UNIVERSITY OF
EASTERN FINLAND
Faculty of Science and Forestry

MODELING OF THE INTERACTIONS BETWEEN NUCLEAR RECEPTOR hCAR AND CO-REGULATOR PEPTIDE

Sun Linlin

Master's thesis

Department of Chemistry

Medicinal Chemistry

411/2012

Abstract

Human constitutive androstane receptor (hCAR, NR1I3) is a member of nuclear receptor superfamily. It functions as a key regulator of the metabolism for a variety of xenobiotics, steroid hormones, bile acids, etc. The co-regulator proteins are indispensable for above functions that are mediated by hCAR. There is usually more than one short length peptide within one co-regulator. These peptides are called nuclear receptor interaction motifs, which are essential for the direct interaction between co-regulator and nuclear receptor (NR). Previous studies suggest that the position of C-terminal helix (H12) of the NRs ligand binding domain (LBD) is a key element that influences such interaction. In co-activators and mediator, the motifs usually share a conserved LXXLL sequence, while the motifs in co-repressors commonly share a longer sequence which is LXXXI/LXXXI/L. A nuclear receptor can specifically bind to these motifs, and display differential recruitment among several motifs in one co-regulator molecule. To understand such specificity of hCAR, the interaction between hCAR-LBD and a series of co-regulator motifs were analyzed in this study using 9 molecular dynamics (MD) simulation systems. The systems consisted of apo/liganded hCAR-LBD and the co-regulator peptide. Due to lack of information about the crystal structures of the studied co-regulator peptides, homology models were used to generate these structures. Analysis on the trajectories from MD simulations and the corresponding final structures suggested that co-repressor peptides were able to induce significant structural changes of hCAR-LBD, whereas the co-activator and mediator peptides only changed the structures subtly. The structural changes at C-terminus of hCAR-LBD and the binding behavior of peptides onto the co-regulator groove indicated that, peptide containing ID2 of NCoR may be responsible for the reorientation of H12 in the presence of inverse agonists. Thus ID2 could be an important motif for the repressive control of hCAR via co-repressor NCoR. For the co-activators and mediator investigated in this work, peptide containing NR1 and NR2 of SRC-1 and NR2 of TRAP may help to maintain the active form of H12 and HX. Therefore, they could also be critical motifs for hCAR-dependent gene regulation by SRC-1 or mediator.

Key words: nuclear receptor, hCAR, molecular dynamics, co-regulator, NCoR, SRC-1, agonist, inverse agonist

Table of contents

Abbreviations

aa.	Amino acids
AD	Activation domain
AF-1	Activation function 1
AF-2	Activation function 2
ANDR	3α-androstenol
APF	Atomic positional fluctuation
AR	Androgen receptor
CAR	Constitutive androstane receptor
CARM1	Coactivator-associated arginine methyl-transferase
CBP	cAMP response element-binding protein-binding protein
CCPR	Cytoplasmic hCAR-retention protein
CITCO	6-(4-Chlorophenyl) imidazo[2,1-b][1,3]thiazole-5-carbaldehyde-O-(3,4-dichlorobenzyl) oxime
CLOTR	Clotrimazole
DAX-1	Dosage-sensitive sex reversal, adrenal hypoplasia critical region, on chromosome X, gene 1
DBD	DNA binding domain
DMSO	Dimethyl sulfoxide
DRIP	Vitamin D receptor interacting protein
EE2	17α-ethynyl-3, 17β-estradiol
ER	Estrogen receptor
ERRs	Estrogen related receptors
FL81	5-(3,4- dimethoxybenzyl)-3-phenyl-4,5-dihydro-isoxazole
FL82	5-benzyl-3-phenyl-4,5-dihydroisoxazole
GR	Glucocorticoid receptor
GRIP/SRC-1	GR-interacting protein
GPS2	G protein pathway suppressor 2
H12	Helix 12
HATs	Histone acetyltransferases
hCAR	Human CAR
HDACs	Histone deacetylases

HNFα	Hepatocyte nuclear factor α
HSP	Heat shock protein
ISWI	Imitation switch
LBD	Ligand binding domain
LBP	Ligand binding pocket
LCoR	Ligand-dependent corepressor
LRH-1	Liver receptor homolog-1
MD	Molecular dynamics
M1H	Mammalian one-hybrid system, reporter gene assays
M2H	mammalian two-hybrid assays
mSin3	Mammalian switch-independent 3 proteins
MTA	Metastasis associated factor
NCoR	Nuclear receptor corepressor
NR	Nuclear receptor
NTD	N-terminal domain
Nurr1	Nuclear receptor related 1 protein
PDB	Protein data bank
PGC-1	PPARγ coactivator-1
PK11195	1-(2-chlorophenyl-nmethylpropyl)-3-isoquinolinecarboxamide
PPARγ	Peroxisome proliferator-activated receptor-gamma
PPP1R16A	Membrane-associated subunit of protein phosphatase 1β
PR	Progesterone receptor
PRMT1	Protein arginine methyltransferase 1
PTMs	Post-translational modifications
PXR	Pregnane X receptor
RAR	Retinoic acid receptor
RD	Repressor domain
Res	Hormone response elements
REA	Repressor of estrogen activity
RIP140	Receptor-interacting protein 140
RMSD	Root mean squares deviation
RXR	Retinoid X receptor

S06772	1-[(2-methylbenzofuran-3-yl)methyl]-3-(thiophen-2-ylmethyl) urea
SHP	Small hetero-dimer partner
SMRT	Silencing mediator for retinoid and thyroid hormone receptors
SRC-1	Steroid receptor coactivator-1
SRCs	The SRC family members
SREBP	Sterol regulatory element binding proteins
SWI/SNF	Switching/sucrose non-fermenting
TBL-1	Transducin-like protein 1
TBL1-R	TBL-1-related protein
TF	Transcription factor
TPP	Triphenyl phosphate
TR	Thyroid hormone receptor
TRAP	Thyroid hormone receptor-associated protein
TRBP	thyroid hormone receptor binding protein
UDP	Uridine diphosphate
VDR	Vitamin D receptor

1 Introduction

1.1 Classification, structure and function of nuclear receptors

Nuclear receptors (NRs) are ligand-regulated transcription factors (TFs) that respond to an input (such as steroids, retinoids, bile acids, heme, xenobiotics) and produce an output (such as gene expression or repression) (Aagaard et al., 2011; Huang et al., 2010; Sladek, 2010; Privalsky, 2004). NRs play an essential role in the regulation of cell differentiation, development, reproduction, metabolism and homeostasis in multi-cellular organisms (Li and Wang., 2010; Perssi and Rosenfeld, 2005; Gronemeyer et al., 2004; Nagy and Schwabe, 2004). The inappropriate function of NR impacts a wide range of pathophysiologies ranging from cancer to metabolic diseases (Trauner et al., 2011; Huang et al., 2010; Khan and Lingrel et al., 2010; Gronemeyer et al., 2004).

NRs bind to their target DNA sequences as homo- or hetero-dimers. In general, NRs regulate gene expression in a ligand-dependent manner. Some of the NRs, such as constitutive androstane receptor (CAR) can also regulate gene expression in the absence of ligand. NR-mediated gene expression is through stepwise and ordered recruitment of various transcription complexes which contain transcription co-regulators (Germain et al., 2006). For decades, the structure and function of NRs have been the targets of research and drug design (Huang et al., 2010; Germain et al., 2006; Mangeldorf et al., 1995).

The sequencing of the human genome has led to the identification of 48 NRs, which can be classified into six evolutionary groups. This classification is based on sequence alignment and phylogenetic tree construction of highly conserved domains (Nuclear Receptor Nomenclature Committee, 1999). The phylogenetic position of each NR is relevant to the DNA -binding and its dimerization abilities (Germain et al., 2006). Alternatively, based on the ligand-binding specificities, NR superfamily can also be divided into three classes: classic receptors, orphan receptors and adopted orphan receptors (Jin and Li., 2010). Classic receptors, such as androgen receptor (AR) and estrogen receptor (ER), are regulated by endocrine ligands. The receptors

without endogenous ligands are identified as orphan receptors, such as small hetero-dimer partner (SHP), estrogen related receptors (ERRs) and hepatocyte nuclear factor α (HNFα). Since the physiological ligands have been identified for orphan receptors, those receptors are thus classified as adopted orphan receptors. CAR is assigned into this class.

In addition, isoforms (products from alternative transcription start sites on the same gene and products of mRNA splice variants) and subtypes (products of closely related genes) are known for most NRs (Germain et al., 2006). These isoforms and subtypes of NRs differ in the regard of ligand binding affinity, transcription activity and distribution in cell and tissues, which contribute complexity for the NR-mediated regulation network (Germain et al, 2004; Steinmetz et al., 2001; Katzenellenbogen et al., 1996).

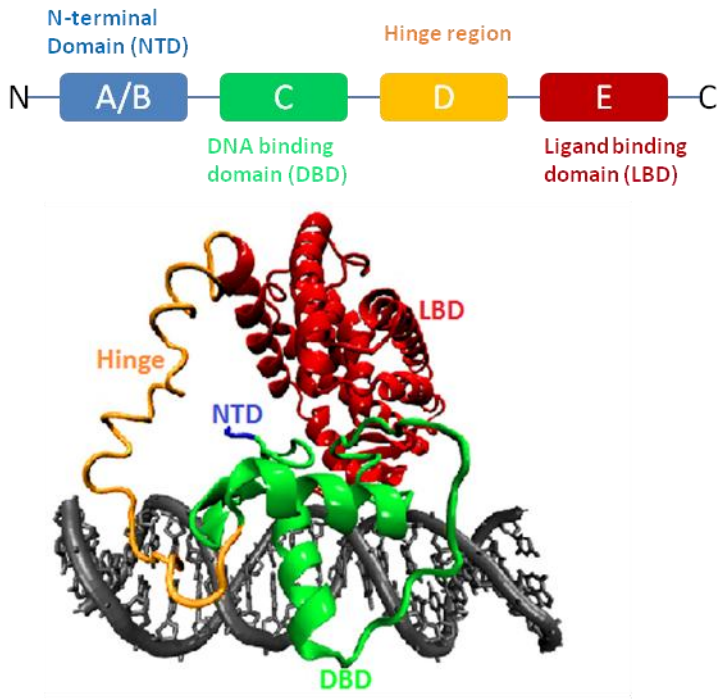

Figure 1. *General structure of nuclear receptors (Aagaard et al., 2011).*

All NRs share high sequence similarity and conserved domains (Jin and Li., 2010). Typically, a NR consists of five functional regions (Fig 1). These regions are designated as N-terminal domain (NTD or A/B domain), DNA binding domain (DBD or C domain), ligand binding

domain (LBD or E domain), a highly variable hinge region between DBD and LBD (or D domain). The importance and the structural properties of these domains are discussed below.

N-terminal domain and Hinge region

These two domains are less conserved compared to DBD and LBD. To date, no crystal structure of NTD has been resolved. This may due to the flexible nature of NTD (Jin and Li., 2010). NTD contains a ligand-independent transactivation function, called activation function 1 (AF1). Among different receptors, AF-1 exhibits distinct structural features and different functions. For example, AF-1 is responsible for the transactivation in the case of AR (Simental et al., 1991), whereas the function of AF-1 could be limited in CAR since it has a very narrow NTD region (Baes et al., 1994). The hinge region D is also poorly conserved and little is known about its structure. It confers the spatial flexibility to the receptors (Aagaard et al., 2011). Moreover, it is reported that this region may harbor nuclear localization signals (Germain et al., 2006).

DNA binding domain

DBD is the most conserved domain. With this domain, NRs bind to specific DNA sequences, called hormone response elements (REs). The core region of this domain is composed by approximate 66 amino acids (Aagaard et al., 2011; Aranda and pascual, 2001). These amino acids fold into a globular domain and are made up of two characteristic cysteine-rich zinc finger motifs (Bain et al., 2007). These two zinc-finger motifs are critical in stabilizing the overall folding of DBD and its DNA-binding activity. Besides the zinc-finger motifs, there are two perpendicular α-helices in this domain: the N-terminal helix (helix I) and the C-terminal helix (helix II) (Bain et al., 2007). Helix I, termed as the recognition helix, locates between the two zinc-finger motifs and interacts with DNA in a sequence-dependent manner. This helix contains a P box, which is defined by residues that are important for sequence-specific DNA binding. On the other hand, helix II contributes to non-specific backbone interactions with DNA (Aagaard et al., 2011). For some NRs, helix II contains the D-box, which is involved in dimerization (Aagaard et al., 2011; Jin and Li, 2010). DBD also harbors the nuclear translocation signals (Germain et al., 2006). And this domain also constitute the dimer interface with the dimer partners (Jin and Li., 2010).

Ligand binding domain

LBD is the second conserved domain of NRs. Numerous crystal structures of NR-LBDs indicate that this domain consists of 11- 13 α helices and 2 – 4 β sheets. These secondary elements are arranged in three layers in tertiary structure and form an anti-parallel α-helical 'sandwich' (Jin and Li, 2010).

Based on the highly organized and well-defined structures, LBD has a number of critical functions. First, it provides a ligand binding pocket (LBP) for endogenous and exdogenous ligands. The LBP locates in the interior of this domain and is formed by a subset of surrounding residues from helices 3, 5, 6, 7, 10 and β-sheets (Steinmetz et al., 2001). The size of the LBP depends on the type of the NRs and the bound ligand. Due to the hydrophobic nature of the LBP, the ligand binding largely relies on hydrophobic interactions (Jin and Li., 2010; Bain et al., 2007). However, some orphan receptors may lack of LBP (e.g. nuclear receptor related 1 protein, so called Nurr1, see Wang et al., 2003) or lack of entry point for cavity (e.g. liver receptor homolog-1 or so-called LRH-1, see Sablin et al., 2003). These orphan receptors may function in an alternative way by being ligand-independent. Second, LBD contains an activation function 2 (AF-2) at helix 12 (H12). In contrast to AF-1, the function of AF-2 is ligand-dependent and is crucial for co-regulator recruitments. Third, LBD can interact with the co-regulators. This domain contains the site for co-regulator binding, namely "co-regulator groove". The groove mainly involves residues from helices 3, 4, and 12. Forth, LBD provides a NR-NR dimerization surface for NRs which function as dimers (Aagaard et al., 2011, Bain et al., 2007).

1.2 Constitutive androstane receptor

1.2.1 Physiological role of CAR

CAR (NR1I3) is a member of NR1I subfamily, which regulates a large set of genes. The classic CAR-regulated genes encode drug-metabolizing enzymes, including phase I cytochromes enzymes, phase II UDP-glucuronosyl transferase, sulfotransferases and multiple transporter proteins (Tolson and Wang., 2010). These enzymes are important in the elimination of xenobiotics. In this context, CAR was firstly recognized as a sensor of xenobiotics, such as drugs

and environmental pollutants. However, in recent years, CAR has been intensively studied due to its significance on a variety of physiological functions (Kachaylo et al., 2011; Masi et al., 2009). For example, CAR mediates the effect of hormonal signals and regulates the detoxification and excretion of toxic endogenous metabolites such as bilirubin and bile acids (Masi et al., 2009; Qatanani et al., 2005). Moreover, CAR is also involved in lipid metabolism and glucose homeostasis (Kachaylo et al., 2011). Based on the diversity of its functions, hCAR is considered not only as an interesting subject of research because of its role in the regulation of drug metabolism, but also a potential drug target for the prevention and treatment of many diseases, especially metabolic-related diseases, such as hepatocelluar carcinoma (Sberna et al., 2011; Dussault et al., 2002).

Unlike classical NRs, CAR is in active state when no ligands bind into the LBP. This feature is termed as constitutive activity (Windshügel et al., 2005; Xu et al., 2004; Frank et al., 2004; Dussault et al., 2002). Two endogenous ligands of hCAR, androstanol and androstenol (ANDR), were found to repress the constitutive activity of CAR. In addition, many xenobiotics, including synthetic compounds display differential effects on CAR-dependent gene regulation by activating or repressing it (Li et al., 2008; Maglich et al., 2003; Tzameli et al., 2000).

CAR is expressed primarily in liver and kidney (Kachaylo et al., 2011). In absence of ligand, it predominantly locates in cytoplasm, and forms complex with other proteins, such as heat shock protein (HSP90), cytoplasmic hCAR-retention protein (CCPR) and the membrane-associated subunit of protein phosphatase 1β (PPP1R16A). Upon ligand binding, human (hCAR) is dephosphorylated, which is followed by its dissociation from the cytoplasmic complex and translocation into the nucleus (Kachaylo et al., 2011; Mutoh et al., 2009). The interference which affects the translocation would also affect the activity of CAR. Subsequent to translocation, CAR forms a hetero-dimer with retinoid X receptor (RXRα), which then binds to the promoter region of the target gene with DBD (Frank et al., 2003). By interacting with multiple protein complexes (such as co-activator complex, polymerase II complex), the expression of the target gene is activated.

1.2.2 Structural features of CAR

Like other NRs, CAR contains five functional regions; the x-ray crystal structure is only available for its LBD. As mentioned above, the N-terminus of CAR is short in length and insignificant in function of AF-1 (Jin and Li., 2010). However, this domain is potentially involved in post-translational modifications (PTMs) and tissue specific activity. Yet the mechanism is not clearly understood (Kachaylo et al., 2011). The hinge region is responsible for rotation of DBD in relative to the position of LBD. DBD domain of CAR, as other NRs, also appears in a globular shape and contains two α-helices perpendicular to one another (Masi et al., 2009). It would also be of great importance to the understanding of CAR function if both DBD and LBD were crystallized together, like for peroxisome proliferator-activated receptor-gamma (PPARγ) (Chandra et al.,2008).

LBD (amino acids 103-348) is composed of 11 α-helices, two 3_{10} helices (designated H2 and H2') and three β-sheets (Xu et al., 2004). In other NRs, helix 10 links to H12 via a flexible loop; but in the case of hCAR, the loop is replaced by a single-turn helix, called HX. Due to the rigidity of HX, the conformational freedom of H12/AF-2 is effectively limited. Thus HX is regarded as potentially important for the constitutive activity of hCAR. The LBP is constituted of residues from helix 2 - 7 and helix 10 and β-sheets regions (Xu et al., 2004). CAR as a xenobiotics sensor has a quite flexible LBP with changeable shape and cavity volume, which enable CAR to accommodate a wide range of ligands (Masi et al., 2009). These ligands can be divided into agonists and inverse agonists, the former can further activate CAR, whereas the latter inhibit the basal transcriptional activity of CAR. This domain is also involved in hetero-dimerization, mainly using helix 10 to form a back-to-back hetero-dimer with RXRα (Xu et al., 2004). Importantly, LBD also plays an essential role in co-regulator recruitment, which largely determines the output of CAR-mediated gene expression, as discussed from sections 1.3 to section 1.5.

1.3 Nuclear receptor co-regulators

1.3.1 Introduction to nuclear receptor co-regulators

NRs modulate transcription through the interaction with co-regulators (O'Malley et al., 2008; Privalsky, 2004). Co-regulators include a large array of molecules, which are generally divided into co-activators, co-repressors and mediator. Co-activators are usually recruited by agonist bound NRs or constitutive active NRs. As the name suggested, co-activators are responsible for the transactivation of target genes. By contrast, co-repressors are usually recruited by ligand-free (apo) and antagonist or inverse agonists bound NRs, and they inhibit the gene expression. Mediator, on the other hand, can either activate or repress the gene expression by interacting with NRs directly or indirectly. Nevertheless, the role of each co-regulator is not fixed. In certain context, co-repressor can function as co-activator and vice versa (Santos et al., 2011; Kato et al., 2011; Lonard and O'Malley., 2007).

To date, there are more than 350 co-regulators that have been reported in the literature, suggesting their critical role in the transcriptional regulation (York and O'Malley., 2010). In fact, many co-regulators work together by forming multi-component protein complexes. The composition of regulatory complexes is subject to dynamic rearrangements in a spatial and temporal manner (Kato et al., 2011; Lonard and O'Malley., 2007; Perssi and Rosenfeld., 2005).

Comparable to 'histone code', the co-regulators can also be differentially 'coded' via PTMs, such as phosphorylation, methylation, and acetylation. These modifications of co-regulators can be trigged by other co-regulators or multiple signaling cascade kinases. Recent studies suggested that each combination of such modifications is expected to have a distinct functional outcome (e.g. O'Malley et al., 2008; Lonard and O'Malley., 2007).This phenomenon is the so-called 'co-regulator codes' (Lonard and O'Malley., 2007). 'Co-regulator codes' potentiate to integrate multiple cellular signals into the event of gene-specific transcription and is considered to play a vital role in the regulation of gene expression (O'Malley et al., 2008).

These co-regulators are not exclusive to NRs; they also intensively participate in other non-NR signal transduction pathways. This feature of co-regulators has further complicate the NR

regulation network (Perssi and Rosenfeld., 2005). Being closely involved in the gene regulation network, the dysfunction of co-regulators can often cause physiological abnormalities and diseases (Hsia et al., 2010).

1.3.2 Co-regulator regulated transcription

Transcription, a key biological process, is the first step of gene expression. Transcription consists of multiple sub-reactions occurring in a specific order. Due to multiple molecules or complexes are needed in this process, transcription can be strongly influenced by many factors. In the case of NR-mediated gene expression, such factors mainly arise from two aspects: the chromatin environment that surrounds the genes and the availability of RNA polymerase II holo-complex (Lonard and O'Malley., 2007). Thus most of the co-regulators are able to affect these two critical factors/conditions. On one hand, many co-regulators tether varied enzymatic activities to the transcriptional complex in order to modify the configuration of chromatin. One the other hand, some co-regulators also serve as bridging agents to connect the receptor to basal transcriptional machinery (including RNA polymerase II holo-complex) for the purpose of regulating target gene expression, such as the mediator.

DNA molecules are packed into a histone protein/DNA structure. The structure is termed chromatin (Hsieh and Fischer., 2005). The compact form of chromatin usually hinders the assembly of transcription complexes and result in the repression of transcription. In case of a more open form of chromatin configuration, the transcription would be allowed to process actively. In order to change the active state of chromatin structure, there are a lot of co-regulators that participate in the reorganization of chromatin structures. Based on their different mechanisms, these co-regulators are divided into three groups: chromatin remodelers, histone chaperones and histone modifiers (Kato et al., 2011).

The chromatin configuration can be modified via the recruitment of chromatin remodeler complexes into the promoter region of target gene (Wolf et al., 2008). Among the reported chromatin remodeling complexes, switch/sucrose non-fermenting (SWI/SNF) complex and imitation switch (ISWI) complex can both activate and repress the chromatin state, whereas Mi2-

type complex appears to repress the chromatin only (Kato et al., 2011). Some subunits within these complexes may direct interact with NRs, and be of great importance by controlling the accessibility of other co-regulators or complexes (Kato et al., 2011).

Histone chaperones, the key actors during histone metabolism, consistently contribute to histone assembly, replacements and exchanges (Koning et al., 2007). By regulating the behavior of histones, histone chaperones are thus able to reorganized the chromatin configuration and affect the functional outcomes of NRs. Hence, histone chaperones can also be classified as co-regulators (Kato et al., 2011).

Based on the hypothesis of histone code, the chromatin configuration is directed by specific combinations of histone modifications (Jenuwein and Allis., 2001). Thus such modification of histone proteins would ultimately allow or block gene expression (Wolf et al., 2008; Glass et al., 1997). Among the reported histone modifications, the histone acetylation is most studied and clearly linked to chromatin activity and transcriptional regulation (Kato et al., 2011). The modification is mainly executed by two types of enzymes: histone acetyltransferases (HATs) and histone deacetylases (HDACs). HATs are enzymes which add the acetyl group to histones, whereas HDACs remove it. By histone acetylation, HATs enhance the target gene accessibility to transcription complex and facilitate the target gene transactivation. On the other hand, by histone deacetylation, HDACs pack the chromatin state tightly and repress of transactivation (Honkakoski and Negishi, 2000). Therefore, HATs are usually included in the co-activator complexes (such as SRCs and CBP/p300 co-activators), whereas HDACs usually form the core subunit of co-repressor complexes (Kato et al., 2011; Guo et al., 2012; Watson et al., 2012). By contrast to the co-regulators that hold HAT or HDAC activities, mediator is less involved in chromatin modifications via histone modifications. Instead, it may function at different steps by introducing the basal transcription machinery to the transcriptional complex that generated by NRs and other co-regulators (Chen and Roeder., 2011; Wärnmark et al., 2001).

NR-mediated gene regulation is a network composed of multiple factors. These factors, as well as all the co-regulators, could be targets of other signaling cascades. This phenomenon is termed as crosstalk. To date, such crosstalk is assumed to occur in at least three ways (Gronemeyer et al.,

2004): (1) interference between NRs and other TFs (Aagaard et al., 2011). For instance, the chromatin modification factors recruited by NRs can either enhance or repress the transcriptional activity of other TFs, who share the same binding profiles with the NRs, (2) PTMs of either NRs or co-regulators. These modifications are of great importance on the activity of NRs and co-regulators. Hence, the factors acting on kinases can also modulate NR activity in ligand-independent manner, (3) 'no-genomic' actions of NRs in ligand-dependent or independent manner (Germain et al., 2006; Gronemeyer et al., 2004).

1.3.3 Co-activators

The SRC family members (SRCs) of co-activators are usually one of the first recruited co-activators by active NRs (Germain et al., 2006). The family members include SRC-1, SRC-1/GRIP1/TIF2, and SRC-3/pCIP/ACTR/AIB1/RAC-3/TRAM-1. These three co-activators mediate the transcription of many genes as a response to a single molecular event and are extensively involved in diverse physiological processes (York and O'Malley., 2010).

SRCs are approximate 160 kDa in size and share 50-55% sequence similarity (Chen et al., 2011). Their crystal structures of full-length sequence are currently not available. Both biological and structural studies have suggested that SRCs share five fundamental and structurally conserved domains (Chen et al., 2011), which include: (1) N-terminal bHLH/PAS (basic helix-loop-helix-per/ARNT/sim) domain. This domain is highly conserved and mainly responsible for the interaction of SRCs with other co-regulators. In addition, the nuclear localization signals are believed to locate in this domain. Thus this domain is also critical in directing the distribution and localization of SRCs; (2) Serine/threonine (S/T)-rich domain. This domain is the popular target for PTMs. These modifications would probably produce differential biological consequences by affecting the localization, activity, stability of SRCs; (3) nuclear receptor interacting domain (RID). In the context of NR-mediated gene regulation, this domain is responsible for direct interaction with the NRs; (4) CBP/p300 interaction domain (CID), is also called activation domain 1 (AD1). AD1 can bind to CBP/p300 and activate the chromatin configuration by histone acetylation; (5) Histone acetyltransferase (HAT) domain or activation domain 2 (AD2). AD2 can

bind to CARM1 (co-activator-associated arginine methyl-transferase) and PRMT1 and enhanced the activation of chromatin by promoting histone methylations.

Beside SRCs, a large number of co-activators have been identified and characterized over years (Thakur and Paramanik., 2009). These co-activators appear to be involved in almost every aspects of gene regulation. For example, in addition to transcription initiation, these co-regulators also play a part in the process of mRNA elongation, splicing, even translation (O'Malley et al., 2008). The functional studies of RID of SRCs, combing the crystal structures of activated LBDs that co-crystallized with short peptides co-activators, an important motif has been discovered. The motif is termed as NR box, and it has the consensus sequence LXXLL, where L represents leucine and X means any amino acids. These NR-boxes are used by co-activators to directly interact with the NRs.

Interestingly, NCoR which commonly appears as co-repressor can also act as co-activator under specific conditions. For example, NCoR was seen to directly associate with co-activator ACTR, and assist the transcriptional activation of thyroid hormone receptor β (TR β) mediated genes (Li et al., 2002).

1.3.4 Co-repressors

Nuclear receptor co-repressor (NCoR) (Hörlein et al., 1995) and silencing mediator for retinoid and thyroid hormone receptors (SMRT) (Chen and Evans, 1995) play an important role in NR transcription repression (Privalsky, 2004; Hsia et al., 2010). Studies on NCoR and SMRT homology domains suggested that they share high sequence similarity and conserved molecular architecture, as well as similar function mechanisms (Privalsky, 2004; Ordentlich et al., 1998; Perissi et al., 1999).

NCoR includes three repression domains (RDs) at N-terminus and three nuclear receptor interaction domain (IDs) at C-terminus, while SMRT includes four RDs at N-terminus and two IDs at C-terminus (Privalsky., 2004). The highly conserved RDs mostly serve as the docking platforms for secondary co-repressors (i.e. other components of the large co-repressor complex,

such as HADCs) to bind either sequentially or simultaneously (Privalsky, 2004). IDs are responsible for the interaction with NRs (Privalsky, 2004; Perissi et al., 1999).

Among the multiple proteins recruited by SMRT and NCoR, HADCs are best characterized and well known for their activity of chromatin condensation. The secondary co-repressors recruited by NCoR and SMRT also include TBL-1 (transducin-like protein 1), TBL1-R (TBL-1-related protein), GPS2 (G protein pathway suppressor 2) and mSin3 (mammalian switch-independent 3 proteins). It has been proposed that these secondary co-repressors may function as scaffolds or assist in repression via distinct mechanisms (Privalsky, 2004). However, the molecular basis for such interactions is still largely unknown. Some indirect evidences also imply that solely SMRT or NCoR binding to NR is not be sufficient for the inactivation of transcription, instead, transcription repression complexes which include multiple co-repressors are needed (Privalsky, 2004).

Co-repressors interact with NRs using IDs which have conserved sequence of I/LXXII (where I is isoleucine, X is any residue (Nagy et al, 1999; Hu and Lazar, 1999; Webb et al., 2000; Perssi and Rosenfeld, 2005) or LXXXI/LXXXI/L (Perissi et al., 1999; Xu et al., 2002). The interaction between the co-repressors (e.g. NCoR and SMRT) and the NRs is based on the binding of these motifs onto the co-regulator groove of NR-LBDs. The binding site of co-repressor IDs with NRs is partially overlapping with the binding site of co-activator NR boxes (Xu et al., 2002).

A new group of co-repressors has been found to interact with agonist bound NRs using LXXLL motifs (Gurevich et al., 2007). This group includes receptor-interacting protein 140 (RIP140), ligand-dependent co-repressor (LCoR), repressor of estrogen activity (REA) and metastasis associated factor (MTA), etc. Within this group, some co-repressors only contain RDs and mediate gene silencing by HDACs recruitment, but others may also contain ADs, which bind to NRs as co-activators (Hsia et al., 2010).

Surprisingly, NRs themselves can also be co-repressors, such as DAX-1 (dosage-sensitive sex reversal, adrenal hypoplasia critical region, on chromosome X, gene 1) and SHP, that act as inhibitory partner for other NRs (Germain et al., 2006).

1.3.5 Nuclear receptor mediator

Mediator, so-called thyroid hormone receptor-associated protein (TRAP), plays an essential role in gene regulation by NRs and other TFs. The function of the mediator is based on its multiple subunits, which have distinct structures and functions. Recent researches (e.g. Malik and Roeder., 2010) have revealed that the mediator is an ordered and sequentially assembled complex, and serves as a platform for other co-regulators. The components of a mediator complex are highly variable (Chen and Roeder., 2011). In general, a mediator complex usually consists of head, middle and tail modules. The middle and tail modules are linked by subunits such as MED1 and MED26 (Malik and Roeder., 2010).

A mediator can have multiple functions. On one hand, the mediator can activate transcription and stimulate basal transcription. One the other hand, mediator can act as co-repressors and inactivate the transcription (Chen and Roeder., 2011). Different from many co-activators and co-repressors, mediator may link the general transcription machinery and RNA polymerase II in a direct way (Chen and Roeder., 2011). Moreover, mediator can recruit histone modifiers and chromatin remodelers, which reorganize the chromatin structure (Chen and Roeder., 2011).

Among these subunits of mediator, MED1 is better characterized. The cell-based assays suggested that MED1 can interact with many NRs, including TR, ER, VDR, GR, retinoic acid receptor (RAR) and RXR. Known from the mouse model, MED1 is responsible for many important NR-regulated functions, such as the PPARγ mediated adipogenesis and CAR-mediated hepatic steatosis, etc. MED1 contains two LXXLL motifs. These two motifs also called NR boxes and are utilized to interact with NRs directly. Similar to what has seen in NR-co-activator interaction, the position of AF-2 can critically affect the interaction between NR boxes of MED1 and NRs. However, NR boxes of mediator are not necessary for the *in vivo* function of NRs, which suggest alternative pathways for mediator to interact with the NRs and being LXXLL independently.

Other subunits of mediator, such as MED14 can specifically interact with AF-1 of NRs, such as GR and PPARγ. Meanwhile, these NRs can also interact with MED1 through AF-2 domain. Such differential regulation is usually determined by the target genes or other factors (Chen and Roeder, 2011). MED25 contains one LXXLL motif and is found to directly associate with HNFα

and regulate a set of genes. MED15 can activate sterol regulatory element binding proteins -1 α (SREBP-1α) and regulate lipid homeostasis, through the recruitment of cofactors that include other mediator subunits and p300/CBP histone acetyltransferases.

1.4 Influence of ligand binding on nuclear receptor structure and co-regulator recruitment

NR-mediated transcription is a chain of biological reactions, which is usually trigged by the binding of ligand into the LBP of the NRs. By definition, agonists are ligands that lock the receptor in the active form and antagonists are ligands that prevent the receptor from adopting active conformation (Germain et al., 2006). Term inverse agonists, refers to antagonists, but is used specifically for the ligands which are able to inhibit the basal transcriptional activity of NRs. For example, different inverse agonists of hCAR can abolish the basal transcriptional activity to a certain extend.

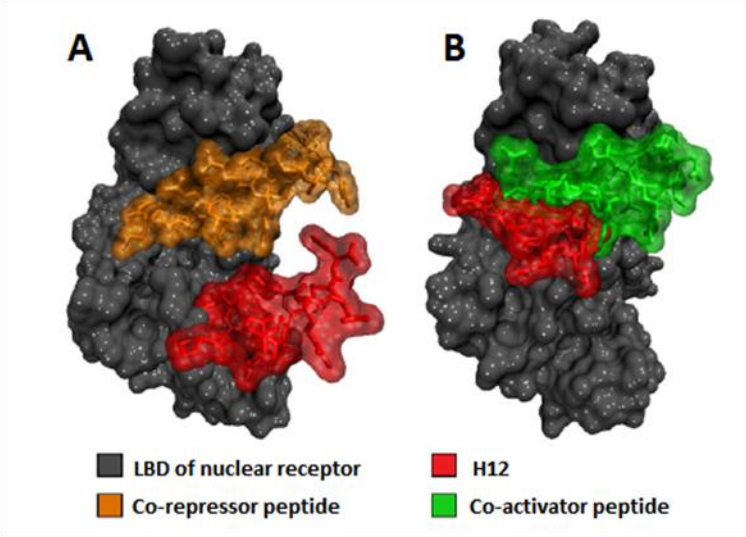

Figure 2. *H12 is repositioned in response to the nature of ligand bound (Aagaard et al., 2011). (A) In the presence of inverse agonist/antagonist, the position of H12 allows the binding of co-repressors through IDs. (B) Binding of agonist switches the H12 into a position that favors the binding of co-activators.*

Structural studies suggested that the active state of the NRs is controlled by the C-terminus of LBD (Aagaard et al., 2011; Germain et al., 2006) (Fig 2). The binding of ligands into the LBP would cause structural changes in the NRs and induce a series of intracellular interactions. Among these changes, the movement of H12 is most evident. When agonist bind into the LBP, H12 tends to fold against the LBD and cover the entrance of the LBP. This change facilitates the recruitment of co-activators and the activation of transcription. In contrast, if the bound ligand is an antagonist or inverse agonist, H12 helix tends to extend away from the core of LBD. Resultantly, co-repressor complexes are recruited by NRs and thus inactivate the transcription. Hence, the position of AF-2 relative to the rest of the LBD is critical for the selection of co-regulators: the active position of H12 favors co-activators recruitment and its inactivate position facilitates co-repressors recruitment (Nagy and Schwabe, 2004; Privalsky, 2004; Bourguet et al., 2000).

Here raises another question: how does the position of H12 enhance of impair the selective binding of co-activators and co-repressors? Seeing from the interface between the short peptide which contained NR box of co-activator and LBD of nuclear receptor, the peptide is held in place via hydrophobic interaction and forms two hydrogen bonds between the peptide backbone atoms and two conserved residues from LBDs (lysine from H3 and glutamate from H12). Because the hydrogen binding requires reasonably close distance and favored orientation between the H12 and co-activator peptide, the active position of H12 induced by agonists is thus considered as important for co-activator recruitment. On the other hand, the X-ray crystal structures suggest that the peptide from IDs of co-repressor extends into the regions which are occupied by active H12 (Xu et al., 2002). Only in the case of inactive H12, NRs favor the interaction with co-repressors. Different from the binding of co-activators, the binding of co-repressors does not rely on conserved hydrogen bonds, but mainly hydrophobic interactions.

A general co-regulator exchange model has been proposed based on current understanding of the regulatory function of co-activators, co-repressors, as well as mediator (Glass and Rosenfeld., 2000). The transcription, as mentioned above, is a sequential process that happens in a specific order, this process may be divided into 5 stages. First, the unliganded or antagonist bound nuclear receptor attaches to specific DNA sequences, and recruits co-repressor complex. HDACs, as one

component of the co-repressor complex, are used to condense the chromatin structure and repress the transcription. Second, upon the binding of agonist, AF-2 of nuclear receptor is activated and facilitates the exchange of the co-repressor complex for the co-activator complex, which most probably contains the histone modifying factors, such as HATs. Third, HATs or other enzymes produce an open chromatin structure via histone modifications. In this step, the other chromatin remodelers may also be involved. Forth, exchange the co-activator complex for mediator complex and recruit RNA polymerase II. Fifth, mediator complex initiate and activate the gene transcription. Based on this model, close cooperation of multiple co-regulator complexes is indispensable for the regulation of gene transcription.

1.5 Nuclear receptor specificity of co-regulator peptides

1.5.1 Nuclear receptor specificity of the NR boxes of co-activators

There are a number of co-regulators that share the conserved NR boxes. These co-regulators include co-activators (such as SRCs, PGC-1, CBP/p300 and TRBP), co-repressors (RIP140, LCoR) and mediator/TRAP. Despite these NR boxes are shared by above-mentioned co-regulators and most of these NR boxes are able to bind to the receptor directly, they are probably not functionally equivalent (Chang et al., 1999). Many findings support the idea that the nuclear receptor binding selectivity can be achieved by altering sequences flanking the LXXLL core motif (Savkur and Burris., 2004; Chang et al., 1999; McInerney et al., 1998). This may explain why NRs usually interact with specific co-regulators. For instance, PPARγ has greater affinity for CBP than for SRC-1, whereas ERα binds SRC-1 better than CBP (Zhou et al., 1998). Interestingly, Wärnmark et al (2010) has reported that the NR boxes of TRAP are differentially recruited by ERα and ERβ. These preferences have been utilized to discriminate between NRs and even nuclear receptor subtypes either in ligand dependent or independent manner (Bramlett et al., 2001; Mclnerney et al., 1998; Darimont et al., 1998).

Single (such as PGC) or multiple copies (such as SRCs) of NR boxes are present in a single co-activator. In case of multiple copies, the NR boxes are usually differentially utilized by different

NRs. For example, SRC-1 contains three NR boxes (NR1, NR2 and NR3), NR2 is sufficient for the activation by of ER, whereas TR and RAR require both NR2 and NR3 with correct spacing between them. PPARγ and PR need both NR1 and NR2, and again require for correct spacing between these two NR boxes (Mclnerney et al., 1998). Biochemical experiments have demonstrated that single fragment of SRC-1 containing two or three NR boxes can interact with both hetero- and homo-dimers, with one NR box associated with each monomer (Nolte et al., 1998; Westin et al., 1998; Gee et al., 1999). This observation suggests that co-regulators containing multiple NR boxes would probably achieve enhanced binding with NR compared to those containing single NR box (Savkur and Burris., 2004).

Murine CAR (mCAR) is proved to interact with co-activators, such as SRCs, ASC-2 and PBP. Of these co-activators, SRC-3 interacts with mCAR through S/T and HAT domains, whereas SRC-1 and SRC-2 interact with mCAR by NR2 (Chen et al., 2011). However, hCAR only shares limited sequence and functional similarity with murine CAR. Thus the hCAR activation mechanism by the recruitment of SRCs might be different from mCAR.

1.5.2 Nuclear receptor specificity of the NR boxes of mediator

Similar to NR boxes in co-activators, the two NR boxes of a mediator subunit MED1 also display preferential binding with certain NRs. For example, steroid hormone receptors, such as ER, show preferred binding to the NR1of TRAP, whereas non-steroid hormone receptors, such as TRα and VDR, show preferred binding to NR2 of TRAP. However, these two motifs are both required for efficient NR-mediated transcription (Chen and Roeder., 2011).

Mediator, as discussed above, functions as recruiter of complexes that interact with the basal transcription machinery. Learning from the co-regulator exchange model, the mediator complex is most probably involved in many gene transcription. Considering the fact that the NR boxes of the mediator are able to directly interact with several NRs, one may assume that hCAR may entitle to the similar interaction with mediator. More research work is needed to validate this idea.

1.5.3 Nuclear receptor specificity of IDs of co-repressors

Co-repressors SMRT and NCoR interact with NRs utilizing the conserved LXXXI/LXXXI/L motif (termed as IDs). SMRT contains two IDs, whereas NCoR contains three (one of which is removed by mRNA splicing in one of the isoforms) (Privalsky., 2004; Nagy et al., 1999). It has been reported that different NRs exhibit different affinities for these IDs (Privalsky., 2004). For instance, RARs preferentially interact with ID2 of SMRT, RXRs can interact with both ID1 in SMRT and ID1 in NCoR, T3Rs interact with ID2 and ID3 of NCoR and ID1 and ID2 of SMRT. These preferences may be caused by sequence variations in the motif itself or other factors, such as sterical influences within co-repressor complex (Perissi et al., 1999). Moreover, the mutation within the adjoining sequences from different motifs is also reported to disrupt the interaction between NRs and co-repressors. Thus these sequences may also be of great importance for the recognition and selection of NRs (Webb et al., 2000).

1.6 Aim of study

This study aimed at investigating the important nuclear receptor interaction motifs of co-regulators that contribute to hCAR specificity. There are usually multiple interaction motifs within each co-regulator. Each of these motifs may underlie critical functions in the activation and repression of hCAR transcriptional activity.

In this study, co-activator SRC-1, co-repressor NCoR and TRAP were chosen to represent different classes of co-regulators of hCAR. The goal was to clarify the differential recruitment of interaction domains of NCoR, SRC-1 and TRAP by hCAR through inspecting the structural changes of NR-ligand-co-regulator complexes during MD simulations. Furthermore, this study was hoped to provide hints for mutagenesis studies in delineating the critical molecular determinants of the interaction between the co-regulator interaction domains of NCoR, SRC-1 and TRAP. In addition, the ligand specificity of these interactions was hoped to be elucidated.

2 Methods and materials

2.1 Model building

The model was based on three essential components: hCAR-LBD, ligand and a peptide segment from co-regulator. The ligand-protein complexes were already available for this work and the docking of ligands has been described in the publication by Jyrkkärinne et al (2012). A number of ligands, which covered a wide range of chemical groups, were selected for this study (Jyrkkärinne et al., 2012; Küblbeck et al., 2011a; Küblbeck et al., 2011b; Jyrkkärinne et al., 2008; Küblbeck et al., 2008; Li et al., 2008; Huang et al., 2004; Maglich et al., 2003) (Table 1, Appendix I). Seven of them are agonists (CITCO, FL81, FL82, permetrin, CLOTR, TPP and artemisin) and eight of them are inverse agonists (EE2, androstanol, ANDR, PK11195, S07662, clomifene, celecoxib and meclizine). Each studied peptide was placed onto the co-regulator groove of liganded or apo hCAR-LBD. MD simulations of 10 ns were performed for these NR-ligand-co-regulator complexes.

Three well known co-regulators were chosen for this study. They are co-activator SRC-1, co-repressor NCoR and TRAP. Short peptide segments were extracted from the interaction domains of these three co-regulators. Previous studies proved that these peptides are sufficient to mediate the gene expression with the help of NRs (Nagy et al., 1999; Hu and Lazar., 1999). These peptides contain ID1 (contains both ID1a and ID1b according to different sequence alignments) and ID2 from NCoR, NR1, NR2 and NR3 (NR 1-3 for short) from SRC-1, and NR1and NR2 (NR1-2 for short) from TRAP. Of these peptides, NR2 of SRC-1 is the only one which has been co-crystallized with hCAR-LBD (Xu et al., 2004). The other peptides were built using homology modeling and are described below.

2.2 Homology modeling

Prior to homology modeling, the sequence alignments of these co-regulator peptides were studied. Many literatures have reported alignments with respect to the first conserved leucine or

isoleucine residue within the conserved nuclear receptor interaction domains of co-regulators (Plevin et al., 2005; Savkur and Burris., 2004; Bramlett et al., 2001; Wärnmark et al., 2001; Heery et al., 2001; Webb et al., 2000; Hu and Lazar., 1999; Perssi et al., 1999; Nolte et al., 1998;

Table 1. *Ligands incorporated in MD simulation systems, with their molecular weight (MW) and in vitro activities.*

Ligand[a]	Molecular formula	Molecular Weight (MW)	*in vitro* activity		
			Act[b]	NCoR act[c]	SRC-1act[c]
CITCO*	$C_{19}H_{12}Cl_3N_3OS$	436.74	17.6 ± 2.5	2.2 ± 0.4	206.7 ± 9.2
FL82*	$C_{16}H_{15}NO$	237.30	14.2 ± 2.3	1.0 ± 0.3	81.7 ± 12.7
FL81*	$C_{18}H_{19}NO_3$	297.35	9.7 ± 4.5	1.5 ± 0.1	160.5 ± 12.1
Permethrin*	$C_{21}H_{20}Cl_2O_3$	391.29	9.2 ± 2.3	2.7 ± 0.3	113.0 ±17.4
CLOTR*	$C_{22}H_{17}ClN_2$	344.84	6.2 ± 1.5	4.9 ± 0.3	50.8 ± 1.9
TPP*	$C_{18}H_{15}O_4P$	326.28	3.5 ± 0.5	2.7 ± 0.3	123.0 ±15.8
Artemisin*	$C_{15}H_{18}O_4$	262.30	2.1 ± 0.7	2.6 ± 0.6	56.3 ± 17.3
EE2**	$C_{20}H_{24}O_2$	296.40	0.1 ± < 0.1	1.5 ± 0.1	3.4 ± 0.3
Androstanol**	$C_{19}H_{32}O$	276.46	0.5 ± < 0.1	19.1 ± 1.0	7.1 ± 0.4
ANDR**	$C_{19}H_{30}O$	274.44	0.2 ± < 0.1	9.7 ± 1.2	10.0 ± 1.1
PK11195**	$C_{21}H_{21}ClN_2O$	352.86	0.6 ± 0.1	23.8 ± 3.7	20.4 ± 4.2
S07662**	$C_{16}H_{16}N_2O_2S$	300.38	0.4 ± 0.1	20.9 ± 10.2	1.9 ± 0.5
Clomifene**	$C_{26}H_{28}ClNO$	405.96	0.4 ± < 0.1	0.6 ± < 0.1	0.7 ± < 0.1
Celecoxib**	$C_{17}H_{14}F_3N_3O_2S$	381.37	0.6 ± 0.1	0.7 ± 0.1	0.9 ± < 0.1
Meclizine**	$C_{25}H_{27}ClN_2$	390.95	1.6 ± 0.8	0.9 ± 0.1	0.8 ± 0.2

[a]*agonist*, inverse agonist***

[b,c]*Jyrkkärinne et al., 2012* [b]*Activity at 10 µM concentration (for CITCO 1µm) in reporter gene assays in mammalian cells, expressed as relative to solvent control ± s.d.* [c] *NCoR and SRC-1 recruitment was measured at 10 µM concentration (for CITCO 1 µM, and for steroids, EE2, androstenol and androstanol at 30 µM) in mammalian two-hybrid assays (M2H), expressed as relative to solvent control ± s.d.*

McInerney et al., 1998). Such alignments, as shown in Figure 3, are well recognized and were used for this study. Based on the sequence alignments, the homology models of ID1 and ID2 of NCoR peptides were build on the basis of the crystal structure of a short SMRT peptide

containing the core residues of ID2 (PDB entry number 1kkq, Xu et al., 2002). Two homology models of NCoR ID1 were built, each corresponding to an alternative alignment. The homology models of NR1and NR3 of SRC-1, together with NR1-2 of TRAP were built using NR2 of SRC-1 as template (PDB entry number 1xvp).

The homology modeling was performed using *Biopolymer* module of SYBYL-X 1.2 (Tripos, St. Louis, MO, USA). In order to test the stability of the built co-regulator peptides, these peptides were minimized by using 1000 steps steepest descents under the condition of AMBER7-FF99 force field and Gasteiger-Hückel point charges. The backbones of the peptides only changed subtly during minimization. However, in order to have more comparable starting conformations of different peptides in MD simulations, these peptides were included into the protein complexes as the original states, which were not minimized. The unfavorable interactions that were caused by homology modeling were removed or minimized in the following minimization procedures.

A

```
SMRT ID2       NMGLEAIIRKALMGKYDQW
NCoR ID2       NLGLEDIIRKALMGSFDDK
NCoR ID1a      LITLADHICQIITQDFARN
NCoR ID1b      ADHICQIITQDFARNQVSS
```

B

```
SRC-1 NR2       ERHKILHRLLQE
SRC-1 NR1       QTSHKLVQLLTT
SRC-1 NR3       KDHQLLRYLLDK
TRAP NR1        SQNPILTSLLQI
TRAP NR2        KNHPMLMNLLKD
```

Figure 3. *(A) Sequence alignment of human co-repressor SMRT and NCoR interaction domains. NCoR ID1a (amino acids 2,048-2,066) and NCoR ID1b (amino acids 2,052-2,070) represent two different alignments of NCoR ID1when aligned with SMRT ID2 (amino acids 2,347-2,365). The alignment of NCoR ID1a emphasizes the long motif LXXXIXXXI/L, while the alignment of NCoR ID1b emphasizes the short motif I/LXXII motif. The alignment of NCoR ID2 (2,261-2,279) is based on both motifs. (B) Sequence alignment of human co-activator SRC-1 (NR1: amino acids 628-639; NR2: amino acids 685 -696; NR3: amino acids 744-755) and human mediator TRAP (NR1: amino acids: 599-610; NR2: amino acids 640-651). This is based on LXXLL motif, which is also termed as NR box. The most important and conserved residues are highlight in grey.*

2.3 Incorporation of the co-regulator peptides

Three homology models of two NCoR IDs were built: NCoR ID1a, ID1b and ID2. NCoR peptides used the same coordination as SMRT and merged onto the co-regulator grooves of hCAR-LBD. This procedure was described in Jyrkkärinne et al, (2012). Peptide SRC-1 NR2 was co-crystallized with hCAR-LBD (1xvp). Hence, the coordination of peptide SRC-1 NR2 from crystal structure (PDB no. 1xvp) was used for the other homology models, which include peptides SRC-1 NR1-2, TRAP NR1-2.

2.4 Set up of the molecular dynamics simulation systems

MD simulations of 10 ns were run for 9 systems (Table 2). Among these MD simulation systems, system I only contains apo and liganded hCAR-LBD, while systems II-IX also contain the co-regulator peptide. Moreover, each system contains 16 subsystems, 15 of them containing ligands and one containing apo-structure (ligand-free structure).

For each subsystem, the hydrogen atoms were first added to protein complexes by using *tleap* module of AMBER10 (Case et al., 2008). The protein complexes, as well as the structural crystal water molecules were then solvated in a periodic water box, also with *tleap*. Force field parameters and partial charges from ff99sb force filed were used for protein (Hornak et al., 2006). For the ligand, the general atomic force field (GAFF) parameter assignments were made by using the *antechamber* module of AMBER10 (Wang et al., 2004), and the atom-centered partial charges were generated by using AM1-BCC method (Jakalian et al., 2000). The explicit TIP3 waters were used for solvation. No salt ions were included in the MD studies.

2.5 Energy minimization

Because peptides were docked onto the co-regulator groove by using the same coordination as SMRT ID2 or SRC-1 NR2 peptides, many unfavorable sterical contacts were produced. Thus

prior to MD simulations, the protein complexes were minimized by using *sander* module of AMBER10. Note that the docking poses of ligands in the LBP were carefully evaluated beforehand and were not considered as the focus of these minimization procedures.

Table 2. *Settings and parameters of MD simulation systems*

System[a]	Components of MD systems[b]		MD parametheres
I	No peptide[c]	hCAR-LBD+ ligand[a]	Force filed for ligand: GAFF Force field for protein: Amber ff99SB Box-size: periodic water box Simulation time: 10 ns Water type: TIP3P Ions: none Environment: Amber 10 Cluster: CSC, Finland
II	NCoR ID2		
III	NCoR ID1a		
IV	NCoR ID1b		
V	SRC-1 NR1		
VI	SRC-1 NR2		
VII	SRC-1 NR3		
VIII	TRAP NR1		
IX	TRAP NR2		

[a]*Each system contains 1 apo structure and 15 liganded structures.*

[b]*The x-ray crystal structure of hCAR ligand binding domain is chain D of PDB entry 1xvp. Of the peptides studied here, only for SRC-1 NR2 there was crystallographic data available (1xvp). Based on the sequence alignment as shown in Figure 3, the other co-activator peptides were generated by homology modeling by using SRC-1 NR2 (1xvp) as template. The co-repressor peptides, on the other hand, were also generated by homology modeling, but by using SMRT ID2 (1kkq) as template. SYBYL was used for the set up of homology models.*

[C]*System I contains no peptide, is regarded as the comparison group.*

The minimization contained two steps. First, the water molecules and the hydrogen atoms of the protein complex were minimized by steepest decent with heavy atoms constrain at the strength of 50 kcal/mol. Second, the protein complex was further minimized by calculating 1000 steps steepest decent and 4000 steps conjugate gradients, but using 50 kcal/mol constraints for heavy atoms excluding the co-regulator peptide and the last four residues of H12. After these two minimization steps, the protein complex was believed to be a good starting point for MD simulations.

2.6 Molecular dynamics simulations

All MD simulation systems were equilibrated by using *sander* module of AMBER10 (Weiser et al., 1999). The solvent box in each subsystem was heated to 300 K over 7.5 ps and equilibrated for 50 ps under the condition of 300 K constant temperature and 1 atm constant pressure, using 50 kcal/mol constraints for protein heavy atoms. However, the constraints were removed in the following procedures. Subsequently, the MD systems were minimized for 500 steps steepest descent and 500 steps conjugate gradients. Then the systems were again heated to 300 K within 7.5 ps, and equilibrated for 300 ps by using time step of 1.5 fs.

The production dynamic runs of 10 ns were calculated by *pmemd* module of AMBER10. The cutoff value for lennard-Jones interaction was set to 8 Å. And the electrostatic interactions were calculated by the particle mesh Ewald (PME) method (Darden et al., 1993). During the MD simulations, the shake algorithm was used to constrain the bonds involving hydrogen atoms to their equilibrium values (Ryckaert et al., 1977).

2.7 Analysis of trajectories and final structures

The trajectories from MD runs were analyzed for root mean square deviation (RMSD), the atomic positional fluctuation (APF) and the protein secondary structure with the *ptraj* module of Amber tools 1.3 (Case et al., 2005). RMSD has been commonly used for evaluating the stability of globular protein conformation (Maiorov and Crippen., 1994). It measures the average distance between the atoms of two superimposed proteins. In order to check the structural stability during MD simulations, the three-dimensional structure of protein complex during MD simulations and the reference protein were superimposed and calculated for RMSD values. The reference protein was the first structure after saving coordinates at *tleap* module. Different from RMSD, APF represents the movements of a single residue before and after MD simulations. APF values often revealed the most flexible residues, which may provide insights to the functionally important structure elements. The stability of protein secondary structures (such as α-helix, β sheets, etc) was also checked.

The final structures from 10ns MD runs were generated using *ambpdb* module of AMBER10. These structures were visually examined within the assistance of SYBYL software. In addition, all figures in this study were prepared by using SYBYL. The Connolly surfaces of the LBP were calculated by *MOLCAD* module in SYBYL by using 1.6 Å probe radius.

2.8 MM-PBSA binding free energy calculation

In addition to trajectory analysis, MM-PBSA ligand-protein interaction energy ($E_{protein\text{-}ligand}$) were calculated by standard MM-PBSA method (Hou et al., 2011; Rastelli et al., 2010, Wang et al., 2001). The calculation was based on 50 snapshots from first nanosecond and another 50 snapshots from the ninth nanosecond of MD simulations. The output energy values were the average free energy of the 50 extracted structures at 1 ns and 9 ns, respectively.

For each snapshot, the ligand-protein interaction energy ($G_{bind} = G_{complex}\text{-}G_{protein}\text{-}G_{ligand}$) was calculated. The absolute energy values of each structure, such as protein and ligands, can be approximately calculated by the sum of molecular mechanical gas-phase energies (E_{MM}), solvation free energies ($G_{solvation}$) and entropy contributions ($T\Delta S$) ($G = E_{MM} + G_{solvation} - T\Delta S$, where $G_{solvation} = G_{GB}+G_{np}$). E_{MM} was calculated by using the *sander* program of AMBER10 with all protein pairwise interactions included and dielectric constant (ε) of 1. $G_{solvation}$ was calculated in the sum of generalized Born equation (G_{GB}) (Onufriev et al., 2000), and non-polar solvation energy which related to solvent-accessible surface areas (Weiser et al., 1999). However, considering the entropy term (($T\Delta S$) is currently very time-consuming and expensive to run (Kongsted et al., 2009; Weis et al., 2006); it was omitted from this calculation.

3 Results and discussion

3.1 Structural stability of molecular dynamics simulation systems

Within the time range of MD simulations, the structural stability of protein complexes was evaluated by root mean square deviation (RMSD, Appendix II). Increase of the RMSD values indicates the decrease in the structural stability in MD simulation systems. In this model, the RMSD values are approximately 4.5 Å at maximum and 1 Å at minimum (Appendix II). Such variation of RMSD is comparable to other MD studies (e.g. Küblbeck et al., 2011a; Windshügel et al., 2005). These values revealed that the overall structure of hCAR-LBD remained stable in this model.

Compared with the data obtained from 9 MD systems, RMSD values calculated for system I (Table 2) and systems V-IX (Table 2) are around 2 Å in average. On the other hand, the RMSD values of systems II-IV (Table 2) are clearly higher, but no greater than 4.5 Å. These above results suggested that the repressive activity of NCoR peptides may be responsible for the relatively high RMSD values in systems II-IV. This may be because the crystal structure of hCAR-LBD that was extracted from CITCO bound hCAR complex is in active state before MD simulation. Therefore, by the interaction of NCoR and hCAR-LBD, the transcriptional active conformation of hCAR can potentially be transformed into less active states. On the other hand, the effect of introducing the co-activator SRC-1 and TRAP peptide would cause fewer changes in such systems. The RMSD values in systems V-IX thus could be relatively lower than systems II-IV. In this context, the original conformation of hCAR at the starting point of MD simulations could critically affect the structural responses of hCAR-LBD complex to the co-regulator peptides.

The system stability was further tested by atomic positional fluctuation, APF (Appendix III). It represents the backbone fluctuation of single residue in the time range of MD simulations. Over 9 simulation systems, helices of hCAR-LBD revealed subtle movements with APF values less than 1 Å. This might be due to the compact architecture of the three-layered helix sandwich, which prevents these residues to move freely. On the other hand, the loops (aa. 143-154 and aa. 298-307) and β-sheets (aa. 210-225) of hCAR-LBD revealed clearly higher flexibility with APF values in

the range of 1 - 4.5 Å. These values are in consistent with previous studies (Küblbeck et al., 2011a). Consequentially, in this respect, these systems are sufficiently stable to simulate the structural changes for further analyzing.

3.2 Molecular dynamics simulations of systems II-IV

3.2.1 Structural changes of hCAR-LBD induced by interaction with IDs of NCoR

The C-terminal residues of hCAR-LBD are essential in stabilizing the position of H12. As suggested by APF values, these residues moved more in systems II-IV compared to system I (Appendix IV, Fig 1 – Fig 4). Thus, by interacting with NCoR peptides, the C-terminus of hCAR-LBD was destabilized. Such destabilization may change the activity of hCAR-LBD.

By including ID2 peptide of NCoR into system II, inverse agonists tended to perturb the helical content (HC %, means the percentage of MD simulation time for the residues to stay in helical conformation) of H12 (Appendix V, Fig 2B), and shifted H12 out of the active position (Fig 4B). Strong inverse agonists, such as S07662 and PK11195, appeared to move H12 toward H10 (Fig 4B), with HC % of H12 decreased to minimum 35% and 13%, respectively (Appendix V, Fig 2B). Interestingly, inverse agonists androstanol and clomifene were seen to dramatically decreased HC % of H12 to less than 8% (Appendix V, Fig 2B), and re-orientated H12 to the direction of HX (Fig 4B). Other inverse agonists (ANDR, celecoxib, meclizine and EE2) that stabilized the C-terminal residues (Appendix V, Fig 2B), only induced minor structural changes (Fig 4B). With regards to agonists, permethrin, CLOTR and artemisin, acted more like inverse agonists, which also destabilize the C-terminal residues (Appendix V, Fig 2A) and move H12 to H10. However, CITCO and FL81, as strong agonists, tended to maintain H12 in a highly stable active state (Fig 4A).

System III included ID1a peptide of NCoR. Within this MD simulation system, 2 out of 8 inverse agonists (PK11195 and androstanol) tended to destabilize the C-terminal residues of hCAR-LBD

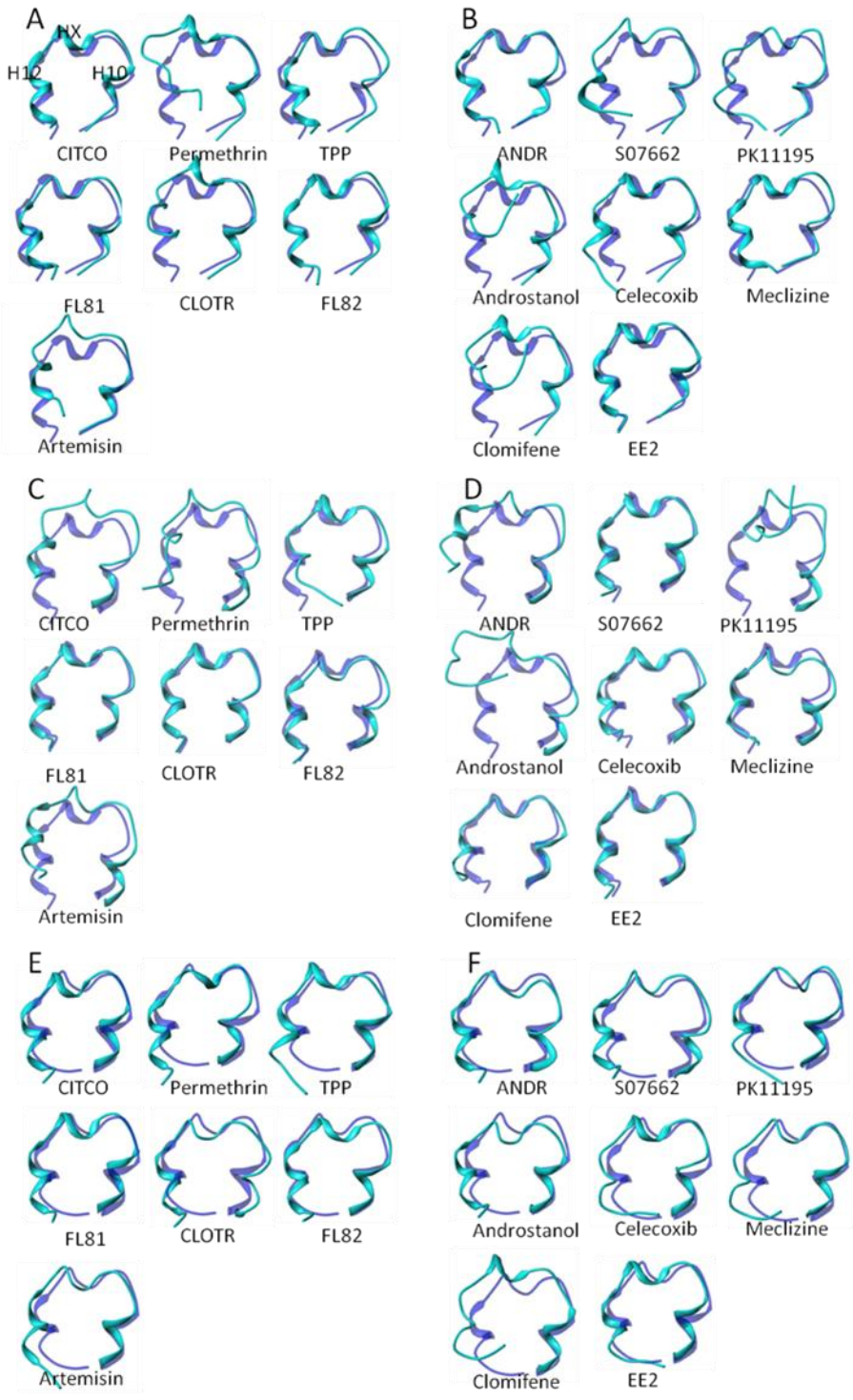

Figure 4. *Positions of H12 in the final structures of the 10 ns MD simulations. (A) agonists and (B) inverse agonists in system II; (C) agonists and (D) inverse agonists in system III; (E) agonists and (F) inverse agonists in system IV. Apo (transparent, blue) is shown as a reference with each liganded structure (cyan).*

and shift H12 to the direction of HX and H10 (Fig 4D). Particularly, PK11195 was seen to decrease HC % of H12 to under 10%, while androstanol decreased the value to 22% at minimum (Appendix V, Fig 3B). Despite S07662 having a better inverse agonist profile, it maintained H12 in the active position (Fig 4D). H12 in the presence of other inverse agonists either moved to the opposite direction of H10 (ANDR), or remained in the active position as what was seen in S07662. On the other hand, agonists FL81, FL82 and CLOTR appeared to stabilize H12 in the active position, while agonist CITCO was seen to greatly deform HX and H12 (Fig 4C). From above, the positions of H12 in the presence of S07662 and CITCO suggested disagreements with the *in vitro* test of ligand-dependent hCAR activity (Table 1).

The second homology model of ID1 motif of NCoR, namely ID1b was included in system IV. Intriguingly, the active position of H12 was maintained by 5 out of 7 agonists (CITCO, permethrin, FL81, CLOTR and FL82) and 3 out of 8 inverse agonists (ANDR, S07662 and androstanol) (Fig 4E and 4F). In the case of other inverse agonists (PK11195, EE2, celecoxib, meclizine and clomifene), H12 remained as in apo-structure (Fig 4F). Based on above findings, ID1b peptide was not able to induce conformational changes towards inactive state of hCAR-LBD.

3.2.2 Binding of NCoR IDs onto hCAR co-regulator groove

The NCoR co-regulator groove is constituted by residues mainly from H3, H4 of hCAR-LBD (Appendix VI, Fig 1). Any movements of the residues that lie in the groove would influence the property of the groove and even the binding of upcoming co-regulators. Such movements were seen in systems II-IV and it caused the dissimilar binding mode of three NCoR peptides. For instance, in apo-structure of systems II-III, H12 adopted active conformation, which prevented efficacious binding of NCoR peptides by introducing sterical hindrances (Appendix VI, Fig 1A and 1B). In apo-structure of system IV, H12 was observed to shift toward H10, and as a result, the peptide was allowed to extend further into the groove and probably achieved enhanced binding. However, the 3-turn helical conformation of ID1a and ID1b (Appendix VI, Fig 1B and 1C) were greatly disturbed.

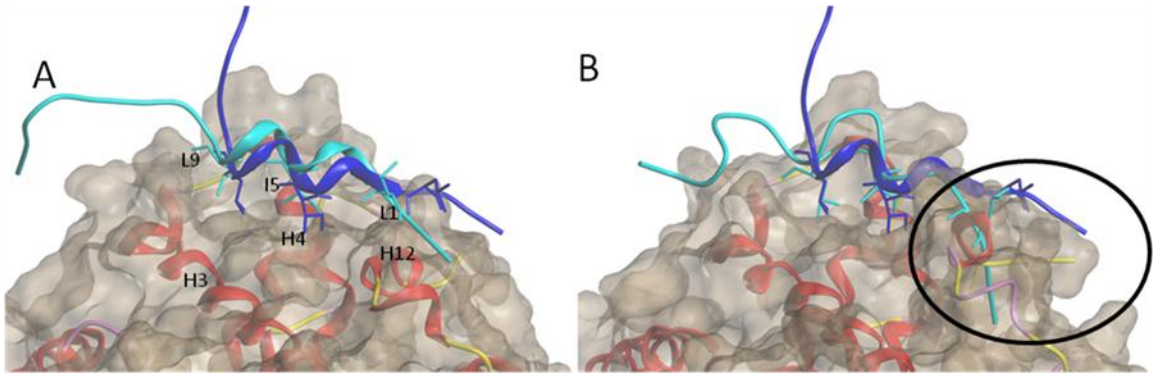

Figure 5*. The NCoR ID2 peptide on hCAR-LBD. (A) represents the co-regulator groove in the presence of CITCO, and (B) represents the co-regulator groove in the presence of S07662. The core residues L1, I5 and L9 of NCoR ID2 on the liganded structures (cyan) are compared to the apo-structure (blue). The molecular surface of hCAR-LBD is shown in grey.The black circule highlight that S07662 liganded structure achieved imporved binding of NCoR ID2.*

The complementary binding of the three core residues (depicted in Appendix VI) into the groove may serve as an indication of strong interaction between hCAR and co-regulator peptides. The binding of ID2 peptide of NCoR onto the groove of CITCO and S07662 liganded structures are pictured in Figure 5. The positions of three core residues of peptide ID2 (L1, I5, L9) are also shown. Based on the above assumption, the S07662 liganded structure achieved improved binding of NCoR ID2 peptide. Different from what was seen in apo-structure, the peptide bound to the bottom of the groove of S07662 liganded structure, and the three core residues intensively interacted with the hydroponic groove (Fig 5B). However, in the presence of CITCO, the core residue L1 of ID2 peptide pointed outwards the groove (Fig 5). Hence the binding of ID2 peptide was probably weakened by CITCO.

The conformation of ID2 peptide of NCoR, as well as the positions of three core residues in the presence of other ligands is shown in Figure 6. Under the influence of inverse agonist, such as PK11195, androstanol and clomifene, the peptide appeared to bind deeply into the groove. This is in line with the inactive positions of H12 in the corresponding structures (Fig 4B). Celecoxib, meclizine, EE2, as suggested by the H12 movements, either enhanced

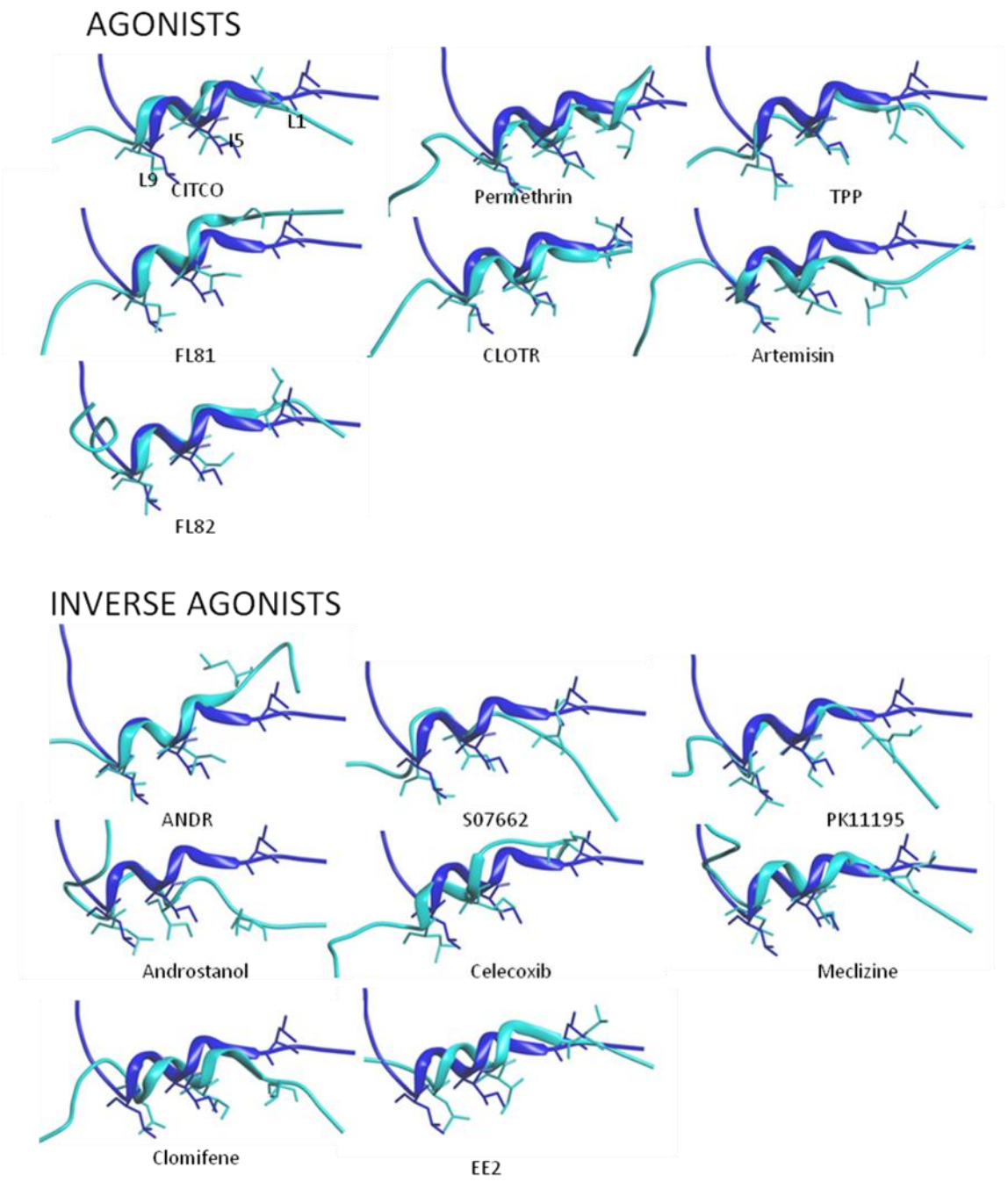

Figure 6. *The core residues L1, I5 and L9 of NCoR ID2 on the liganded structures (cyan), compared to the apo-structure (blue).*

the binding of NCoR ID2 to a small extent (meclizine) or highly resembled the binding of peptide in apo-structure (EE2 and celecoxib). The binding of peptide under the effect of agonists also differed from one to another. Permethrin, TPP, artemisin that shifted H12 to H10, indicated better

binding of the peptide. This can be explained by their weak or modest NCoR binding affinity: permethrin, TPP and artemisin that each increased 2.7, 2.7 and 2.6 fold of NCoR recruitment compared to apo in M2H assays (Table 1). CLOTR, which yielded 4.9 fold increases in NCoR recruitment, were also found to enhance the binding of the peptide. CITCO, FL81, and FL82, as potent agonists, maintained the active state of H12 and in the meantime, disfavored the binding of the co-repressor peptide ID2.

Notably, the N-terminal residues of the peptide ID2 of NCoR tended to move toward the bottom site of the groove in order to enhance the interaction between L1 and the groove, especially in the presence of inverse agonist. However, ANDR was the only exception compared to other inverse agonists. Since the ANDR liganded complex induced a clear shift of L1 to the opposite side of the peptide and hCAR interacting interface, the interaction between hCAR and the peptide ID2 might be weakened or disfavored.

The interaction between peptide ID1a of NCoR and hCAR-LBD groove was enhanced by PK11195 and androstanol (Appendix VII, Fig 1). However, other inverse agonists, including S07662, failed to do so. The homology model of ID1b, on the other hand, failed to bind to the groove in any liganded structures (Appendix VII, Fig 2). Compared to peptide ID2, it seems that the homology models of ID1a and ID1b acted in a very different way. Moreover, due to the fact that even strong inverse agonists conferred to active state in the presence of ID1a and ID1b, the structural changes in system III and IV are inconsistent with the experimental data (Table 1). In addition, the role of ligands in ID1 interaction remained unclear.

3.2.3 Differences between ID1 and ID2 motifs of co-repressor NCoR

Various degrees of peptide helical content perturbation was seen in the three NCoR simulation systems (II-IV). In system II, the 3-turn helical conformation of peptide ID2 was successfully maintained in 13 out of 15 liganded structures (Appendix VIII, Fig 1A). However, most of the liganded structures induced by peptide ID1a and peptide ID1b failed to keep such conformation (Appendix VIII, Fig 1B and 1C). Learning from previous studies on molecular determinants of NR-co-repressor interaction, and referring to the crystal structures of NCoR ID1 and SMRT IDs,

the 3-turn helical conformation is regarded as important for the repressive activity of NCoR and SMRT (Phelan et al., 2010; Xu et al., 2002; Perissi et al., 1999). Thus, the movements of H12 of hCAR-LBD (as described in section 3.2.1) and the peptide binding behavior onto the co-regulator groove (as described in section 3.2.2), and the high stability of 3-turn helical conformation of NCoR ID2 peptide revealed that ID2 is probably the interaction motifs that specifically interact with hCAR. Conversely, the peptides of ID1a and ID1b with disturbed helical conformation during the MD simulations, combing the structural changes of H12 and peptide binding in system III and system IV, may suggest weakened peptide interaction to the hCAR groove.

In fact, the arguments on whether ID1 and ID2 of NCoR utilize the same or the distinct mechanism to interact with NRs yet have no answer (Phelan et al., 2010). However, ID1 and ID2 act distinctively in this model. This may be caused by the inaccurate structures of these two motifs, which were generated by homology modeling using ID2 of SMRT as template. Since NCoR ID2 shares greater sequence similarity with SMRT ID2 (Fig 3), it is possible that in this study ID2 has more accurate peptide conformation than ID1a and ID1b. Yet it is not clear how such assumed accuracy (or inaccuracy of NCoR ID1a and ID1b) could influence the modeling systems. But it is certain that the sequence alignment for homology modeling has played an important role in the model performance. These differences between ID1a and ID1b modeling results implied that the core residues or even the flanking residues of the IDs should be maintained in certain conformation, in order to achieve strengthened NCoR binding affinity.

In addition, when comparing the ID2 binding mode of NCoR to that of SMRT (Jyrkkärinne et al., 2012), the three-turn helical conformations of both NCoR and SMRT peptides are maintained. Differently, the core residues of SMRT appeared at the same side and all interact with the co-regulator groove, whereas in NCoR they do not.

3.3 Molecular dynamics simulations of systems V-VII

3.3.1 Structural changes of hCAR-LBD induced by interaction with NR boxes of SRC-1

The low RMSD values in systems V-VII suggested that the complexes of hCAR have limited movements during MD simulations. APF values (Appendix IV, Fig 5 – Fig 7) suggested the stability of C-terminal residues was enhanced by agonists and slightly destabilized by inverse agonists. This is in agreement with the nature of ligands: (1) according to previous study (Windshügel et al., 2011), agonists are presumably to maintain or precede the active form of hCAR. Thus in this model, agonist-bound structure are obligated to fewer movements in C-terminus; (2) inverse agonists are ligands who potentiate the perturbation of the active form of hCAR. Instead of C-terminus stabilization, they intend to destabilize it.

In system V that included NR1 box of SRC-1, the helical conformation of HX appeared to be enhanced by agonists, while decreased by inverse agonists (Appendix V, Fig 5). However, H10 and H12 were very stable, despite that the bound ligand could be either an agonist or an inverse agonist. Importantly, the positions of H12 only changed subtly (Appendix IX, Fig 2). For most hCAR complexes, H12 was maintained in the active form (Fig 7). However, there was one exception: H12 in androstanol liganded structure moved towards H10. This implies that androstanol may inhibit the binding between hCAR and co-activator peptides. From above, there are only few differences that can be identified between the behavior of C-terminal residues (esp. the positions of H12) in the presence of agonists and inverse agonists. Accordingly, it would be difficult to analyze the effect of the ligand binding based on the performance of this MD system. The APF values in this system are lower than that of system I. This suggests that the peptide containing NR1 box may help to stabilize the active form of hCAR-LBD.

In system VI, there were no apparent changes in the helical stability of H10 and HX between agonists and inverse agonists liganded structures (Appendix V, Fig 6). However, inverse agonists such as clomifene, EE2, PK11195 and androstanol were found to slightly decreased the helical stability of H12 (Appendix V, Fig 6) and moved H12 out of the active conformation (Fig 7D and

Appendix IX, Fig 3B). This was not seen in the case of any agonists. The inverse agonist induced movements of H12 would probably impair the binding of co-activators. Based on above findings, one can assume that NR2 box of SRC-1 may be potentially important for the activity of hCAR in a ligand specific manner.

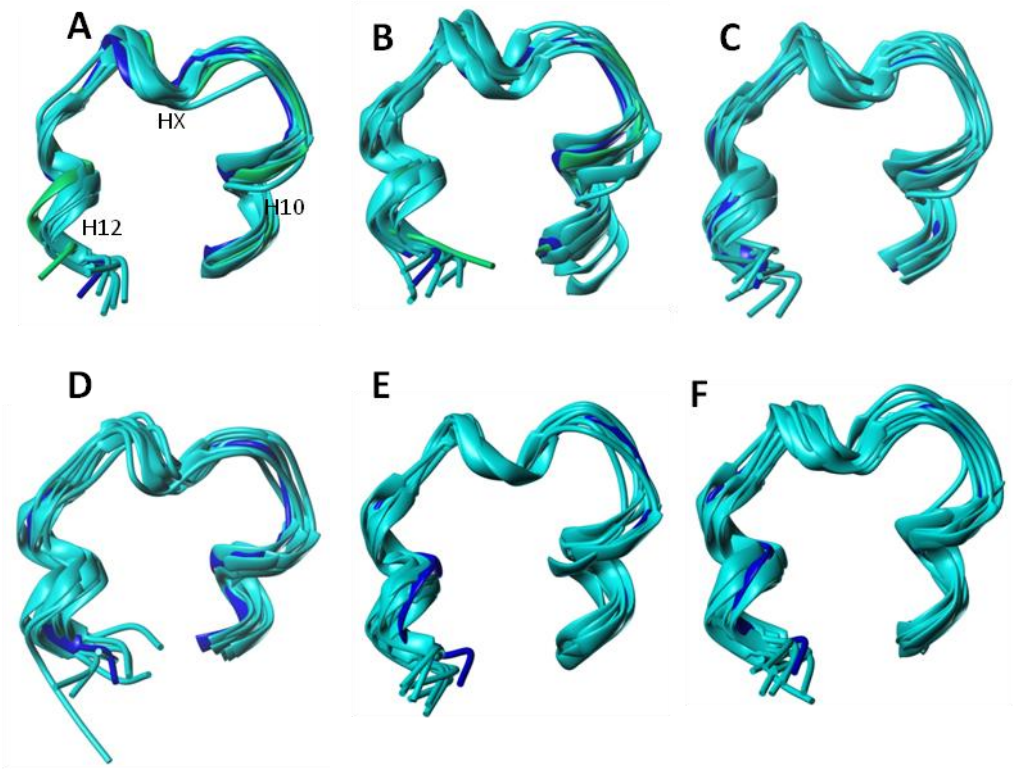

***Figure** 7. Positions of H12 in the final structures from the 10 ns MD simulations. (A) agonists and (B) inverse agonists liganded structures in system V; (C) agonists and (D) inverse agonists liganded structures in system VI; (E) agonists and (F) inverse agonists liganded structures in system VII. Apo (blue) is shown as a reference with each liganded structure (cyan). The green ribbon in (A) is FL81 and in (B) is androstanol.*

In system VII, the co-regulator peptide containing NR3 box of SRC-1 was included into hCAR complexes. Artemisin appeared to destabilize the helical content of both H10 and HX, while S07662 and meclizine appeared to drive C-terminus of H10 out of the helical conformation (Appendix V, Fig 7). In the presence of other ligands, the three helices at c-terminus were highly stabilized (Appendix V, Fig 7). The active positions of H12 were maintained and exhibited no clear differences from one ligand to another (Appendix IX, Fig 4).

3.3.2 Binding of SRC-1 NR boxes onto hCAR co-regulator groove

In systems V-VII, the co-activator groove is formed by H3, H4 and H12 of hCAR-LBD. In the apo-structure of these systems, H12 remained in the active position as before MD simulations and the peptides from SRC-1 were stabilized in 2-helical conformation with only subtle movements (Appendix VI, Fig 2).

The binding of NR boxes of SRC-1 can be affected by ligand binding. The interaction between peptide containing NR1 box of SRC-1 and hCAR-LBD is enhanced by both CITCO and S07662 compared to apo-structure (Fig 8A and 8B). But in system VI, peptide containing NR2 box moved away from the groove of S07662 bound hCAR-LBD complex (Fig 8D). In system VII, the binding of CITCO and S07662 had no significant influences on the binding of peptide containing NR3 box with the C-terminal residues of the peptide move slightly (Fig 8E and 8F).

The positions of core residues in co-regulator interaction motifs were evaluated for each liganded structure in the presence of NR1-3 boxes (Appendix VII, Fig 3 – Fig 5). Based on the positions of co-regulator core residues, the binding in liganded structure were compared to apo. In system V, it seemed that both agonists (CITCO, TPP) and inverse agonists (S07662, androstanol, EE2, meclizine) were able to strengthen the interaction between peptide containing NR1 box and hCAR-LBD (Appendix VII, Fig 3). In system VI, agonists CLOTR and artemisin enhanced the binding of peptide containing NR2 box, while agonists TPP, FL82 and inverse agonist S07662 tended to destabilize the peptide and weaken the binding of peptides (Appendix VII, Fig 4). In system VII, 2 agonists (CLOTR, and FL82) and 4 inverse agonists (ANDR, androstanol, celecoxib and PK11195) enhanced the binding of NR3 peptide (Appendix VII, Fig 5). Based on above observations, the binding of co-activator peptide not only depends on the bound ligand, but also rely on the type or the flanking sequences of the peptides themselves.

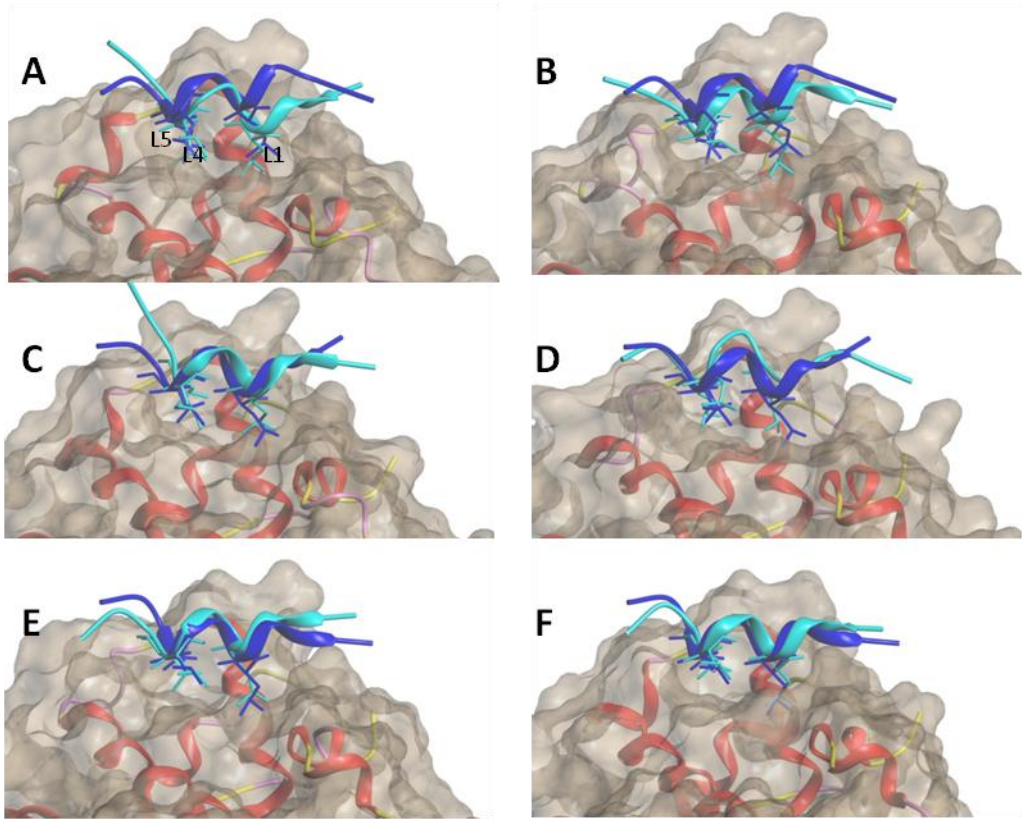

Figure 8. *The co-regulator groove of hCAR with peptides from co-activator SRC-1. The left column compares the binding of (A) NR1, (C) NR2 and (E) NR3 peptide on CITCO liganded structures to apo-structure. The right column compares the binding of (B) NR1, (D) NR2 and (F) NR3 peptide on S07662 liganded structures to apo-structure. The molecular surface of hCAR-LBD is shown in grey. SRC-1 peptides from apo-structure is shown in blue and change into cyan in liganded structure.*

3.3.3 Differences between NR1, NR2 and NR3 boxes of co-activator SRC-1

Based on the theory of 'mouse-trap' model of NR ligand binding (Savkur and Burris., 2004) and the crystal structures of SRC-1 peptides, the strong interaction between NR boxes and co-regulator groove relies on the relative position of H12 to NR box (Windshügel et al., 2005). In systems V-VII, H12 was maintained in the active position (see section 3.3.1). The peptides containing NR boxes were stabilized in 2-turn helical conformation (Appendix V, Fig 5 - Fig 7) with few movements compared to apo-structure (Appendix VII, Fig 3 - Fig 5). It seems that the three NR boxes all facilitate the interaction of SRC1 peptides with hCAR-LBD.

Different from system V and VII, the binding of peptide with hCAR-LBD was significantly different between agonist and inverse agonist liganded structures in system VI. First, the active position of H12 was maintained by agonists, whereas inverse agonists moved H12 toward H10 (see section 3.3.1). Second, NR2 peptide in system VI was slightly destabilized (HC% > 74%) by many ligands (Appendix VIII, Fig 2B). In particular, K688 and I689 that compose the N-terminus of NR2 helix were released from helical conformation in 2 out of 7 agonists bound structures (FL81 and FL82) and 4 out of 8 inverse bound structures (S07662, ANDR, EE2, celecoxib). Since the helical conformations of NR boxes were destabilized, the peptide binding affinity would probably be weakened, especially in the presence of inverse agonist.

On a minor note, CITCO bound structure in the presence of NR3 peptide of SRC-1 yielded 2.5 Å RMSD at the time point of 6.8 ns (Appendix II, Fig 7A). This value is one of the greatest fluctuations within systems V-VII. Since CITCO obtained less favorable ligand-protein interaction energy in system VII (see section 3.8), it is suspected that the fluctuation revealed by RMSD values may lead to the changes of ligand-protein interaction energy.

3.4 Molecular dynamics simulations of system VIII-IX

3.4.1 Structural changes of hCAR-LBD induced by interaction with NR boxes of TRAP

The RMSD values in systems VIII-IX are within the range of 1 - 2 Å. These values suggest that the peptides from TRAP have stabilized the protein complexes during MD simulations. As suggested by APF values (Appendix IV, Fig 8 – Fig 9), a few ligands tended to destabilize the C-terminus of hCAR-LBD. These ligands include TPP (APF of residue 337 > 2 Å), CITCO (APF of residue 337 > 1.4 Å), clomifene (APF of residue 346 > 1 Å) in system VIII and PK11195 (APF of residue 337 > 1.9 Å) in system IX. However, based on the low APF values and high HC % values (Appendix V, Fig 8 - 9) in the C-terminus of most liganded structures, TRAP peptides were regarded as important to stabilize the C-terminus of hCAR. In this regard, the behaviors of TRAP peptides resemble the SRC-1 peptides, but differ from NCoR peptides.

Figure 9 illustrates the positions of C-terminal residues in both systems (see also Appendix IX, Fig 5 – Fig 6). In system VIII, agonists and inverse agonists were able to maintain H12 in active position. Differently, ligands in system IX tended to move H12 upwards. Moreover, in system IX, inverse agonists tended to shift H12 toward H10 to a small extent, while agonist did not. However, since the *in vitro* data of the recruitment of TRAP peptides into hCAR are not available, it is difficult to interpret the consequences on hCAR activity due to movements of H12 and other C-terminal residues.

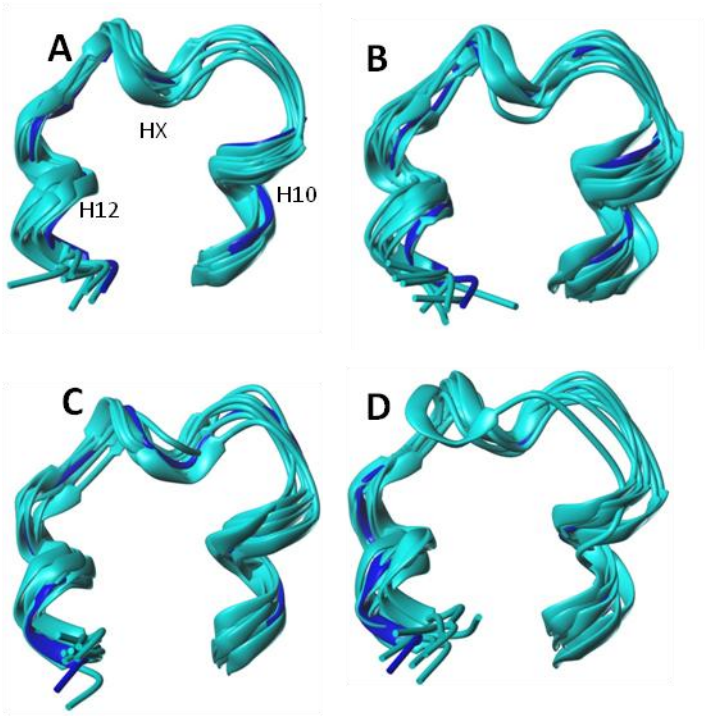

Figure 9. *Positions of H12 in the final structures from the 10 ns MD simulations. (A) agonists and (B) inverse agonists liganded structures in system VIII; (C) agonists and (D) inverse agonists liganded structures in system IX. Apo (blue) is shown as a reference with each liganded structure (cyan).*

3.4.2 Binding of TRAP NR boxes onto hCAR co-regulator groove

The TRAP peptides bound to the co-regulator groove that formed by residues from H3, H4 and H12 of hCAR-LBD (Appendix VI, Fig 3). The two-turn helical conformation of TRAP was

maintained in both apo-structures. In comparison to apo, NR1 departed away from the co-regulator groove in the presence of CITCO (Fig 10A), while S07662 seemed to neither enhance nor weaken the binding of NR1 box (Fig 10B). However, peptide containing NR2 in CITCO and S07662 liganded structures remained in the same position as apo (Fig 10C and 10D). Based on the positions of core residues of peptides, the binding of two NR boxes of TRAP in the presence of diverse ligands were analyzed. It has been found that the peptide containing NR1 tended to depart away from groove in 11 out of 15 liganded structures (5 agonists: CITCO, permethrin, TPP, FL81and artemisin; 6 inverse agonists: ANDR, PK11195, androstanol, celecoxib, meclizine and EE2) (Fig 11A and 11B). By contrast, in system IX, the core-residues of NR2 peptide remained unchanged compared to that of apo (Fig 11C and 11D). For both systems, there were no clear differences in the binding of TRAP between agonists and inverse agonists liganded structures.

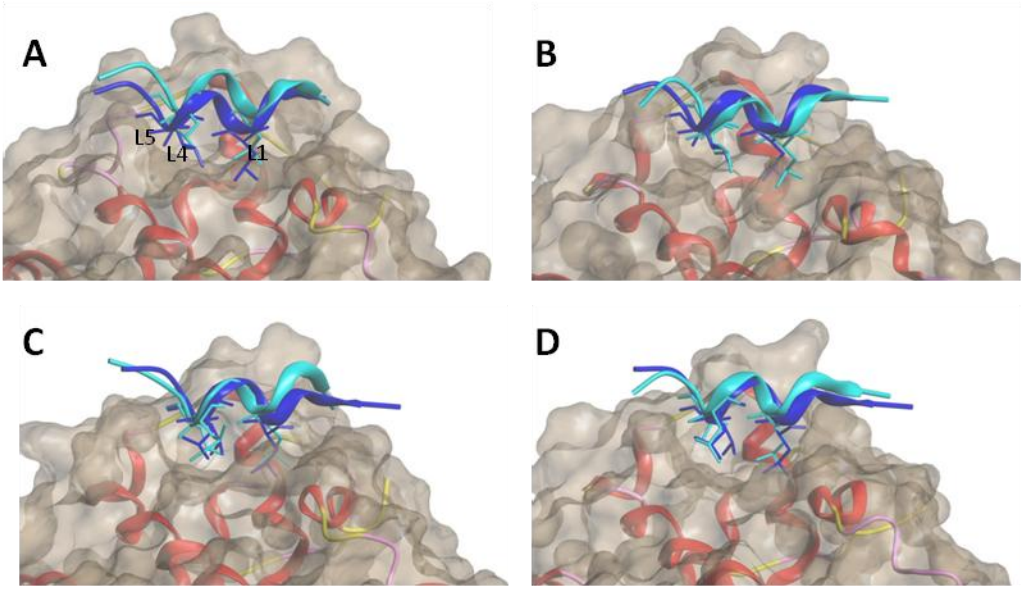

Figure 10. *The co-regulator groove of hCAR with TRAP. The left column compares the binding of (A) NR1 and (C) NR2 peptide on CITCO liganded structures to apo-structure. The right column compares the binding of (B) NR1 and (D) NR2 peptide on S07662 liganded structures to apo-structure. The molecular surface of hCAR-LBD is shown in grey. SRC-1 peptides from apo-structure is shown in blue and change into cyan in liganded structure.*

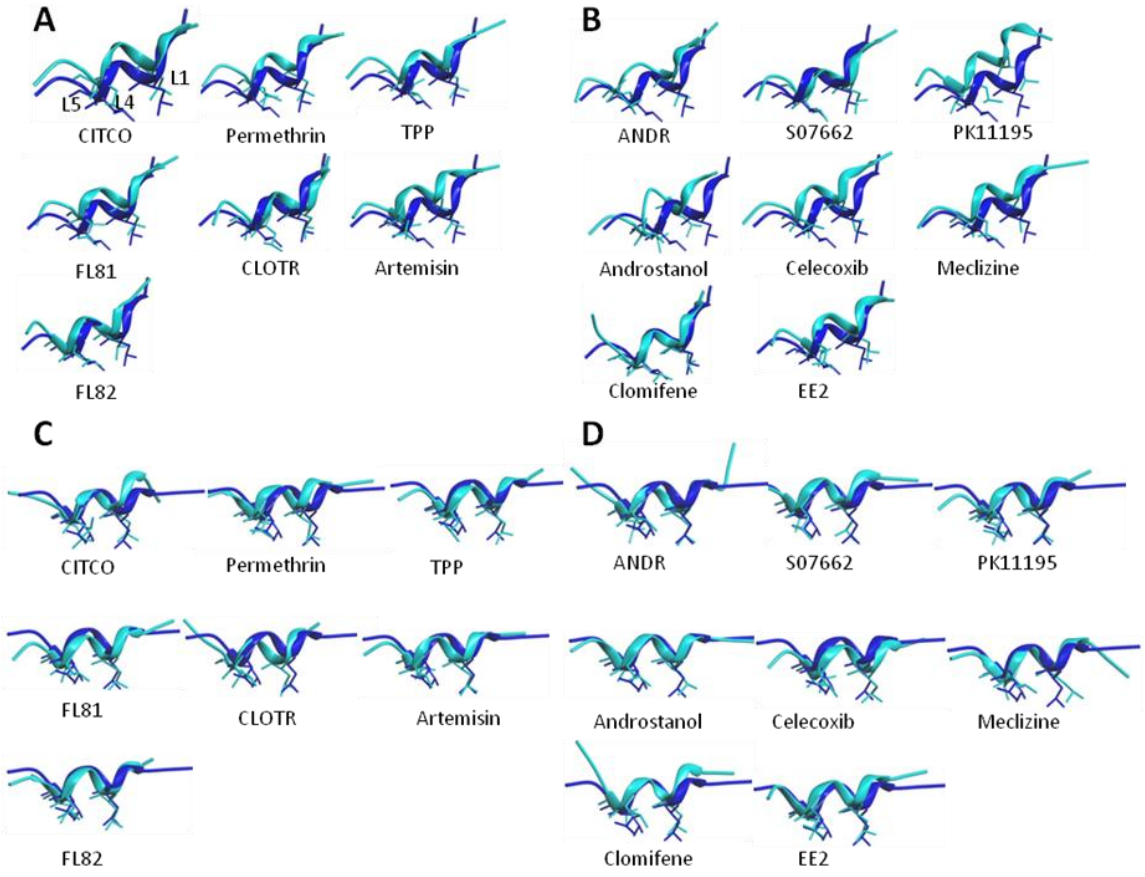

Figure 11. *The core residues L1, L4 and L5 of TRAP NR1 on the (A) agonist and (B) inverse agonist liganded structures compared to the apo-structure (blue). The core residues L1, L4 and L5 of TRAP NR2 on the (C) agonist and (D) inverse agonist liganded structures compared to the apo-structure (blue).*

3.4.3 Differences between NR1 and NR2 boxes of mediator TRAP

Based on the analysis regarding systems VIII and IX, several structural features that involved NR1 and NR2 of TRAP were evident. First, the active position of H12 was maintained in both systems; the helical stability of H12 was enhanced by the two NR boxes in comparison to system I. Second, the 2-turn helical conformation of TRAP peptides was maintained in both apo and liganded structures (Appendix VIII, Fig 3). Third, NR1 box tended to depart away from hCAR as compared to apo, while NR2 peptide tended to maintain in the same position as apo.

Because the *in vitro* activity of TRAP regarding hCAR interaction is currently unavailable, the role of NR1 and NR2 in the TRAP-dependent hCAR regulation remains to be solved. Based on this study, the distinct binding mode of NR1 and NR2 suggested that NR2 box would probably interact with hCAR with higher preference than NR1 box. It has been reported that VDR can preferentially recruit NR2 box of TRAP (Rachez et al., 1999), thus this preference might be maintained for its close relative, hCAR.

3.5 Changes in the stability of HX

HX is a four-residue helical structure that connects H10 to H12. HX is known for its rigidity and potential importance on hCAR constitutive activity (Xu et al., 2004). Nettles et al (2005) further suggested that HX plays an important role in the allosteric communication between dimeric partners. And on the basis of such communication, the activity of NRs can be finely tuned. Moreover, Wright et al (2011) have proved that HX dynamics is critical for the activity of murine CAR. This may also hold true for hCAR. In the data of this study, peptides from co-activator SRC-1 and mediator TRAP were observed to maintain the high helical content of HX in the presence of most ligands (Appendix X). By contrast, the three peptides from NCoR appeared to destabilize the helical content of HX, especially in the presence of inverse agonists (Appendix X).

Helical content stability of HX in all simulation systems was dependent both on ligands and co-regulator peptides. In the absence of co-regulator peptide, the inverse agonists were likely to stabilize HX, while agonists were not (Fig 12). But in the case of the many co-regulator peptides (ID2, ID1a and ID1b of NCoR, NR1 box of SRC-1 and NR1-2 boxes of TRAP), HX was stabilized by agonists to a greater extent than by inverse agonists. It is noteworthy that in system V, which contained NR1 box of SRC-1, the average HC % value of agonists is up to 78.22%, which is 87% higher compared to HC % of inverse agonists. However, SRC-1 NR2 and 3 exhibited no major differences between agonists and inverse agonists bound structures.

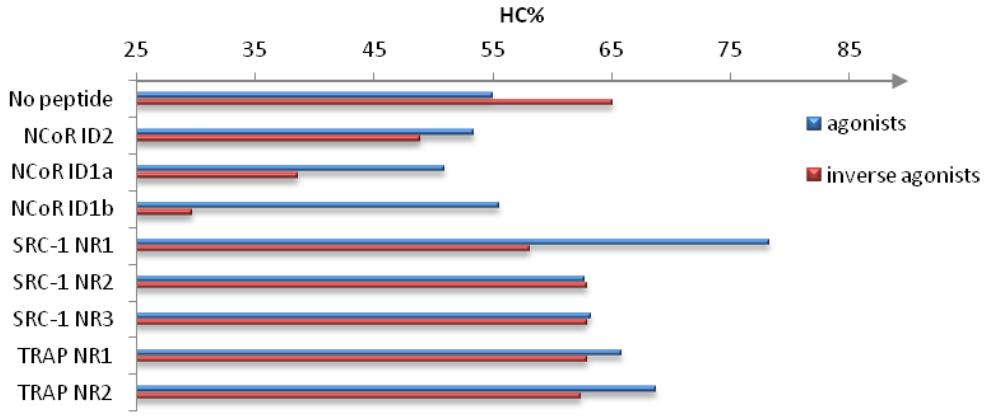

Figure 12. *Helical content (HC %) of the HX helical conformation during MD simulations for 9 MD systems. The average value of HC % is compared between the agonists and inverse agonists liganded structures. Since the in vitro data shows that clomifene, meclizine and celecoxib are not able to recruit NCoR, these three ligands were excluded for calculating the average HC % values in the ligand structures of inverse agonists.*

3.6 Changes in the stability of H2-H3 loop

The APF values suggested that the loop connecting H2 to H3 (aa. 143-154) is probably the most flexible part of hCAR-LBD (Appendix II). In systems I, III and VIII, the loop appeared to be stabilized in apo, but moved more in the presence of ligands, especially inverse agonists (Appendix XI, Fig 1, Fig 3 and Fig 8). In contrast, other systems were seen to achieve most flexible loop in the absence of ligand (apo). Thus, ligand can help to stabilize or destabilize this loop under different context. Moreover, agonists appeared to have few effects on this loop, while inverse agonists tended to destabilize it. This was also seen in the modeling studies with SMRT and hCAR (Jyrkkärinne et al., 2012).

The loop changes in apo and four liganded structures in systems II-IX were compared to system I (Fig 13). First, in apo-structures, most peptides contributed to the destabilization of this loop with the exception of NCoR ID1a in system III and TRAP NR1 in system VIII. Second, upon the binding of strong agonists, such as CITCO and permethrin, the loop appeared to be stabilized by most co-regulator peptides (Fig 13B and 13C). Third, in case of strong inverse agonists, the stability of this loop seemed to be reduced by most co-regulator peptides: 5 out of 8 tested

peptides (SRC-1 NR2 and 3, NCoR ID1 and 2b, TRAP NR1) in S07662 (Fig 13D) and 6 out of 8 (SRC-1 NR1, 2 and 3, NCoR ID1a, TRAP NR1 and 2) in PK11195 (Fig 13E). From above, one can assume that the loop changes rely on the binding of co-regulators and the nature of ligand.

The loop is in a position that has few or no direct interaction with ligand or LBP. However, it may serve as one of the ligand entry sites (Jyrkkärinne et al., 2012; Renaud et al., 1995; Martinez et al., 2005). The large fluctuation of the loop would probably result in the opening of the LBP. For instance, celecoxib, clomifene, meclizine and permethrin in system I, which had large fluctuation in H2-H3 loop region, all appeared to have open cavity (Fig 14).

3.7 Changes in the shape and volume of the ligand binding pocket

Ligands bind to the LBP of hCAR mainly through hydrophobic interaction. The pocket is known for its elasticity and the ability to accommodate a wide range of ligands. In this study, the LBP over 9 simulation systems were checked. Both the ligand and the co-regulator peptides were found to induce the changes of either the shape or the volume of the LBP.

In each system, the apo-structure usually had the smallest volume of cavity (Table 3). It seems that the cavity starts to expand when the ligand enters inside. Supportively, in system II, clomifene has achieved a close cavity (1027 $Å^3$), which is 110% larger than the cavity of apo (487 $Å^3$) and 65% larger than that of FL82 (624 $Å^3$). Like other ligands, CITCO also expanded the volume of the cavity in most MD systems (systems I-IV and VI-IX). Such as in system VII, CITCO achieved a 58% larger cavity than apo (CITCO: 709 $Å^3$; apo: 450 $Å^3$). However, the LBP of CITCO (539 $Å^3$) is 10% smaller than the cavity volume of apo (600 $Å^3$) in system V. Since CITCO has high MW, the shrinkage of the cavity was most likely caused by the enhanced interaction between CITCO and the LBP residues. Potentially, this may be related to the strong activation potential of SRC-1 NR1 box and the strong agonism of CTICO.

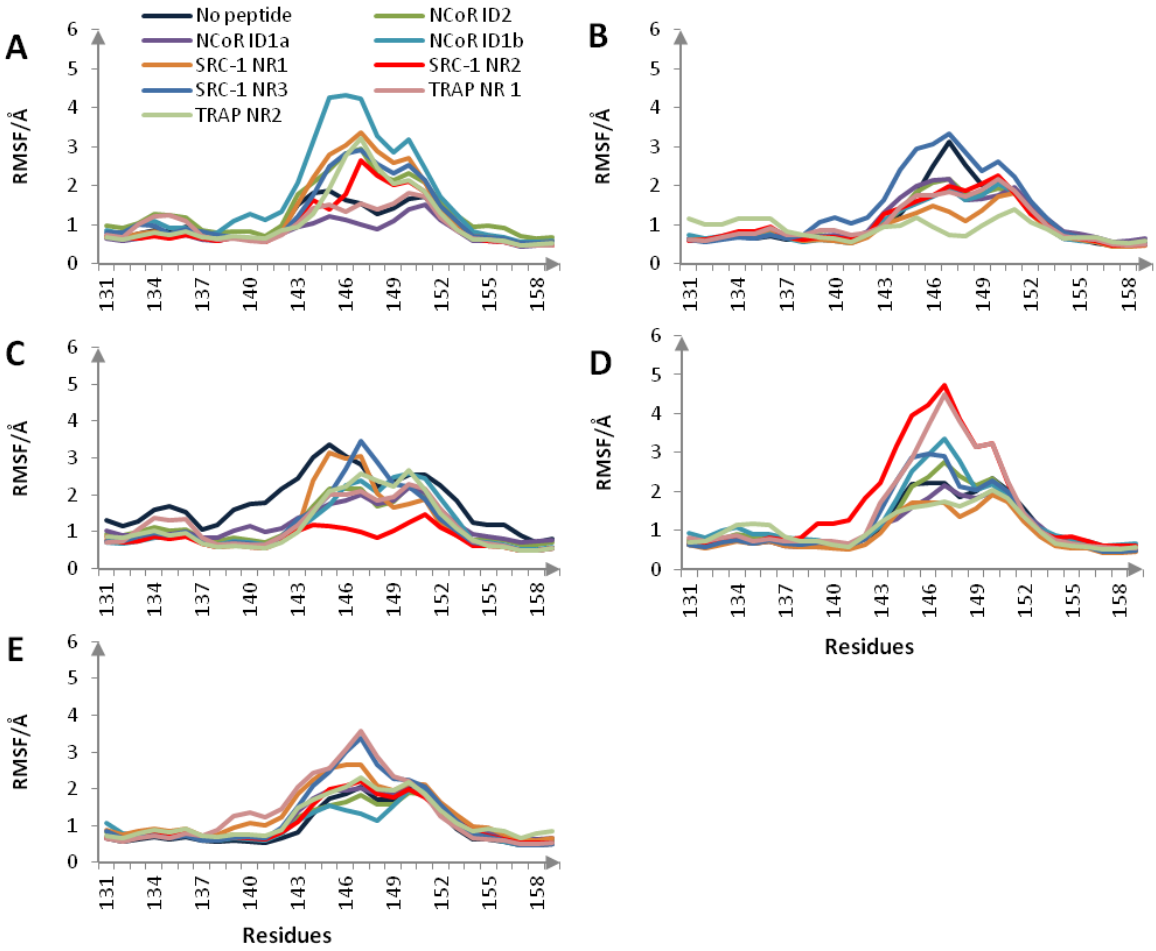

Figure 13. *APF values of the backbone atoms of hCAR-LBD during the 10 ns MD simulations. H2-H3 loop in (A) apo-structure and in the liganded structures of (B) CITCO, (C) permethrin, (D) S07662, and (E) PK11195.*

There are in total 14 pockets which opened in the final structures from 10 ns of MD simulations (Table 3). They are all from the liganded structures: 5 in system I (permethrin, ANDR, clomifene, celecoxib and meclizine), 2 in system II (FL81 and artemisin), 2 in system III (artemisin and clomifene), one in system VII (clomifene), 3 in system VIII (FL81, EE2 and meclizine) and one in system IX (meclizine). Since the unstable LBP will ultimately affect the stability of the overall structure, and destroy the structural basis for the interaction of co-regulators or transcriptional machines, the opening of the cavities has most probably great effect on the function of hCAR.

Table 3. *The volume of the ligand binding pocket in 9 MD simulation systems, the unit for the volume is* $Å^3$.

Ligand[a]	System								
	I	II	III	IV	V	VI	VII	VIII	IX
APO	471	487	388	541	600	413	450	437	441
CITCO*	609	722	769	716	539	682	709	661	741
FL82*	599	624	632	557	604	712	575	635	576
FL81*	652	n.a.(1)	702	670	657	625	670	n.a.(1)	672
Permethrin*	n.a.(1)	896	814	722	795	787	772	787	777
CLOTR*	657	686	720	793	792	683	791	683	699
TPP*	716	691	647	674	649	721	767	589	627
Artemisin*	624	n.a.(2)	n.a.(2)	528	556	684	589	646	564
EE2**	710	748	645	631	690	717	704	n.a.(2)	716
Androstanol**	705	626	717	696	736	794	669	733	690
ANDR**	n.a.(2)	673	667	766	643	652	716	639	697
PK11195**	665	699	790	734	685	806	769	764	946
S07662**	577	709	669	600	651	603	636	636	618
Clomifene**	n.a.(1)	1027	n.a.(2)	900	831	790	n.a.(1)	840	798
Celecoxib**	n.a.(2)	721	742	703	677	619	763	844	585
Meclizine**	n.a.(1)	777	777	795	679	788	873	n.a.(1)	n.a.(1)

[a]*agonist*, inverse agonist***

n.a. states the ligand binding pocket is open and the volume is thus not measurable. The number in bracket represents the sites where the pocket opens: (1) the H2-H3 loop region; (2) near H12.

In general, there were two sites where the cavity opened: (1) the H2-H3 loop region, such as FL81 in system II (Fig 14); (2) with six structures near H12, ANDR and celecoxib in system I, artemisin in system II, artemisin and clomifene in system III, and EE2 in system VIII. In case of (2), the opening site extended to the surface of hCAR-LBD and therefore probably occupied the place for co-regulator binding, thus it is suspected that the interaction between the co-regulator peptide and hCAR would be greatly weakened.

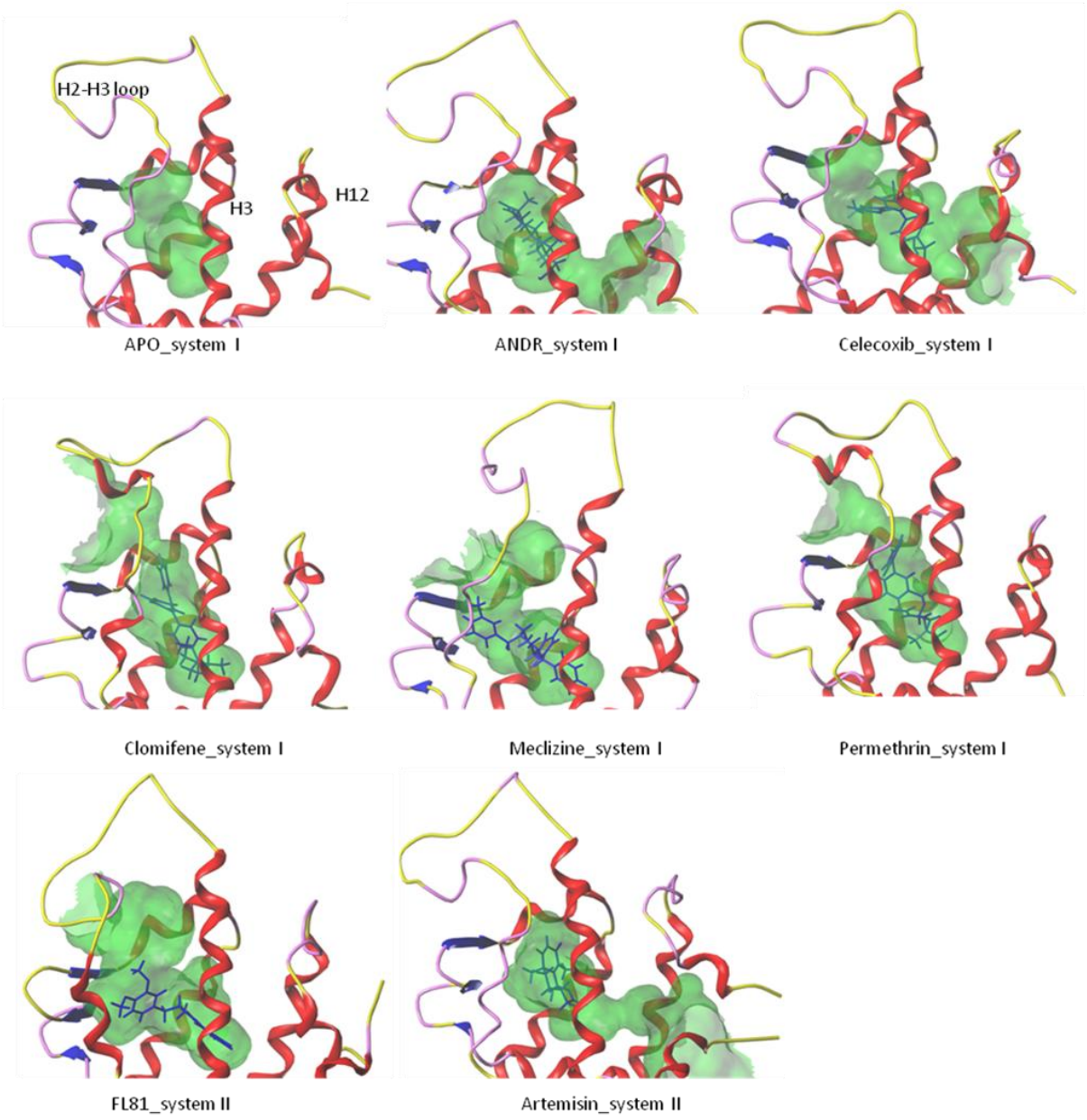

Figure 14. *The opening of the ligand binding pockets of hCAR-LBD after 10 ns MD simulations: ANDR, celecoxib, clomifene, meclizine and permethrin liganded structures in system I, and FL81 and artemisin liganded structures in system II.*

3.8 MM-PBSA ligand-protein interaction energy

Protein-ligand interaction energy ($E_{protein\text{-}ligand}$) can be used to compare the binding affinities of different ligands. Since the co-regulator peptides have impact on the shape of the LBP, as well as overall structure, the binding of co-regulator peptides can be regarded as indirectly related to these protein-ligand interaction energy values. In practice, the interpretation of these changes can be demanding due to several reasons: (1) when calculating the interaction energy, the entropy calculation was left out in the convenience of computing time. Thus the calculated values may have discrepancy with the real energy values (Kongsted et al., 2009); (2) LBP is highly flexible, not all the structural changes of NRs are predictable upon the binding of diverse ligands (Jin and Li., 2010). However, the energy values may provide supplementary information for further studies.

Küblbeck et al (2011a) have reported a good correlation between *in vitro* activities and protein-agonist interaction energy from the 1 ns MD simulations which exclude co-regulator peptides. However, in this study, there was not that good correlation between the calculated interaction energy and experimental data. It is true that the strong agonists correlate to favorable interaction energy, such as CITCO, permethrin and FL81(Appendix XII). The less potent agonists, such as CLOTR, artemisin and TPP have less favorable interaction energy. The major discrepancy was with FL82: though it is a strong agonist, it had less favorable calculated interaction energy. On the other hand, within the range of inverse agonists, the interaction energy is not relevant to the potency of antagonism, but depends on the co-regulator peptides and other factors, such as molecular size. It is possible that the favorable interaction energies of clomifene and meclizine are due to their high MW and many hydrophobic interactions with residues from LBP.

For each simulation, E_{1ns} and E_{9ns} values were calculated. E_{1ns} represents the ligand-protein binding energy at 1 ns and accordingly, E_{9ns} represents the energy at 9 ns of MD simulations. The differences (E_{1ns}-E_{9ns}) can indicate that whether the interaction between ligand and the LBP was strengthened (E_{1ns}-$E_{9ns} > 0$) or weakened (E_{1ns}-$E_{9ns} < 0$) during the MD simulations. The major energy deviations were observed in SRC-1 NR3 complexed structures (Fig 15). For instance, the

binding energy of TPP increased by 11 kcal/mol, while with clomifene (-9 kcal/mol) and meclizine (-4 kcal/mol) the changes were to the opposite. In addition to SRC-1 NR3, with NCoR ID1a and TRAP NR1, there were a few larger changes during the MD simulations; with other peptides, the interaction energies did not change much.

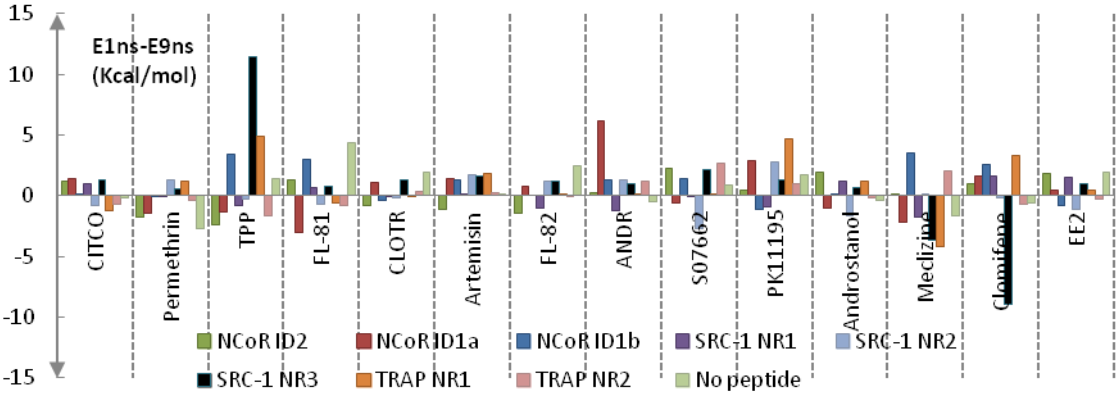

Figure 15. *Energy differences (E_{1ns}-E_{9ns}) (celecoxib was not calculated due to software deficiency) for each ligands in 9 MD systems. When the value is positive ($E_{1ns} > E_{9ns}$), the ligand binding is suggested to be enhanced during the process of MD simulations. But when the value is negative, the ligand binding suggested to become less favorable.*

To further validate the role of co-regulator peptides, the energy differences between co-regulator peptide-containing systems (II to IX) and system I (the system that contains no peptides and services as a reference with each peptide-containing system) were calculated (E_I -E_{II-IX}). When the value is positive, the co-regulator peptide is proposed to have enhanced the ligand binding, and vice versa. As shown in Fig 16, SRC-1 NR-3 and NCoR ID1a are responsible for the major changes. In the presence of SRC-1 NR3, great energy bonus was achieved by TPP (10 kcal/mol) and CLOTR (6 kcal/mol), but CITCO, clomifene and meclizine dropped down significantly by -11 kcal/mol, -9 kcal/mol, -6 kcal/mol, respectively. Surprisingly, NCoR ID1a encouraged the ligand binding of each ligand; the energy bonus was within the range of 9 kcal/mol (ANDR) to 1.45 kcal/mol (EE2).

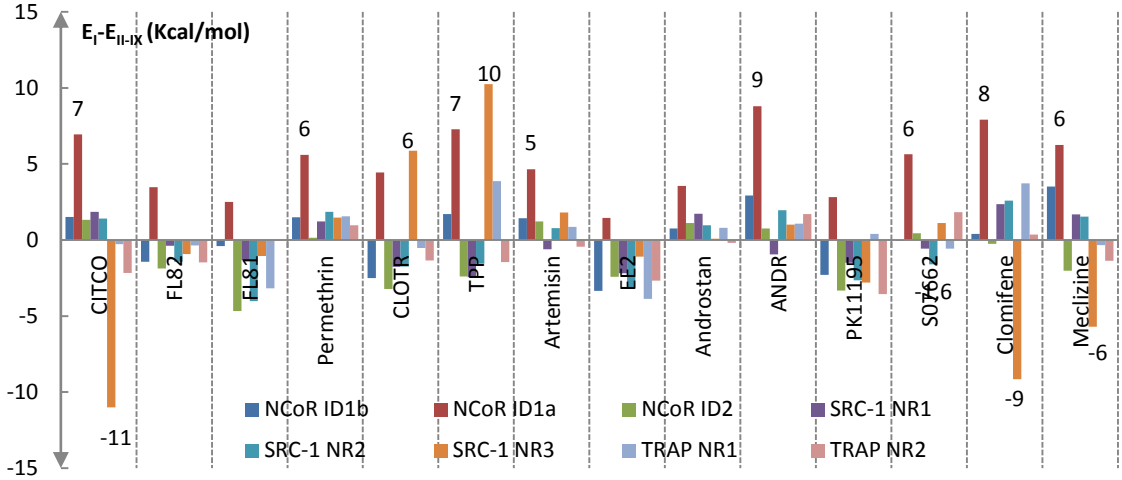

Figure 16. *The energy differences (E_I-E_{II-IX}) that calculated by energy values of the comparison group, system I (E_I) deduct that of systems II-IX (E_{II-IX}). The energy values are from E_{9ns} of each MD simulation. For example, the energy value of CITCO in system I at 9th ns of MD (-46.73 Kcal/mol) deduct the energy value of CITCO in the presence of SRC-1 NR3 (-35.7 Kcal/mol), yielded -11 Kcal/mol energy differences. When value is positive, the ligand-protein binding energy is suggested to be more favorable in the presence of specific co-regulator peptides. But when the value is negative, the existing co-regulator peptides might destabilize the interaction between ligand and LBP of hCAR-LBD.*

4 Conclusions

This study analyzed the preference of multiple co-regulator motifs to interact with hCAR. 9 MD simulation systems were constructed, with special interest in the structural changes of hCAR-LBD during the interaction with co-regulator motifs and ligands. These tested motifs included 3 classes, namely (1) ID1 (including ID1a and ID1b) and ID2 of co-repressor NCoR; (2) NR1-3 boxes of co-activator SRC-1; (3) NR1-2 boxes of TRAP. The ligands included 7 agonists and 8 inverse agonists. The stability analysis suggested that these systems are stable enough to simulate the structural changes of hCAR complexes during the interaction. Moreover, the modeled structure changes are comparable with experimental data for MD systems with ID2 of NCoR, NR1 and NR2 of SRC-1, respectively. However, due to the complexity of the *in vitro* and *in vivo* conditions, further studies are needed to verify and improve the model reliability.

Based on the results of this study, in co-regulator-motif class (1), the binding preference of ID2 seemed to be higher than ID1. This was deducted from several observations: (1) under the influence of ID2, H12 moved out of the active position in the presence of inverse agonists; (2) peptide containing ID2 was stabilized in 3-turn helical conformation; (3) the binding was enhanced between peptide and hCAR-LBD by the approaching of the core residues of ID2 towards the groove. In addition, the two homology models of ID1 (ID1a and ID1b) that were based on alternative sequence alignments, exhibited distinct structural features. Therefore, it would be interesting to discuss how the different structures of co-regulator motifs could relate to their activities; which one is more correct alignment.

The structural changes intrigued by NR boxes of SRC-1, co-regulator-motif class (2), were less pronounced compared to that of co-regulator-motif class (1). These NR boxes tended to maintain the active state of H12 of hCAR-LBD. However, among these NR boxes, the ligand-protein interaction energy was less favorable in the presence of NR3 compared with NR1 and NR2. Therefore, the interaction of NR1 and NR2 with hCAR-LBD is probably stronger than with NR3. Several features in the interactions involving NR1 and NR2 were evident: (1) NR1 was found to enhance the stability of HX and this is in line with the study of Wright et al (2011), which proved the importance of HX stability for hCAR activation upon agonist binding; (2) NR2 induced clear differences between liganded structures of agonists and inverse agonists: H12 remained in active

position in the presence of agonist, but moved out of the active position in the presence of inverse agonists. Such differences were not seen in the case of NR1 and NR3.

In co-regulator-motif class (3), the NR1 motif of TRAP may be not favored in the interaction with hCAR because the peptide was seen to depart away from the co-regulator groove. TRAP NR2, on the other hand, may interact with hCAR in a ligand-independent manner, since NR2 bound to the groove of liganded structures in similar manner as in the apo-structure.

However, the major deficiency in this study probably was that all the peptides except one (SRC-1 NR2) were based on the homology modeling. Thus the modeled peptides may disagree with the real structures and influence the performance of this model. For instance, the crystal structure of NCoR ID1 peptide that has been co-crystallized with Rev-erba (Phelan et al., 2010) is dissimilar to the homology models in this study. There are also many ligands that bind to hCAR with low affinity, which bring difficulties to rationalize the structural changes of hCAR caused by of ligand binding. The solving of additional x-ray crystal structures of hCAR and co-regulator peptides, the finding of more potent ligands and the acquiring of *in vitro* data for more hCAR/co-regulator interactions, would enable the further validation of the model.

5 Acknowledgements

This work was conducted under the supervision of Ph.D. Johanna Jyrkkärinne and Ph.D. Tuomo Laitinen from School of Pharmacy, University of Eastern Finland. I would like to extend my grateful thanks to both of them for their guidance on my research. Ph.D. Tuomo Laitinen and Ph.D. Maija Lahtela-Kakkonen are thanked for reviewing this thesis. I would also like to thank my colleagues working in the modeling group of Prof.Antti Poso. They have brought so much joy and laughter to me during the hard working.

I would like to thank Professor Tapani Pakkanen for his care on my study during the last two years. I also want to thank all of my friends for cheering me up when I was lost in the endless-like modeling, data processing and thesis writing. Especially, I have to thank my family, Jinnan Gong, who has been helping with the linguistic consulting. It's been a long journey and I couldn't have done it without above supports. Thank you!

6 References

Aagaard M. M., Siersbaek R., Mandrup S. Molecular basis for gene-specific transactivation by nuclear receptors. *Biochim Biophys Acta.* **2011,** *1812*, 824–35.

Aranda, A.; Pascual, A. Nuclear hormone receptors and gene expression *Physiol. Rev.* **2001**, *81*, 1269-1304.

Baes, M.; Gulick, T.; Choi, H. S.; Martinoli, M. G.; Simha, D.; Moore, D. D. A new orphan member of the nuclear hormone receptor superfamily that interacts with a subset of retinoic acid response elements *Mol. Cell. Biol.* **1994**, *14*, 1544-1552.

Bain, D. L.; Heneghan, A. F.; Connaghan-Jones, K. D.; Miura, M. T. Nuclear receptor structure: implications for function *Annu. Rev. Physiol.* **2007**, *69*, 201-220.

Berman, H. M.; Westbrook, J.; Feng, Z.; Gilliland, G.; Bhat, T. N.; Weissig, H.; Shindyalov, I. N.; Bourne, P. E. The Protein Data Bank *Nucleic Acids Res.* **2000**, *28*, 235-242.

Bourguet, W.; Germain, P.; Gronemeyer, H. Nuclear receptor ligand-binding domains: three-dimensional structures, molecular interactions and pharmacological implications *Trends Pharmacol. Sci.* **2000**, *21*, 381-388.

Bramlett, K. S.; Wu, Y., Burris T.P. Ligands Specify Coactivator Nuclear Receptor (NR) Box Affinity for Estrogen Receptor Subtypes *Molecular Endocrinology* **2001**, *15*, 909-922.

Case, D. A.; Cheatham, T. E. III.; Darden, T.; Gohlke, H.; Luo, R.; Merz, K. M. Jr.; Onufriev, A.; Simmerling, C.; Wang, B.; Woods, R. The Amber Biomolecular Simulation Programs. *J. Computat. Chem.* **2005**, *26*, 1668-1688.

Case, D. A.; Darden, T. A.; Cheatham, T. E. III.; Simmerling, C. L.; Wang, J.; Duke, R. E.; Luo, R.; Crowley, M.; Walker, R. C.; Zhang, W.; Merz, K. M.; Wang, B.; Hayik, S.; Roitberg, A.; Seabra, G.; Kolossváry, I.; Wong, K. F.; Paesani, F.; Vanicek, J.; Wu, X.; Brozell, S. R.; Steinbrecher, T.; Gohlke, H.; Yang, L.; Tan, C.; Mongan, J.; Hornak, V.; Cui, G.; Mathews, D. H.; Seetin, M. G.; Sagui, C.; Babin, V.; Kollman, P. A. **2008**. AMBER 10, University of California, San Francisco.

Chandra, V.; Huang, P.; Hamuro, Y.; Raghuram, S.; Wang, Y.; Burris, T. P.; Rastinejad, F. Structure of the intact PPAR-gamma-RXR- nuclear receptor complex on DNA *Nature* **2008**, *456*, 350-356.

Chang, C.; Norris, J. D.; Gron, H.; Paige, L. A.; Hamilton, P. T.; Kenan, D. J.; Fowlkes, D.; McDonnell, D. P. Dissection of the LXXLL nuclear receptor-coactivator interaction motif using combinatorial peptide libraries: discovery of peptide antagonists of estrogen receptors alpha and beta *Mol. Cell. Biol.* **1999**, *19*, 8226-8239.

Chen, J. D.; Evans, R. M. A transcriptional co-repressor that interacts with nuclear hormone receptors *Nature* **1995**, *377*, 454-457.

Chen, T.; Chen, Q.; Xu, Y.; Zhou, Q.; Zhu, J.; Zhang, H.; Wu, Q.; Xu, J.; Yu, C. SRC-3 is required for CAR-regulated hepatocyte proliferation and drug metabolism. *J. Hepatol.* **2012**, *56*, 210-217.

Chen, W.; Roeder, R. G. Mediator-dependent nuclear receptor function. *Semin. Cell Dev. Biol.* **2011**, *22*, 749-758.

Darden, T.; York, D.; Pedersen, L. mesh Ewald: An N.log(N) Method for Ewald Sums in Large Systems. *J. Chem. Phys.* **1993**, *12*, 10089-10092.

Darimont, B. D.; Wagner, R. L.; Apriletti, J. W.; Stallcup, M. R.; Kushner, P. J.; Baxter, J. D.; Fletterick, R. J.; Yamamoto, K. R. Structure and specificity of nuclear receptor-coactivator interactions *Genes Dev.* **1998**, *12*, 3343-3356.

De Koning, L.; Corpet, A.; Haber, J. E.; Almouzni, G. Histone chaperones: an escort network regulating histone traffic *Nat. Struct. Mol. Biol.* **2007**, *14*, 997-1007.

di Masi, A.; Marinis, E. D.; Ascenzi, P.; Marino, M. Nuclear receptors CAR and PXR: Molecular, functional, and biomedical aspects. *Mol. Aspects Med.* **2009**, *30*, 297-343.

Dussault, I.; Lin, M.; Hollister, K.; Fan, M.; Termini, J.; Sherman, M. A.; Forman, B. M. A structural model of the constitutive androstane receptor defines novel interactions that mediate ligand-independent activity *Mol. Cell. Biol.* **2002**, *22*, 5270-5280.

Frank, C.; Gonzalez, M. M.; Oinonen, C.; Dunlop, T. W.; Carlberg, C. Characterization of DNA complexes formed by the nuclear receptor constitutive androstane receptor *J. Biol. Chem.* **2003**, *278*, 43299-43310.

Frank, C.; Molnar, F.; Matilainen, M.; Lempiainen, H.; Carlberg, C. Agonist-dependent and agonist-independent transactivations of the human constitutive androstane receptor are modulated by specific amino acid pairs *J. Biol. Chem.* **2004**, *279*, 33558-33566.

Gee, A. C.; Carlson, K. E.; Martini, P. G.; Katzenellenbogen, B. S.; Katzenellenbogen, J. A. Coactivator peptides have a differential stabilizing effect on the binding of estrogens and antiestrogens with the estrogen receptor *Mol. Endocrinol.* **1999**, *13*, 1912-1923.

Germain, P.; Kammerer, S.; Perez, E.; Peluso-Iltis, C.; Tortolani, D.; Zusi, F. C.; Starrett, J.; Lapointe, P.; Daris, J. P.; Marinier, A.; de Lera, A. R.; Rochel, N.; Gronemeyer, H. Rational design of RAR-selective ligands revealed by RARbeta crystal stucture *EMBO Rep.* **2004**, *5*, 877-882.

Germain, P.; Staels, B.; Dacquet, C.; Spedding, M.; Laudet, V. Overview of Nomenclature of Nuclear Receptors *Pharmacol. Rev.* **2006**, *58*, 685-704.

Glass, C. K.; Rosenfeld, M. G. The coregulator exchange in transcriptional functions of nuclear receptors *Genes Dev.* **2000**, *14*, 121-141.

Glass, C. K.; Rose, D. W.; Rosenfeld, M. G. Nuclear receptor coactivators. *Curr. Opin. Cell Biol.* **1997**, *9*, 222-232.

Gronemeyer, H.; Gustafsson, J. A.; Laudet, V. Principles for modulation of the nuclear receptor superfamily *Nat. Rev. Drug Discov.* **2004**, *3*, 950-964.

Guo, C.; Gow, C. H.; Li, Y.; Gardner, A.; Khan, S.; Zhang, J. Regulated clearance of histone deacetylase 3 protects independent formation of nuclear receptor corepressor complexes *J. Biol. Chem.* **2012**, *287*, 12111-12120.

Gurevich, I.; Flores, A. M.; Aneskievich, B. J. Corepressors of agonist-bound nuclear receptors *Toxicol. Appl. Pharmacol.* **2007**, *223*, 288-298.

Heery, D. M.; Hoare, S.; Hussain, S.; Parker, M. G.; Sheppard, H. Core LXXLL motif sequences in CREB-binding protein, SRC1, and RIP140 define affinity and selectivity for steroid and retinoid receptors *J. Biol. Chem.* **2001**, *276*, 6695-6702.

Honkakoski, P.; Negishi, M. Regulation of cytochrome P450 (CYP) genes by nuclear receptors *Biochem. J.* **2000**, *347*, 321-337.

Hörlein, A. J.; Naar, A. M.; Heinzel, T.; Torchia, J.; Gloss, B.; Kurokawa, R.; Ryan, A.; Kamei, Y.; Soderstrom, M.; Glass, C. K. Ligand-independent repression by the thyroid hormone receptor mediated by a nuclear receptor co-repressor *Nature* **1995**, *377*, 397-404.

Hornak, V.; Abel, R.; Okur, A.; Strockbine, B.; Roitberg, A.; Simmerling, C. Comparison of Multiple Amber Force Fields and Development of Improved Protein Backbone Parameters. *Proteins.* **2006**, *65*, 712-725.

Hou, T.; Wang, J.; Li, Y.; Wang, W. Assessing the performance of the MM/PBSA and MM/GBSA methods. 1. The accuracy of binding free energy calculations based on molecular dynamics simulations *J. Chem. Inf. Model.* **2011**, *51*, 69-82.

Hsia, E. Y.; Goodson, M. L.; Zou, J. X.; Privalsky, M. L.; Chen, H. W. Nuclear receptor coregulators as a new paradigm for therapeutic targeting *Adv. Drug Deliv. Rev.* **2010**, *62*, 1227-1237.

Hsieh, T. F.; Fischer, R. L. Biology of chromatin dynamics *Annu. Rev. Plant. Biol.* **2005**, *56*, 327-351.

Hu, X.; Lazar, M. A. The CoRNR motif controls the recruitment of corepressors by nuclear hormone receptors *Nature* **1999**, *402*, 93-96.

Huang, P.; Chandra, V.; Rastinejad, F. Structural overview of the nuclear receptor superfamily: insights into physiology and therapeutics *Annu. Rev. Physiol.* **2010**, *72*, 247-272.

Huang, W.; Zhang, J.; Wei, P.; Schrader, W. T.; Moore, D. D. Meclizine is an agonist ligand for mouse constitutive androstane receptor (CAR) and an inverse agonist for human CAR *Mol. Endocrinol.* **2004**, *18*, 2402-2408.

Jakalian, A.; Bush, B. L.; Jack, D. B.; Bayly, C. I. Fast, Efficient Generation of High-Quality Atomic Charges. AM1-BCC Model: I. Method. *J. Comput. Chem.* **2000**, *21*, 132-146.

Jenuwein, T.; Allis, C. D. Translating the histone code *Science* **2001**, *293*, 1074-1080.

Jin, L.; Li, Y. Structural and functional insights into nuclear receptor signaling *Adv. Drug Deliv. Rev.* **2010**.

Jyrkkärinne, J.; Küblbeck, J.; Pulkkinen, J.; Honkakoski, P.; Laatikainen, R.; Poso, A.; Laitinen, T. Molecular Dynamics Simulations for Human CAR Inverse Agonists *J. Chem. Inf. Model.* **2012**.

Jyrkkärinne, J.; Windshügel, B.; Ronkko, T.; Tervo, A. J.; Küblbeck, J.; Lahtela-Kakkonen, M.; Sippl, W.; Poso, A.; Honkakoski, P. Insights into ligand-elicited activation of human constitutive androstane receptor based on novel agonists and three-dimensional quantitative structure-activity relationship *J. Med. Chem.* **2008**, *51*, 7181-7192.

Kachaylo, E. M.; Pustylnyak, V. O.; Lyakhovich, V. V.; Gulyaeva, L. F. Constitutive androstane receptor (CAR) is a xenosensor and target for therapy *Biochemistry (Mosc)* **2011**, *76*, 1087-1097.

Kato, S.; Yokoyama, A.; Fujiki, R. Nuclear receptor coregulators merge transcriptional coregulation with epigenetic regulation *Trends Biochem. Sci.* **2011**.

Katzenelienbogen, J. A.; Katzenellenbogen, B. S. Nuclear hormone receptors: ligand-activated regulators of transcription and diverse cell responses. *Chem. Biol.* **1996**, *3*, 529-536.

Khan, S.; Lingrel, J. B. Thematic minireview series on nuclear receptors in biology and diseases *J. Biol. Chem.* **2010**, *285*, 38741-38742.

Kongsted, J.; Ryde, U. An improved method to predict the entropy term with the MM/PBSA approach *J. Comput. Aided Mol. Des.* **2009**, *23*, 63-71.

Küblbeck, J.; Laitinen, T.; Jyrkkärinne, J.; Rousu, T.; Tolonen, A.; Abel, T.; Kortelainen, T.; Uusitalo, J.; Korjamo, T.; Honkakoski, P.; Molnár, F. Use of comprehensive screening methods to detect selective human CAR activators. *Biochem. Pharmacol.* **2011a**, *82*, 1994-2007.

Küblbeck, J.; Jyrkkärinne, J.; Molnar, F.; Kuningas, T.; Patel, J.; Windshügel, B.; Nevalainen, T.; Laitinen, T.; Sippl, W.; Poso, A.; Honkakoski, P. New in Vitro Tools to Study Human Constitutive Androstane Receptor (CAR) Biology: Discovery and Comparison of Human CAR Inverse Agonists *Mol. Pharm.* **2011b**.

Küblbeck, J.; Jyrkkärinne, J.; Poso, A.; Turpeinen, M.; Sippl, W.; Honkakoski, P.; Windshügel, B. Discovery of substituted sulfonamides and thiazolidin-4-one derivatives as agonists of human constitutive androstane receptor *Biochem. Pharmacol.* **2008**, *76*, 1288-1297.

Li, H.; Wang, H. Activation of xenobiotic receptors: driving into the nucleus *Expert Opin. Drug Metab. Toxicol.* **2010**, *6*, 409-426.

Li, L.; Chen, T.; Stanton, J. D.; Sueyoshi, T.; Negishi, M.; Wang, H. The peripheral benzodiazepine receptor ligand 1-(2-chlorophenyl-methylpropyl)-3-isoquinoline-carboxamide is a novel antagonist of human constitutive androstane receptor *Mol. Pharmacol.* **2008**, *74*, 443-453.

Li, X.; Kimbrel, E. A.; Kenan, D. J.; McDonnell, D. P. Direct interactions between corepressors and coactivators permit the integration of nuclear receptor-mediated repression and activation *Mol. Endocrinol.* **2002**, *16*, 1482-1491.

Lingrel, J. B.; Khan, S. Prologue to thematic minireview series: Nuclear Receptors in Biology and Diseases *J. Biol. Chem.* **2010**.

Lonard, D. M.; O'Malley, B. W. Nuclear receptor coregulators: judges, juries, and executioners of cellular regulation *Mol. Cell* **2007**, *27*, 691-700.

Maglich, J. M.; Parks, D. J.; Moore, L. B.; Collins, J. L.; Goodwin, B.; Billin, A. N.; Stoltz, C. A.; Kliewer, S. A.; Lambert, M. H.; Willson, T. M.; Moore, J. T. Identification of a novel human constitutive androstane receptor (CAR) agonist and its use in the identification of CAR target genes *J. Biol. Chem.* **2003**, *278*, 17277-17283.

Malik, S.; Roeder, R. G. The metazoan Mediator co-activator complex as an integrative hub for transcriptional regulation *Nature Reviews Genetics* **2010**.

Maiorov, V. N.; Crippen, G. M. Significance of root-mean-square deviation in comparing three-dimensional structures of globular proteins *J. Mol. Biol.* **1994**, *235*, 625-634.

Mangelsdorf, D. J.; Thummel, C.; Beato, M.; Herrlich, P.; Schütz, G.; Umesono, K.; Blumberg, B.; Kastner, P.; Mark, M.; Chambon, P.; Evans, R. M. The nuclear receptor superfamily: The second decade. *Cell* **1995**, *83*, 835-839.

Martínez, L.; Sonoda, M. T.; Webb, P.; Baxter, J. D.; Skaf, M. S.; Polikarpov, I. Molecular dynamics simulations reveal multiple pathways of ligand dissociation from thyroid hormone receptors Biophys. J. **2005**, *89*, 2011−2023.

McInerney, E. M.; Rose, D. W.; Flynn, S. E.; Westin, S.; Mullen, T. -.; Krones, A.; Inostroza, J.; Torchia, J.; Nolte, R. T.; Assa-Munt, N.; Milburn, M. V.; Glass, C. K.; Rosenfeld, M. G. Determinants of coactivator LXXLL motif specificity in nuclear receptor transcriptional activation *Genes Dev.* **1998**, *12*, 3357-3368.

Mutoh, S.; Osabe, M.; Inoue, K.; Moore, R.; Pedersen, L.; Perera, L.; Rebolloso, Y.; Sueyoshi, T.; Negishi, M. Dephosphorylation of threonine 38 is required for nuclear translocation and activation of human xenobiotic receptor CAR (NR1I3) *J. Biol. Chem.* **2009**, *284*, 34785-34792.

Nagy, L.; Kao, H. Y.; Love, J. D.; Li, C.; Banayo, E.; Gooch, J. T.; Krishna, V.; Chatterjee, K.; Evans, R. M.; Schwabe, J. W. Mechanism of corepressor binding and release from nuclear hormone receptors *Genes Dev.* **1999**, *13*, 3209-3216.

Nagy, L.; Schwabe, J. W. Mechanism of the nuclear receptor molecular switch *Trends Biochem. Sci.* **2004**, *29*, 317-324.

Nettles, K. W.; Greene, G. L. Ligand control of coregulator recruitment to nuclear receptors *Annu. Rev. Physiol.* **2005**, *67*, 309-333.

Nolte, R. T.; Wisely, G. B.; Westin, S.; Cobb, J. E.; Lambert, M. H.; Kurokawa, R.; Rosenfeld, M. G.; Willson, T. M.; Glass, C. K.; Milburn, M. V. Ligand binding and co-activator assembly of the peroxisome proliferator-activated receptor-gamma *Nature* **1998**, *395*, 137-143.

Nuclear Receptors Nomenclature Committee A unified nomenclature system for the nuclear receptor superfamily *Cell* **1999**, *97*, 161-163.

O'Malley, B. W.; Qin, J.; Lanz, R. B. Cracking the coregulator codes. *Curr. Opin. Cell Biol.* **2008**, *20*, 310-315.

Onufriev, A.; Bashford, D.; Case, D. A. Modification of the Generalized Born Model Suitable for Macromolecules. *J. Phys. Chem. B.* **2000**, *104*, 3712–3720.

Ordentlich, P.; Downes, M.; Evans, R. M. Corepressors and nuclear hormone receptor function *Curr. Top. Microbiol. Immunol.* **2001**, *254*, 101-116.

Perissi, V.; Staszewski, L. M.; McInerney, E. M.; Kurokawa, R.; Krones, A.; Rose, D. W.; Lambert, M. H.; Milburn, M. V.; Glass, C. K.; Rosenfeld, M. G. Molecular determinants of nuclear receptor-corepressor interaction *Genes Dev.* **1999**, *13*, 3198-3208.

Perissi, V.; Rosenfeld, M. G. Controlling nuclear receptors: the circular logic of cofactor cycles *Nature Reviews Molecular Cell Biology* **2005**, *6*, 542-554.

Phelan, C. A.; Gampe, R. T.,Jr; Lambert, M. H.; Parks, D. J.; Montana, V.; Bynum, J.; Broderick, T. M.; Hu, X.; Williams, S. P.; Nolte, R. T.; Lazar, M. A. Structure of Rev-erbalpha bound to N-CoR reveals a unique mechanism of nuclear receptor-co-repressor interaction *Nat. Struct. Mol. Biol.* **2010**, *17*, 808-814.

Plevin, M. J.; Mills, M. M.; Ikura, M. The LxxLL motif: a multifunctional binding sequence in transcriptional regulation *Trends Biochem. Sci.* **2005**, *30*, 66-69.

Privalsky, M. L. The role of corepressors in transcriptional regulation by nuclear hormone receptors *Annu. Rev. Physiol.* **2004**, *66*, 315-360.

Qatanani, M.; Zhang, J.; Moore, D. D. Role of the constitutive androstane receptor in xenobiotic-induced thyroid hormone metabolism *Endocrinology* **2005**, *146*, 995-1002.

Rachez, C.; Lemon, B. D.; Suldan, Z.; Bromleigh, V.; Gamble, M.; Naar, A. M.; Erdjument-Bromage, H.; Tempst, P.; Freedman, L. P. Ligand-dependent transcription activation by nuclear receptors requires the DRIP complex Nature 1999, 398, 824-828.

Rastelli, G.; Del Rio, A.; Degliesposti, G.; Sgobba, M. Fast and accurate predictions of binding free energies using MM-PBSA and MM-GBSA *J. Comput. Chem.* **2010**, *31*, 797-810.

Renaud, J. P.; Rochel, N.; Ruff, M.; Vivat, V.; Chambon, P.; Gronemeyer, H.; Moras, D. Crystal structure of the RAR-gamma ligand-binding domain bound to all-trans retinoic acid. *Nature* **1995**, *378*, 681−689.

Ryckaert, J. P.; Ciccotti, G.; Berendsen, H. J. C. Numerical integration of the Cartesian Equations of Motion of a System With Constraints: Molecular Dynamics of N-alkanes. *J. Comput. Physics.* **1977**, *23*, 327-341.

Sablin, E. P.; Krylova, I. N.; Fletterick, R. J.; Ingraham, H. A. Structural Basis for Ligand-Independent Activation of the Orphan Nuclear Receptor LRH-1 *Mol. Cell* **2003**, *11*, 1575-1585.

Santos, G. M.; Fairall, L.; Schwabe, J. W. Negative regulation by nuclear receptors: a plethora of mechanisms *Trends Endocrinol. Metab.* **2011**, *22*, 87-93.

Savkur, R. S.; Burris, T. P. The coactivator LXXLL nuclear receptor recognition motif *J. Pept. Res.* **2004**, *63*, 207-212.

Sberna, A. L.; Assem, M.; Xiao, R.; Ayers, S.; Gautier, T.; Guiu, B.; Deckert, V.; Chevriaux, A.; Grober, J.; Le Guern, N.; Pais de Barros, J. P.; Moore, D. D.; Lagrost, L.; Masson, D. Constitutive androstane receptor activation

decreases plasma apolipoprotein B-containing lipoproteins and atherosclerosis in low-density lipoprotein receptor-deficient mice *Arterioscler. Thromb. Vasc. Biol.* **2011**, *31*, 2232-2239.

Simental, J. A.; Sar, M.; Lane, M. V.; French, F. S.; Wilson, E. M. Transcriptional activation and nuclear targeting signals of the human androgen receptor *J. Biol. Chem.* **1991**, *266*, 510-518.

Sladek, F. M. What are nuclear receptor ligands? *Mol. Cell. Endocrinol.* **2011**, *334*, 3-13.

Steinmetz, A. C.; Renaud, J. P.; Moras, D. Binding of ligands and activation of transcription by nuclear receptors *Annu. Rev. Biophys. Biomol. Struct.* **2001**, *30*, 329-359.

Thakur, M. K.; Paramanik, V. Role of steroid hormone coregulators in health and disease *Horm. Res.* **2009**, *71*, 194-200.

Tolson, A. H.; Wang, H. Regulation of drug-metabolizing enzymes by xenobiotic receptors: PXR and CAR *Adv. Drug Deliv. Rev.* **2010**, *62*, 1238-1249.

Trauner, M.; Halilbasic, E. Nuclear Receptors as New Perspective for the Management of Liver Diseases. *Gastroenterology* **2011**, *140*, 1120-1125.e12.

Tzameli, I.; Pissios, P.; Schuetz, E. G.; Moore, D. D. The xenobiotic compound 1,4-bis[2-(3,5-dichloropyridyloxy)]benzene is an agonist ligand for the nuclear receptor CAR *Mol. Cell. Biol.* **2000**, *20*, 2951-2958.

Wang, Z.; Benoit, G.; Liu, J.; Prasad, S.; Aarnisalo, P.; Liu, X.; Xu, H.; Walker, N. P.; Perlmann, T. Structure and function of Nurr1 identifies a class of ligand-independent nuclear receptors *Nature* **2003**, *423*, 555-560.

Wang, J.; Morin, P.; Wang, W.; Kollman, P. A. Use of MM-PBSA in reproducing the binding free energies to HIV-1 RT of TIBO derivatives and predicting the binding mode to HIV-1 RT of efavirenz by docking and MM-PBSA *J. Am. Chem. Soc.* **2001**, *123*, 5221-5230.

Wang, J.; Wolf, R. M.; Caldwell, J. W.; Kollman, P. A.; Case, D. A. Development and Testing of a General Amber Force Field. *J. Comput. Chem.* **2004**, *25*, 1157-1174.

Wärnmark, A.; Almlof, T.; Leers, J.; Gustafsson, J. A.; Treuter, E. Differential recruitment of the mammalian mediator subunit TRAP220 by estrogen receptors ERalpha and ERbeta *J. Biol. Chem.* **2001**, *276*, 23397-23404.

Watson, P. J.; Fairall, L.; Schwabe, J. W. R. Nuclear hormone receptor co-repressors: Structure and function. *Mol. Cell. Endocrinol.* **2012**, *348*, 440-449.

Webb, P.; Anderson, C. M.; Valentine, C.; Nguyen, P.; Marimuthu, A.; West, B. L.; Baxter, J. D.; Kushner, P. J. The nuclear receptor corepressor (N-CoR) contains three isoleucine motifs (I/LXXII) that serve as receptor interaction domains (IDs) *Mol. Endocrinol.* **2000**, *14*, 1976-1985.

Weis, A.; Katebzadeh, K.; Soderhjelm, P.; Nilsson, I.; Ryde, U. Ligand affinities predicted with the MM/PBSA method: dependence on the simulation method and the force field *J. Med. Chem.* **2006**, *49*, 6596-6606.

Weiser, J.; Shenkin, P. S.; Still, W.C. Approximate Solvent-Accessible Surface Areas from Tetrahedrally Directed Neighbor Densities. *J. Computat. Chem.* **1999**, *20*, 217–230.

Westin, S.; Kurokawa, R.; Nolte, R. T.; Wisely, G. B.; McInerney, E. M.; Rose, D. W.; Milburn, M. V.; Rosenfeld, M. G.; Glass, C. K. Interactions controlling the assembly of nuclear-receptor hetero-dimers and co-activators *Nature* **1998**, *395*, 199-202.

Windshügel, B.; Jyrkkärinne, J.; Poso, A.; Honkakoski, P.; Sippl, W. Molecular dynamics simulations of the human CAR ligand-binding domain: deciphering the molecular basis for constitutive activity *J. Mol. Model.* **2005**, *11*, 69-79.

Windshügel, B.; Poso, A. Constitutive activity and ligand-dependent activation of the nuclear receptor CAR-insights from molecular dynamics simulations *Journal of Molecular Recognition* **2011**, *24*, 875-882.

Wolf, I. M.; Heitzer, M. D.; Grubisha, M.; DeFranco, D. B. Coactivators and nuclear receptor transactivation *J. Cell. Biochem.* **2008**, *104*, 1580-1586.

Wong, S.; Amaro, R. E.; McCammon, J. A. MM-PBSA Captures Key Role of Intercalating Water Molecules at a Protein-Protein Interface *J. Chem. Theory Comput.* **2009**, *5*, 422-429.

Wright, E.; Busby, S. A.; Wisecarver, S.; Vincent, J.; Griffin, P. R.; Fernandez, E. J. Helix 11 Dynamics Is Critical for Constitutive Androstane Receptor Activity. *Structure* **2011**, *19*, 37-44.

Xu, H. E.; Stanley, T. B.; Montana, V. G.; Lambert, M. H.; Shearer, B. G.; Cobb, J. E.; McKee, D. D.; Galardi, C. M.; Plunket, K. D.; Nolte, R. T.; Parks, D. J.; Moore, J. T.; Kliewer, S. A.; Willson, T. M.; Stimmel, J. B. Structural basis for antagonist-mediated recruitment of nuclear co-repressors by PPARalpha *Nature* **2002**, *415*, 813-817.

Xu, R. X.; Lambert, M. H.; Wisely, B. B.; Warren, E. N.; Weinert, E. E.; Waitt, G. M.; Williams, J. D.; Collins, J. L.; Moore, L. B.; Willson, T. M.; Moore, J. T. A Structural Basis for Constitutive Activity in the Human CAR/RXRα Hetero-dimer. *Mol. Cell* **2004**, *16*, 919-928.

York, B.; O'Malley, B. W. Steroid receptor coactivator (SRC) family: Masters of systems biology *J. Biol. Chem.* **2010**.

Zhou, G.; Cummings, R.; Li, Y.; Mitra, S.; Wilkinson, H. A.; Elbrecht, A.; Hermes, J. D.; Schaeffer, J. M.; Smith, R. G.; Moller, D. E. Nuclear receptors have distinct affinities for coactivators: characterization by fluorescence resonance energy transfer *Mol. Endocrinol.* **1998**, *12*, 1594-1604.

7 Appendices

List of Appendices

Appendix I: Structure information of ligands

Appendix II: Root mean square deviations (RMSD) of the alpha carbon atoms of hCAR-LBD during 10 ns MD simulations

Appendix III: The atomic positional fluctuation (APF) values of the hCAR-LBD backbone atoms

Appendix IV: APF values of the C-terminal residues of hCAR-LBD

Appendix V: Helical content (HC %) (% of the MD time when the residues stay in helical conformation) of the C-terminal residues of hCAR-LBD

Appendix VI: The binding of apo-hCAR with co-regulator peptides

Appendix VII: The core residues co-regulator peptides on the liganded structures

Appendix VIII: Helical content (HC %) of the co-regulator peptides during MD simulations

Appendix IX: Positions of H12 in the final structures from 10 ns MD simulations

Appendix X: The helical content (% of MD simulation time when HX was stabilized in helical conformation) of HX

Appendix XI: APF values of the H2-H3 loop of hCAR-LBD

Appendix XII: The ligand-protein interaction energy that were calculated with MM-PBSA method

Appendix I. Structure information of ligands.

Agonist	Structure	Inverse agonist	Structure
CITCO $C_{19}H_{12}Cl_3N_3OS$	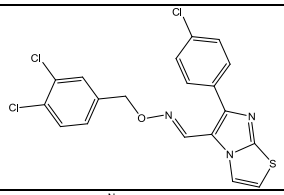	EE2 $C_{20}H_{24}O_2$	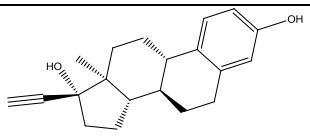
FL82 $C_{16}H_{15}NO$	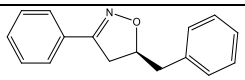	Androstanol $C_{19}H_{32}O$	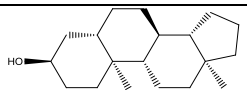
FL81 $C_{18}H_{19}NO_3$	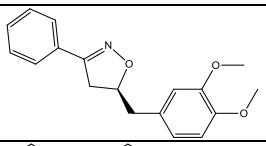	ANDR $C_{19}H_{30}O$	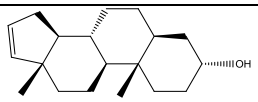
Permethrin $C_{21}H_{20}Cl_2O_3$	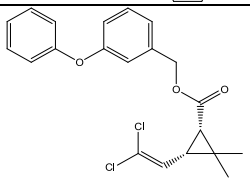	PK11195 $C_{21}H_{21}ClN_2O$	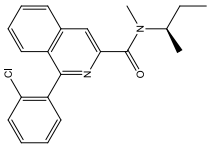
CLOTR $C_{22}H_{17}ClN_2$	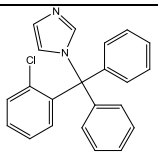	S07662 $C_{16}H_{16}N_2O_2S$	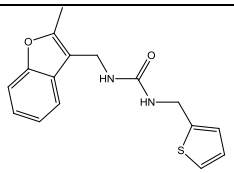
TPP $C_{18}H_{15}O_4P$	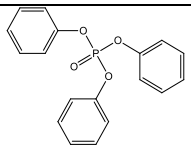	Clomifene $C_{26}H_{28}ClNO$	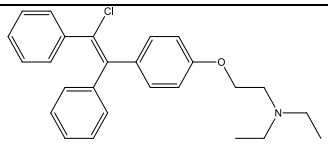
Artemisin $C_{15}H_{18}O_4$	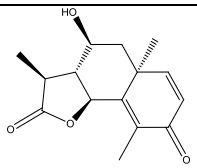	Celecoxib $C_{17}H_{14}F_3N_3O_2S$	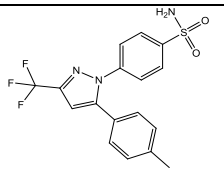
		Meclizine $C_{25}H_{27}ClN_2$	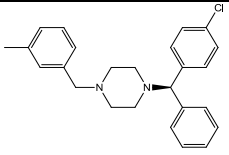

Appendix II. Root mean square deviations (RMSD) of the alpha carbon atoms of hCAR-LBD during 10 ns MD simulations

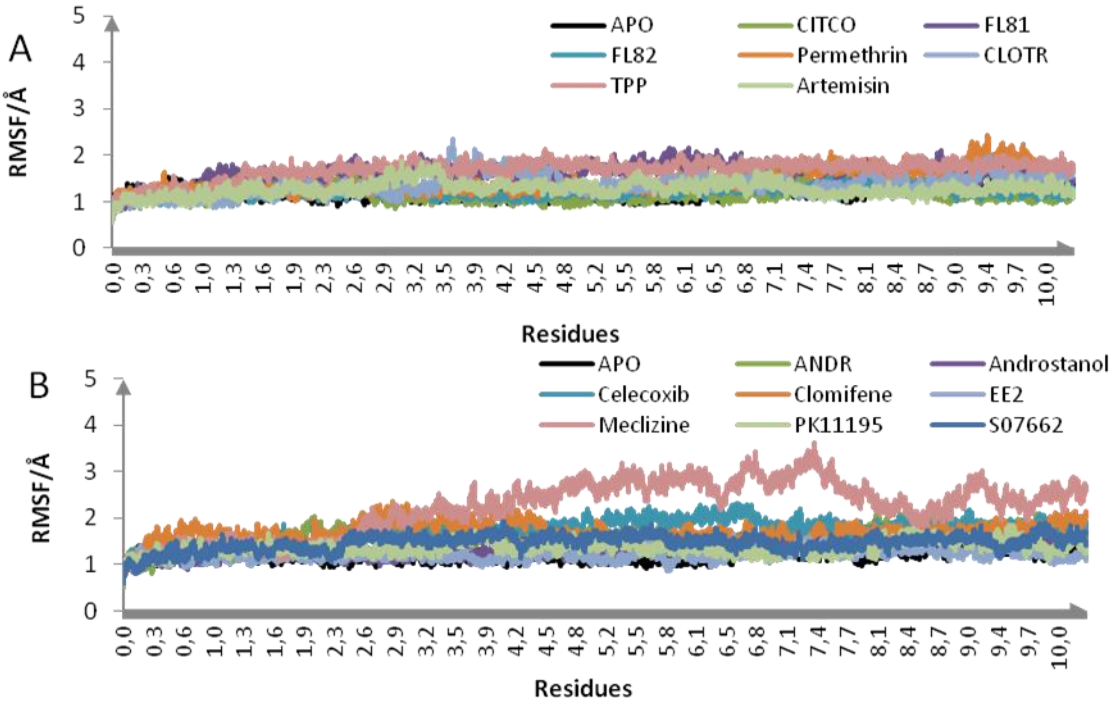

Figure 1. RMSD of system I in the presence of (A) agonists and (B) inverse agonists.

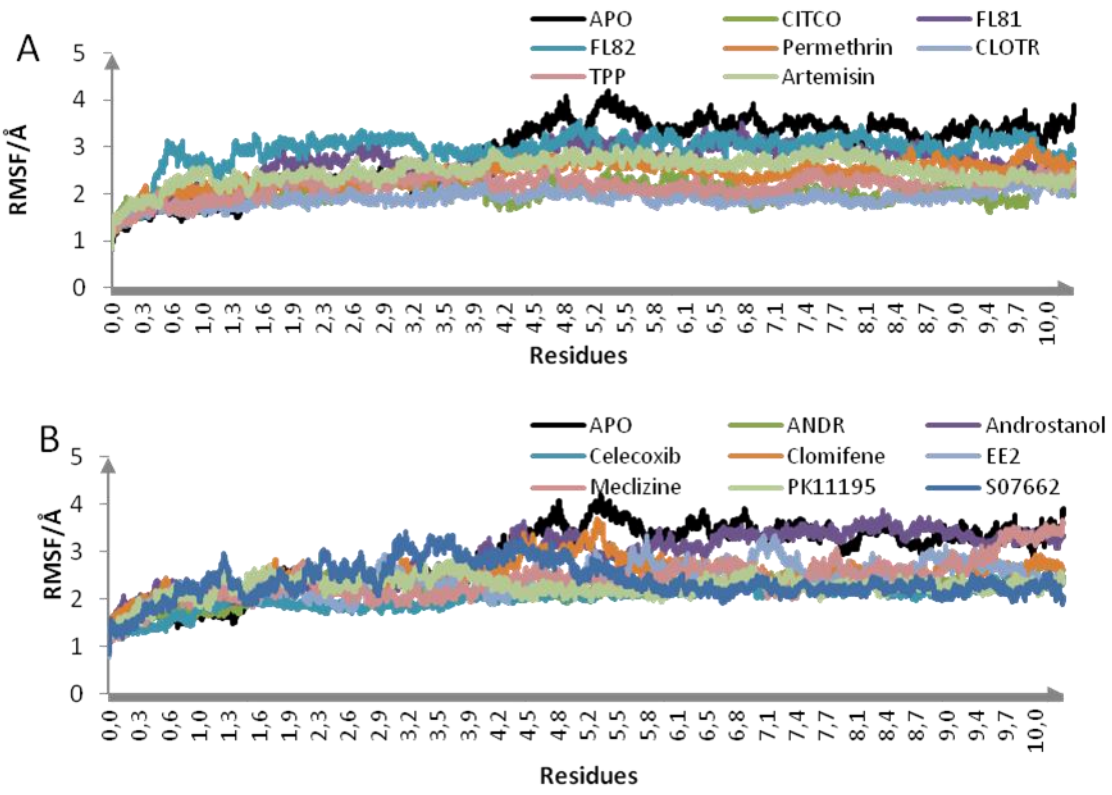

Figure 2. RMSD of system II in the presence of (A) agonists and (B) inverse agonists.

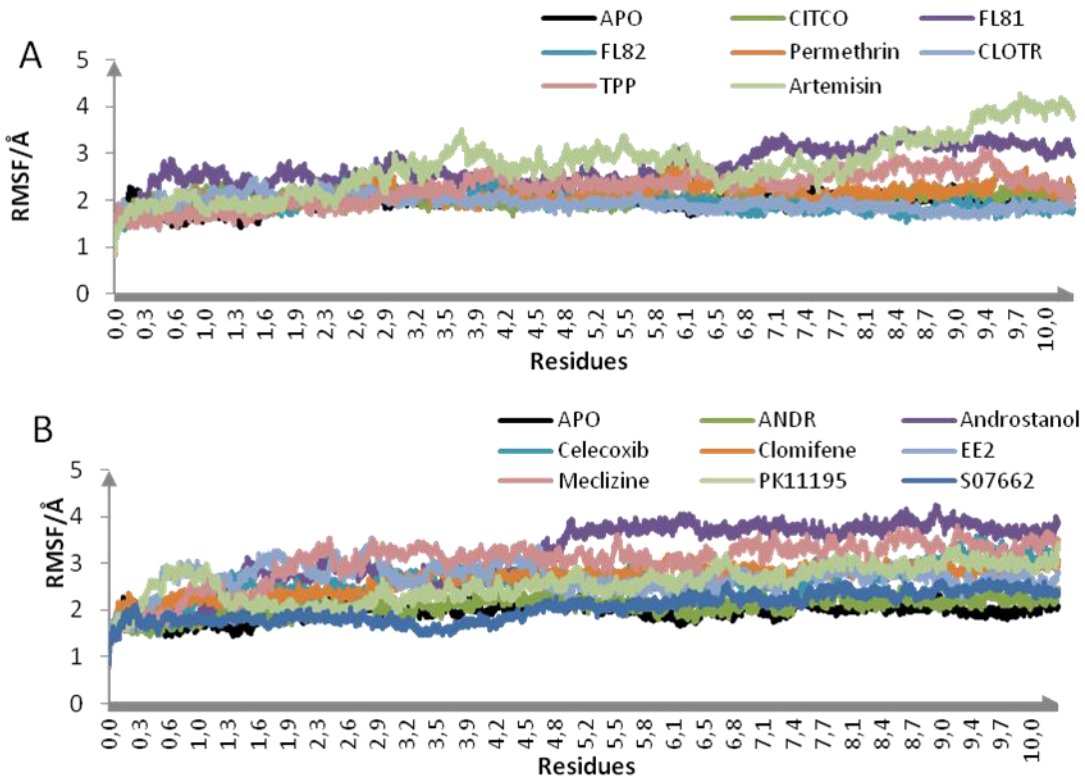

Figure 3. RMSD of system III in the presence of (A) agonists and (B) inverse agonists.

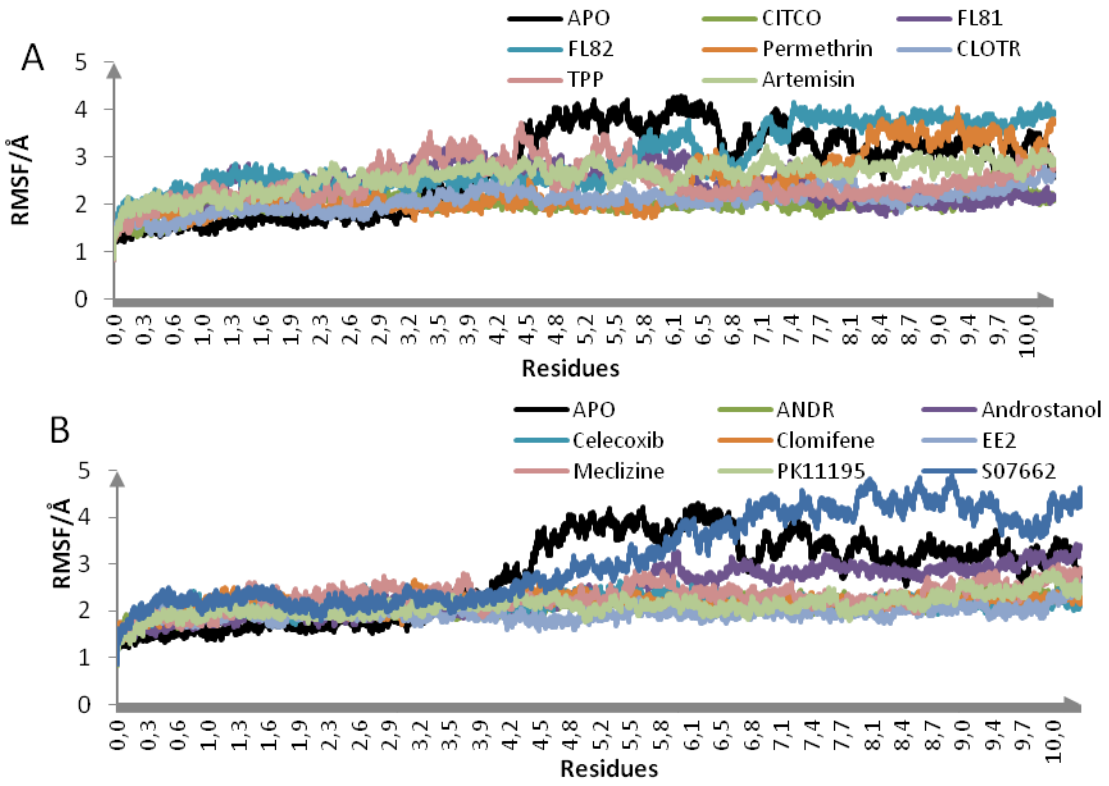

Figure 4. RMSD of system IV in the presence of (A) agonists and (B) inverse agonists.

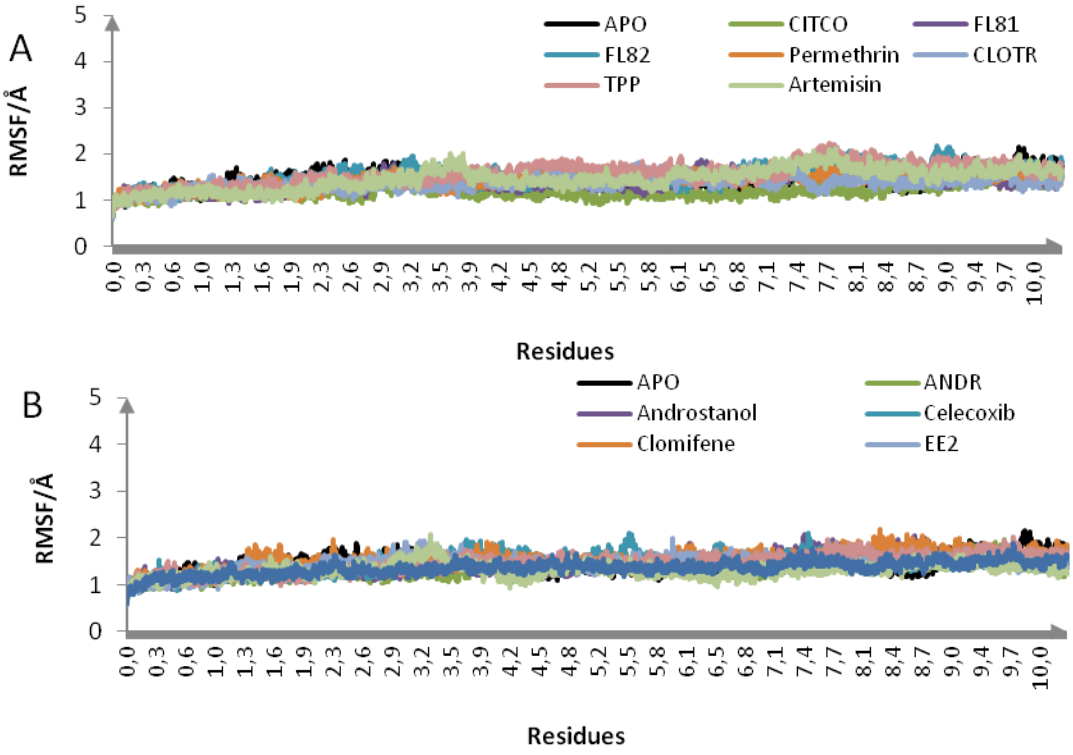

Figure 5. RMSD of system V in the presence of (A) agonists and (B) inverse agonists.

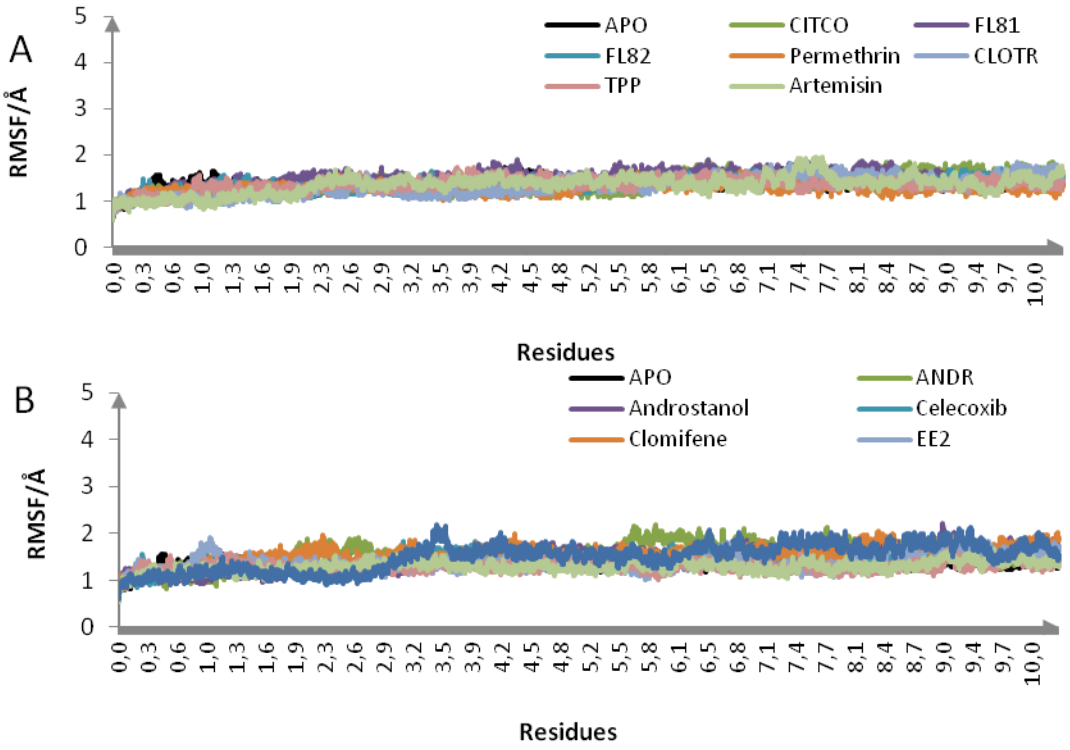

Figure 6. RMSD of system VI in the presence of (A) agonists and (B) inverse agonists.

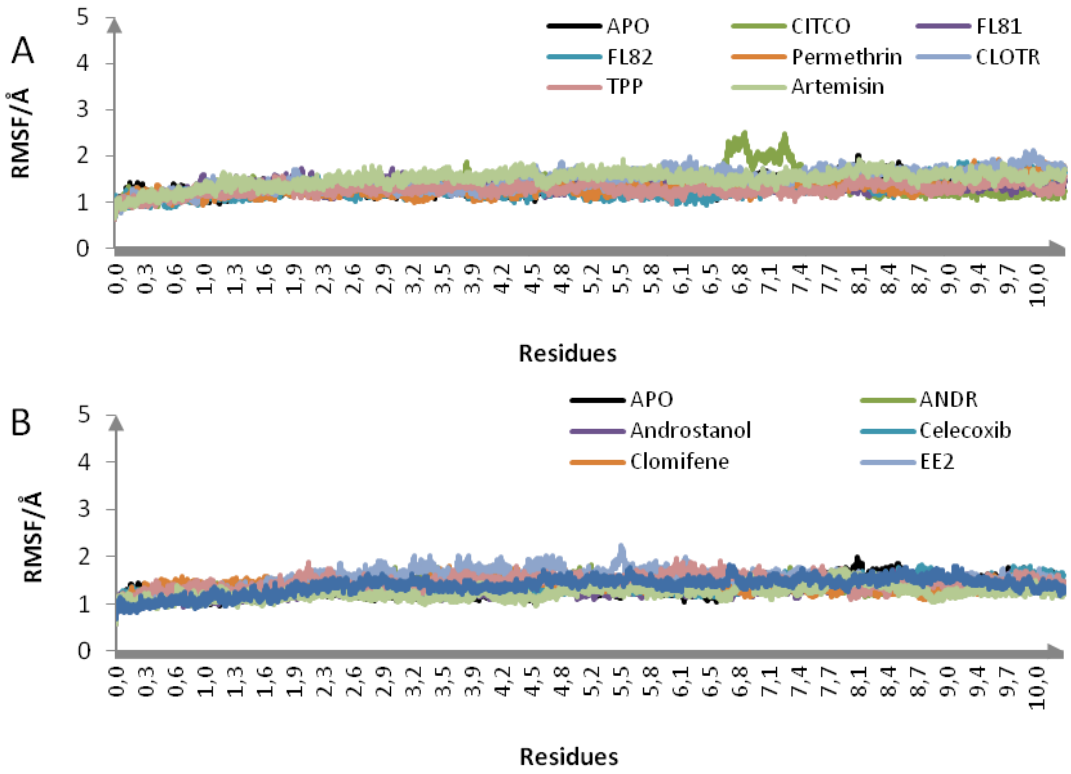

Figure 7. RMSD of system VII in the presence of (A) agonists and (B) inverse agonists.

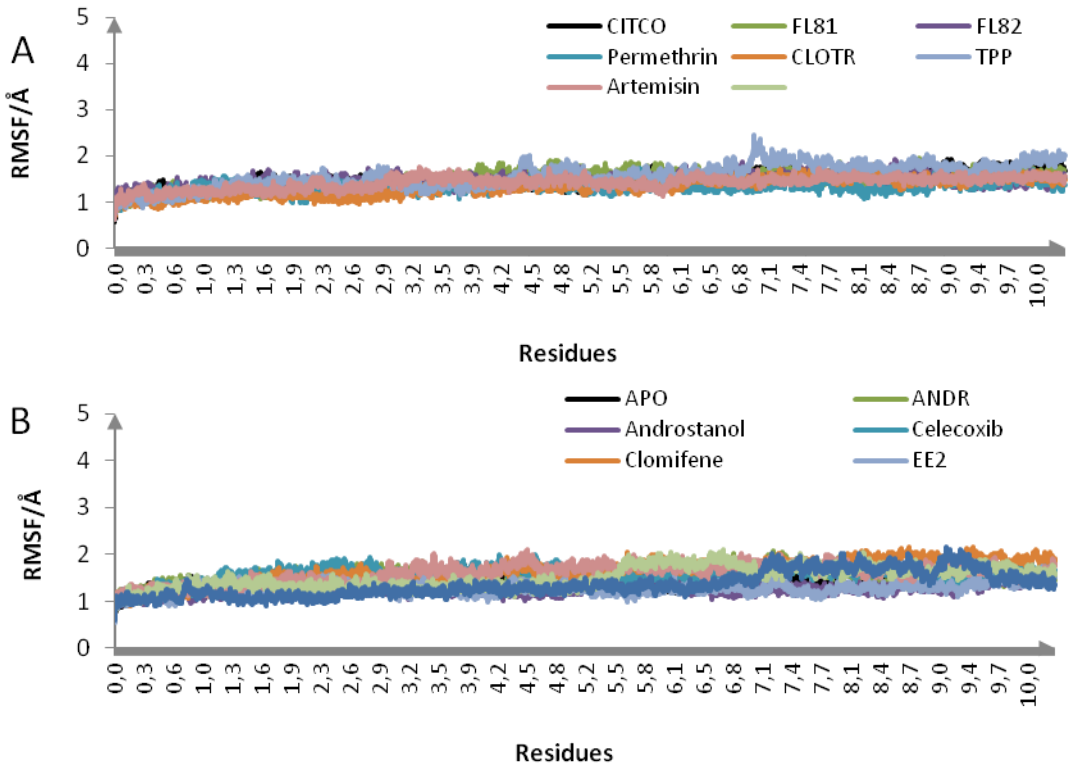

Figure 8. RMSD of system VIII in the presence of (A) agonists and (B) inverse agonists.

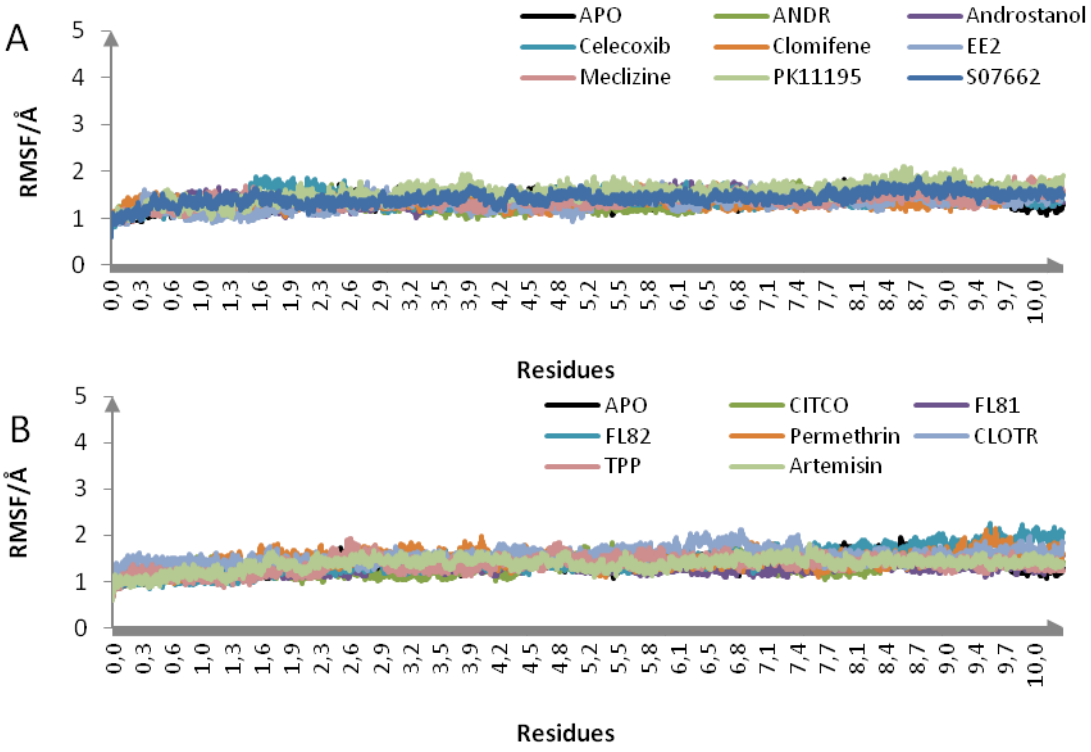

Figure 9. RMSD of system IX in the presence of (A) agonists and (B) inverse agonists.

Appendix III. The atomic positional fluctuation (APF) values of the hCAR-LBD backbone atoms

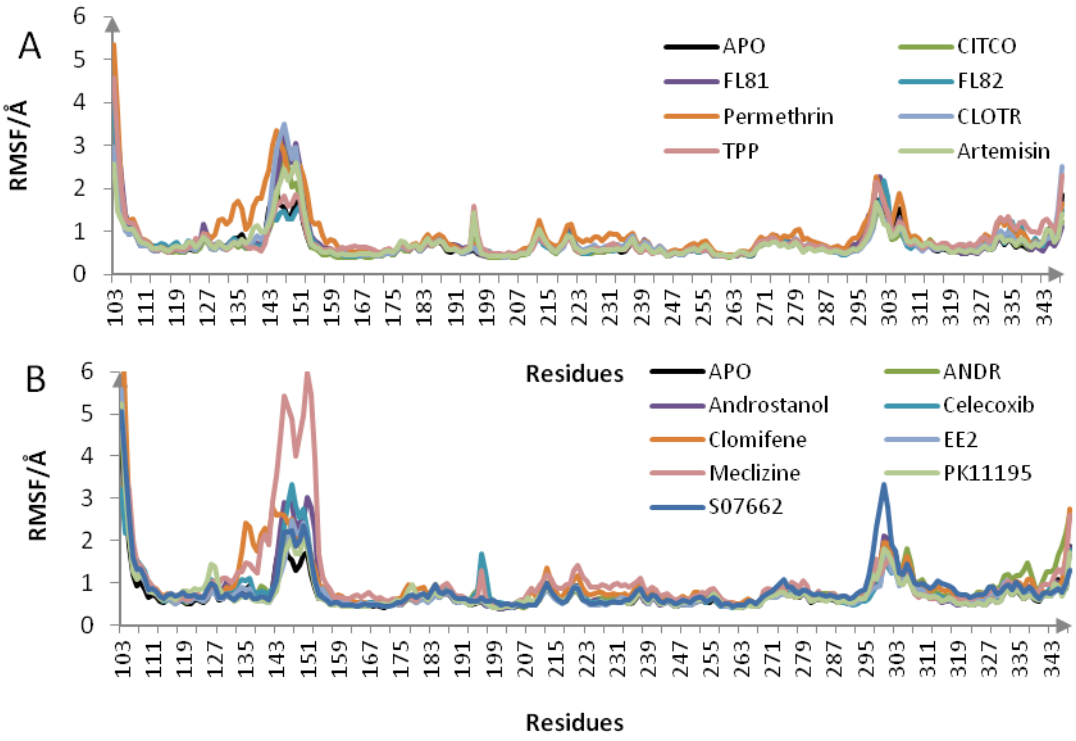

Figure **1.** APF values of system I in the presence of (A) agonists and (B) inverse agonists.

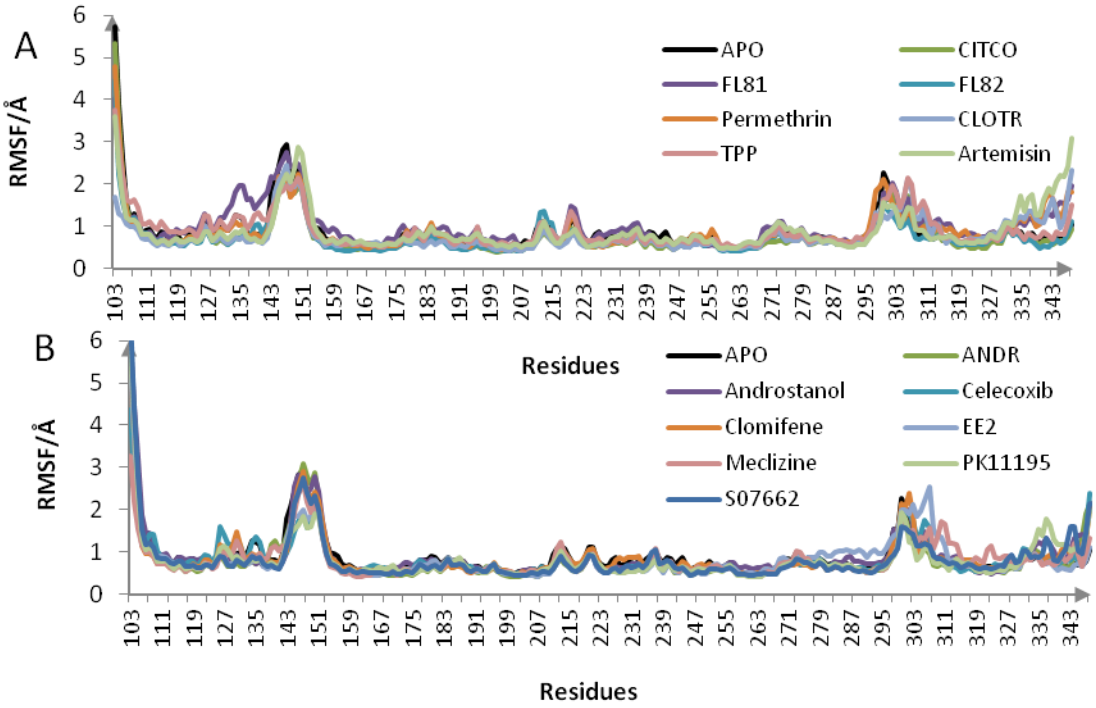

Figure 2. APF values of system II in the presence of (A) agonists and (B) inverse agonists.

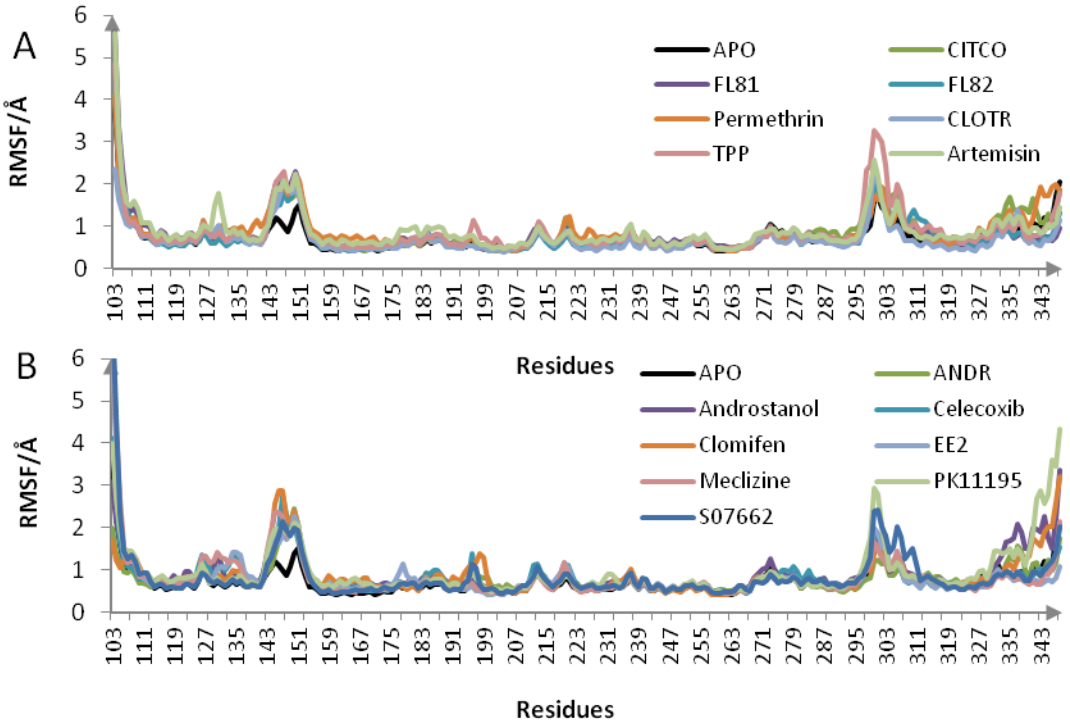

Figure 3. APF values of system III in the presence of (A) agonists and (B) inverse agonists.

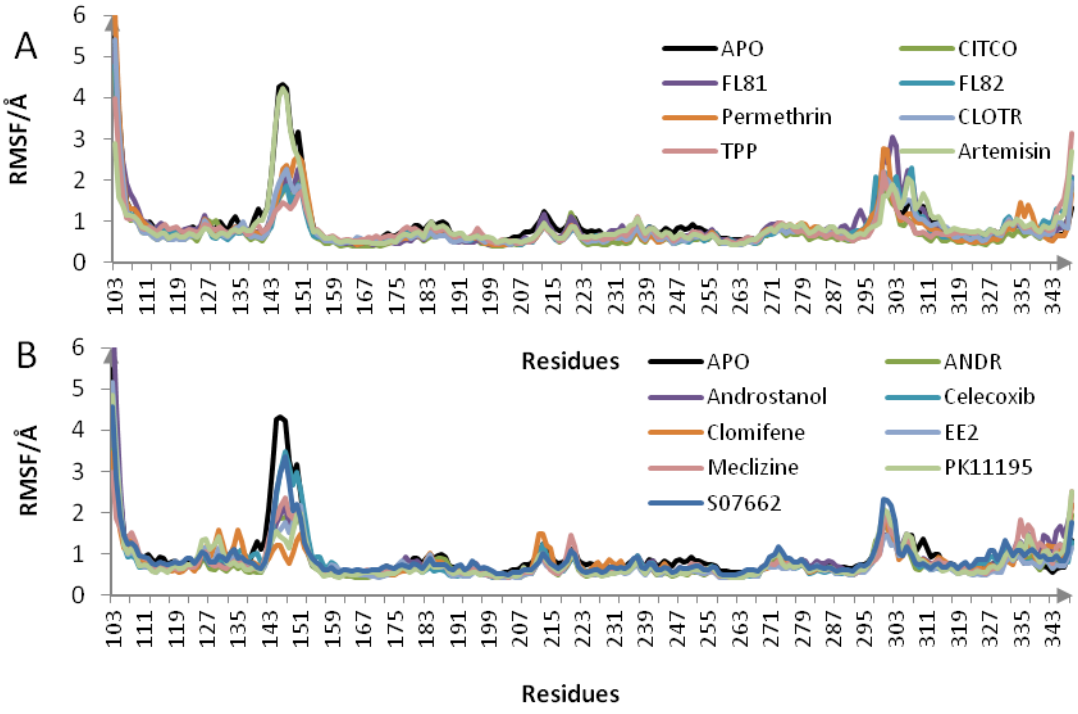

Figure 4. APF values of system IV in the presence of (A) agonists and (B) inverse agonists.

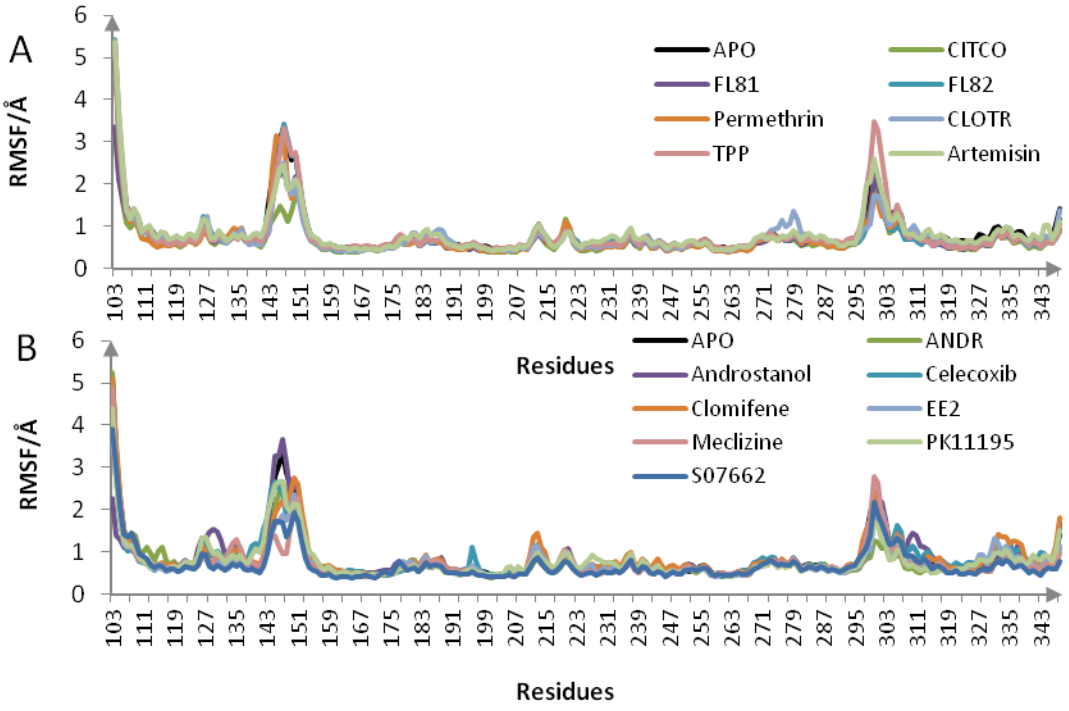

Figure 5. APF values of system V in the presence of (A) agonists and (B) inverse agonists.

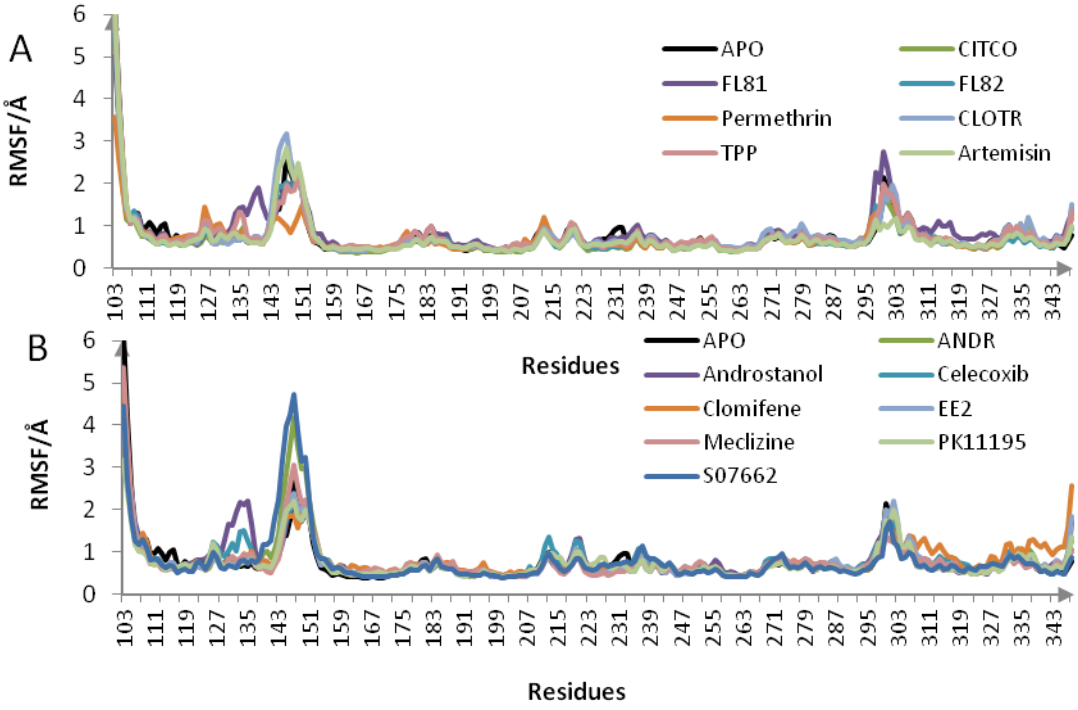

Figure 6. APF values of system VI in the presence of (A) agonists and (B) inverse agonists.

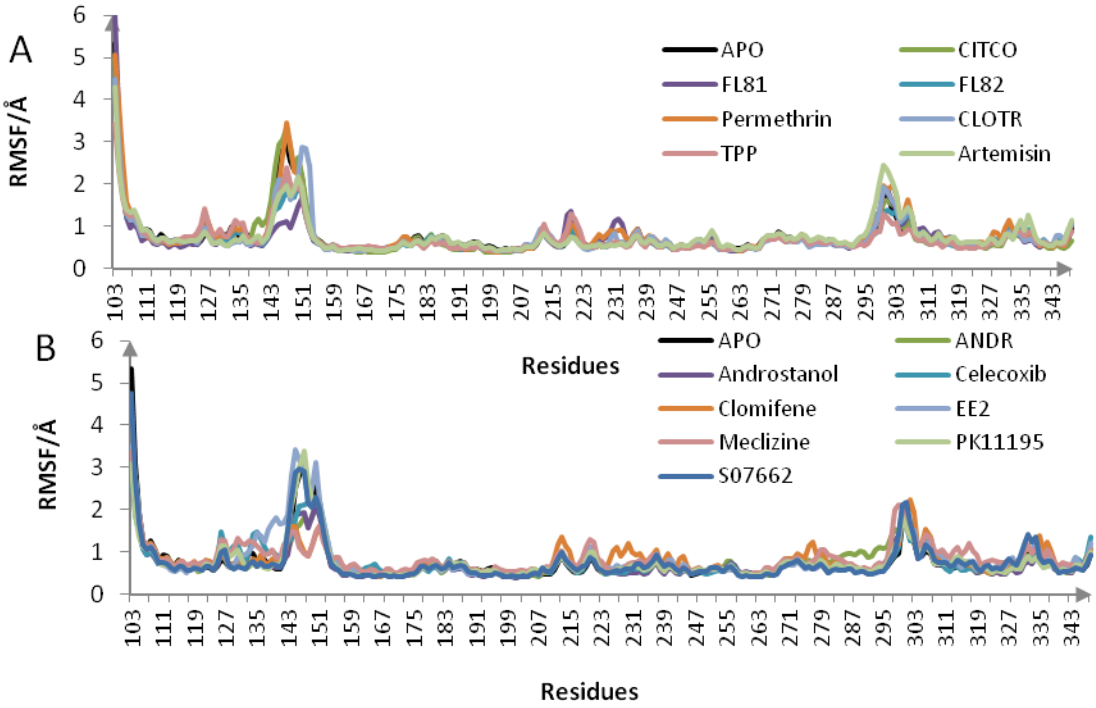

Figure 7. APF values of system VII in the presence of (A) agonists and (B) inverse agonists.

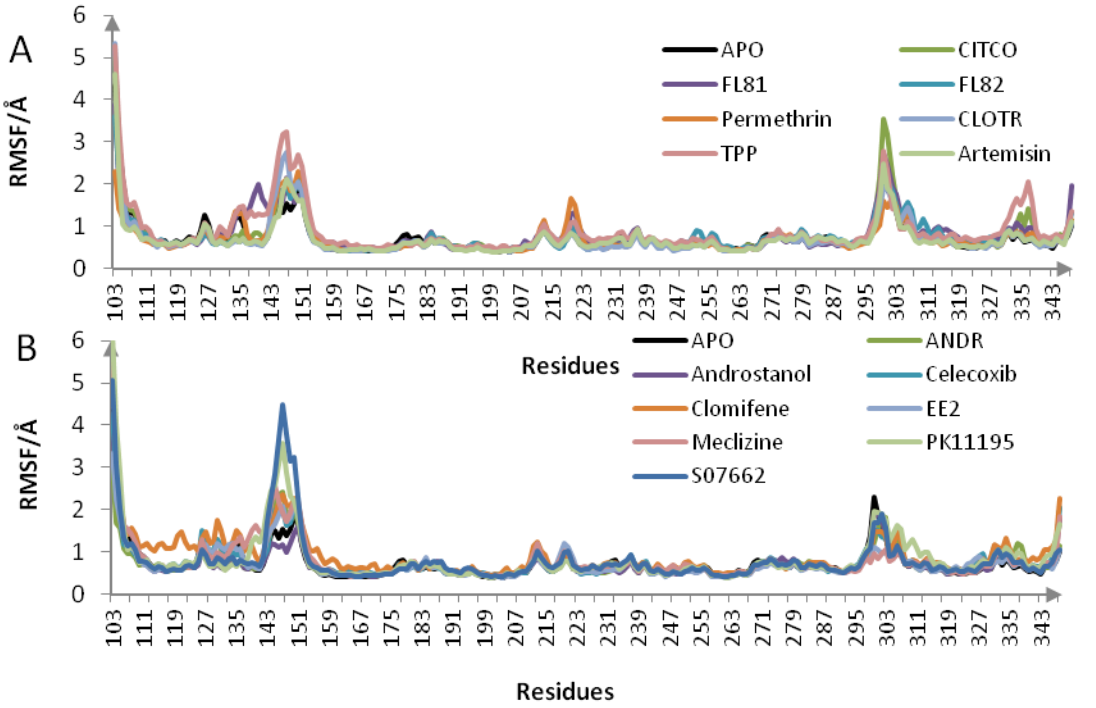

Figure 8. APF values of system VIII in the presence of (A) agonists and (B) inverse agonists.

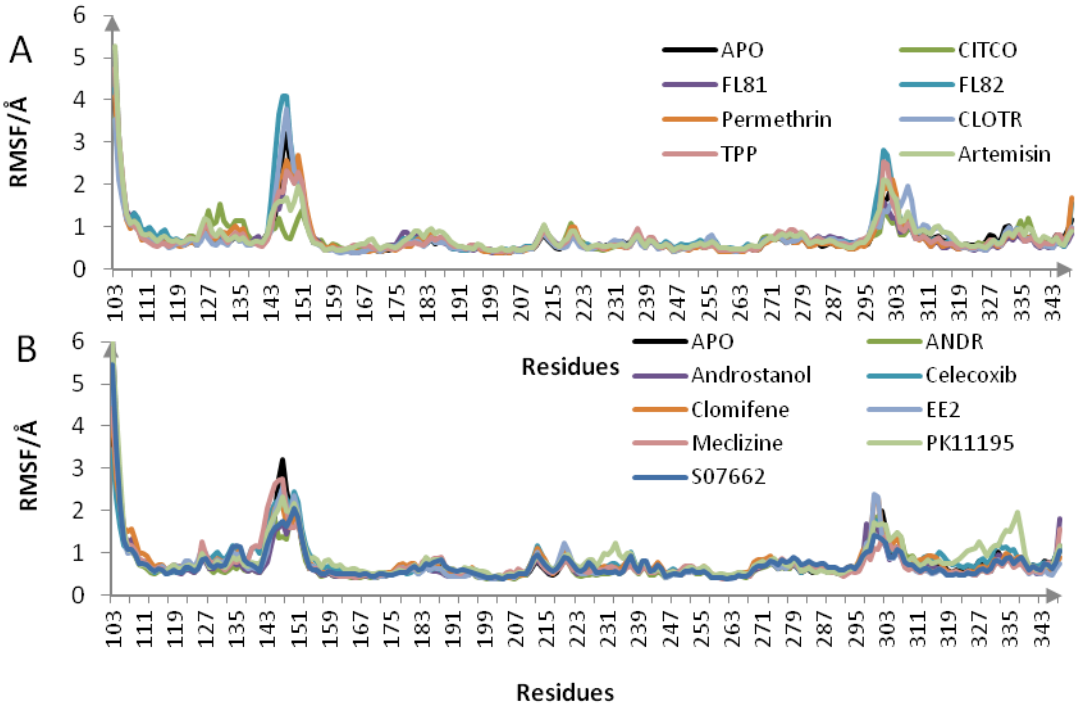

Figure 9. APF values of system IX in the presence of (A) agonists and (B) inverse agonists.

Appendix IV. APF values of the C-terminal residues of hCAR-LBD

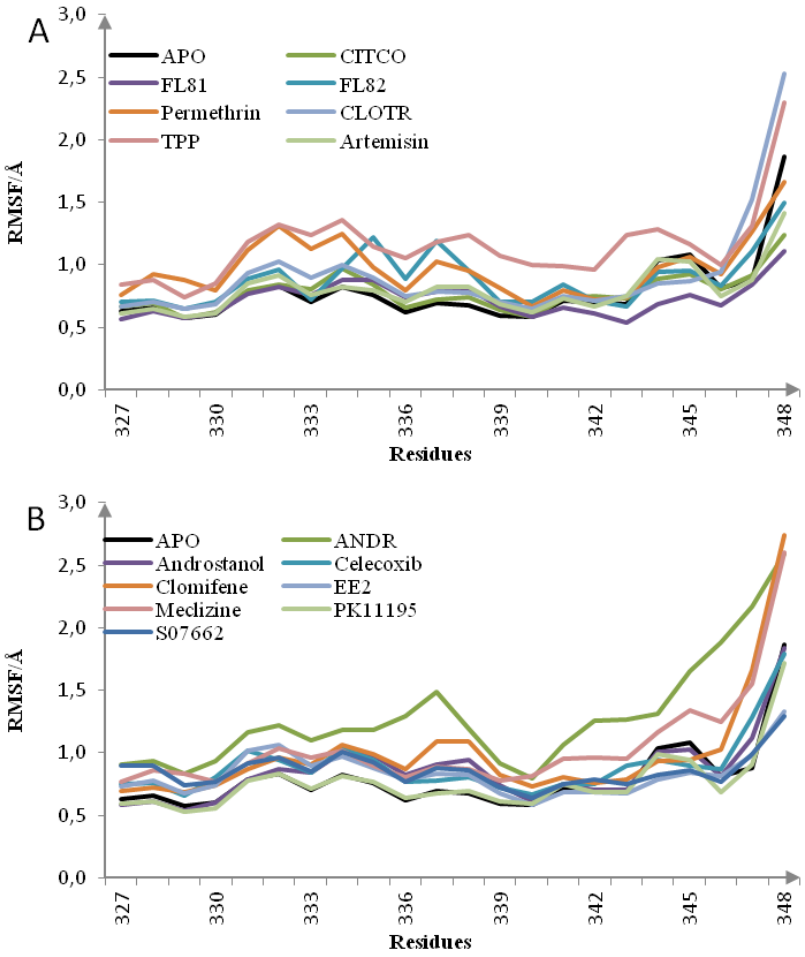

Figure 1. APF values of the C-terminal residues of hCAR-LBD in system I. (A) agonists. B) inverse agonists.

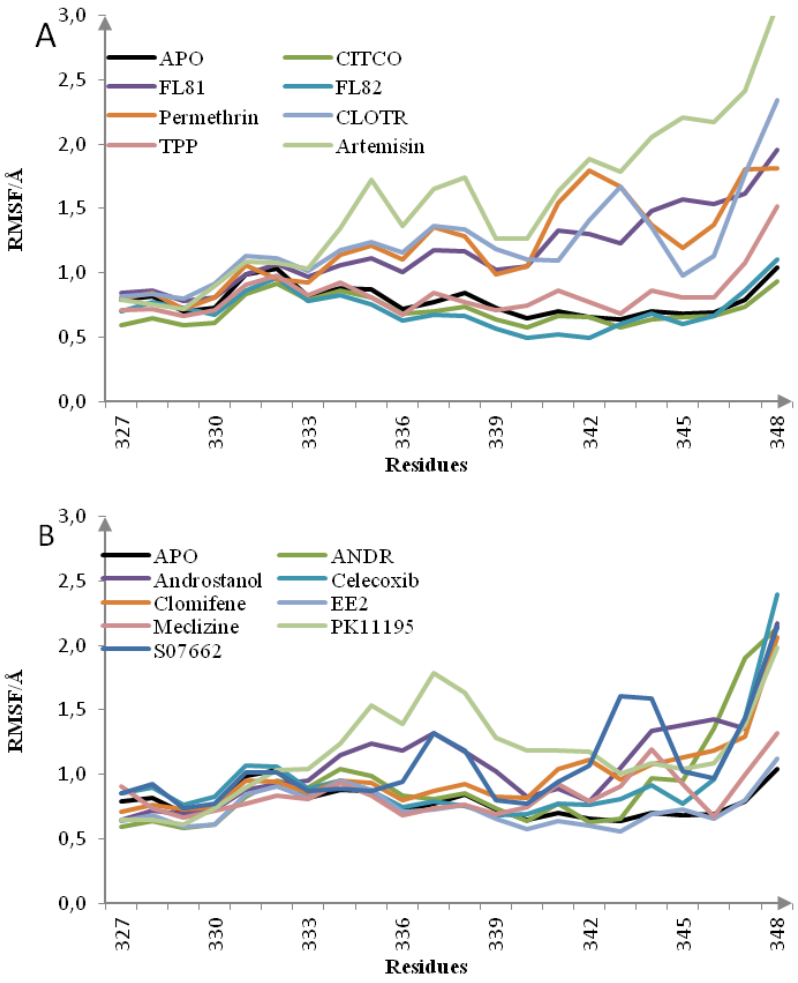

Figure 2. APF values of the C-terminal residues of hCAR-LBD in system II. (A) agonists. B) inverse agonists.

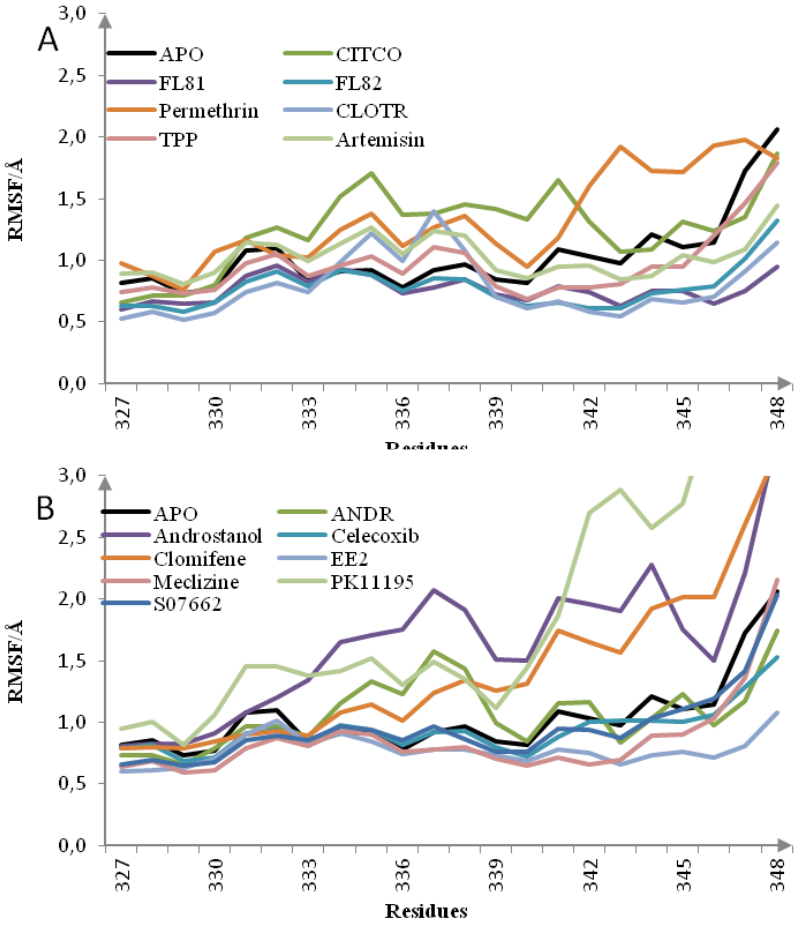

Figure 3. APF values of the C-terminal residues of hCAR-LBD in system III. (A) agonists. B) inverse agonists.

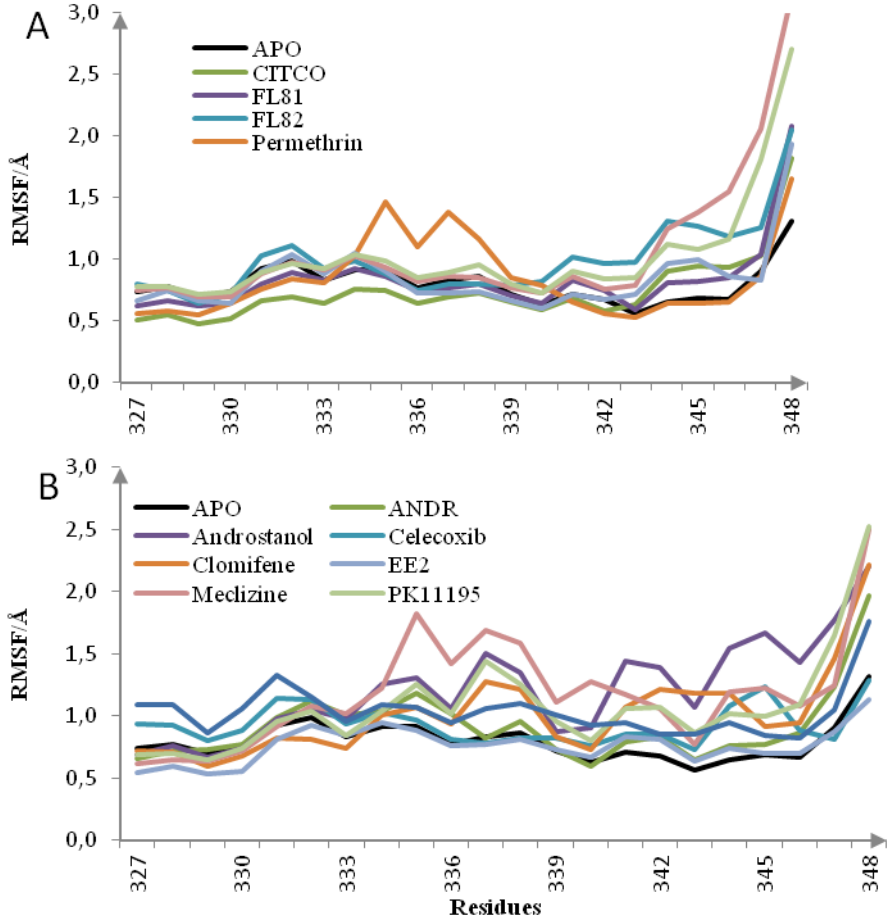

Figure 4. APF values of the C-terminal residues of hCAR-LBD in system IV. (A) agonists. B) inverse agonists.

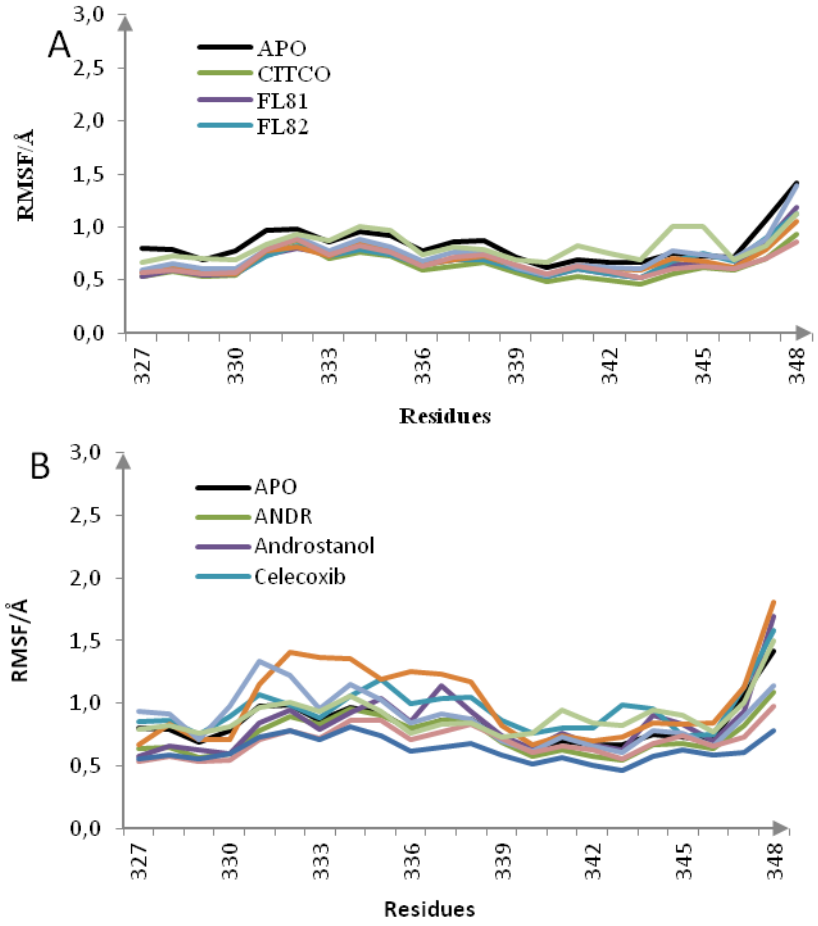

Figure 5. APF values of the C-terminal residues of hCAR-LBD in system V. (A) agonists. B) inverse agonists.

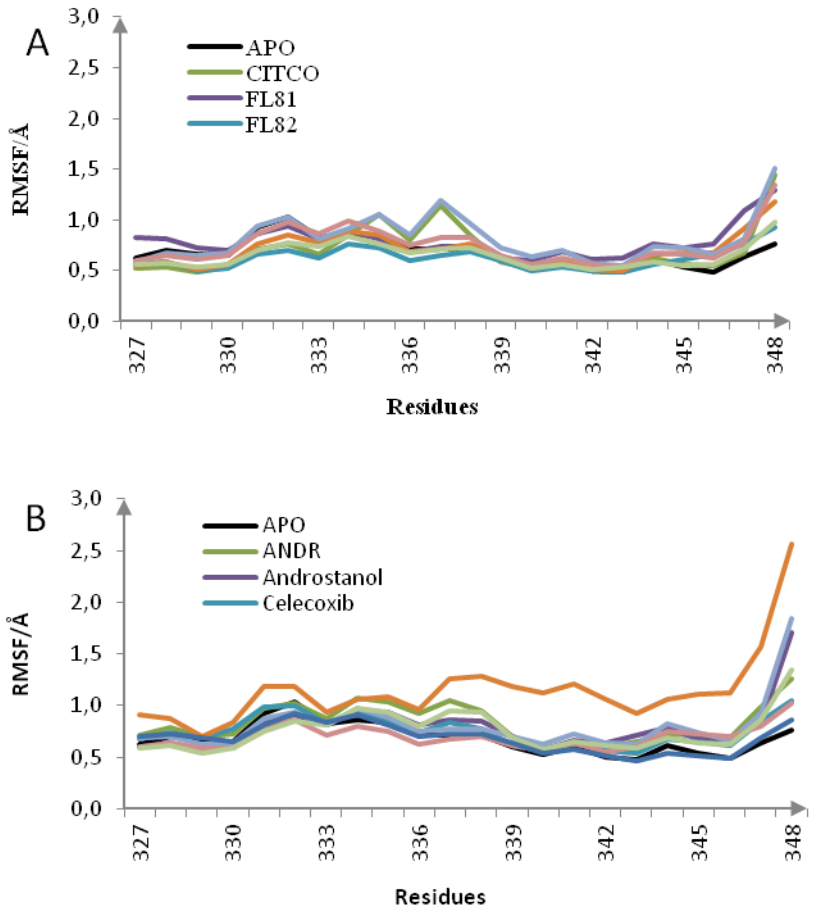

Figure 6. APF values of the C-terminal residues of hCAR-LBD in system VI. (A) agonists. B) inverse agonists.

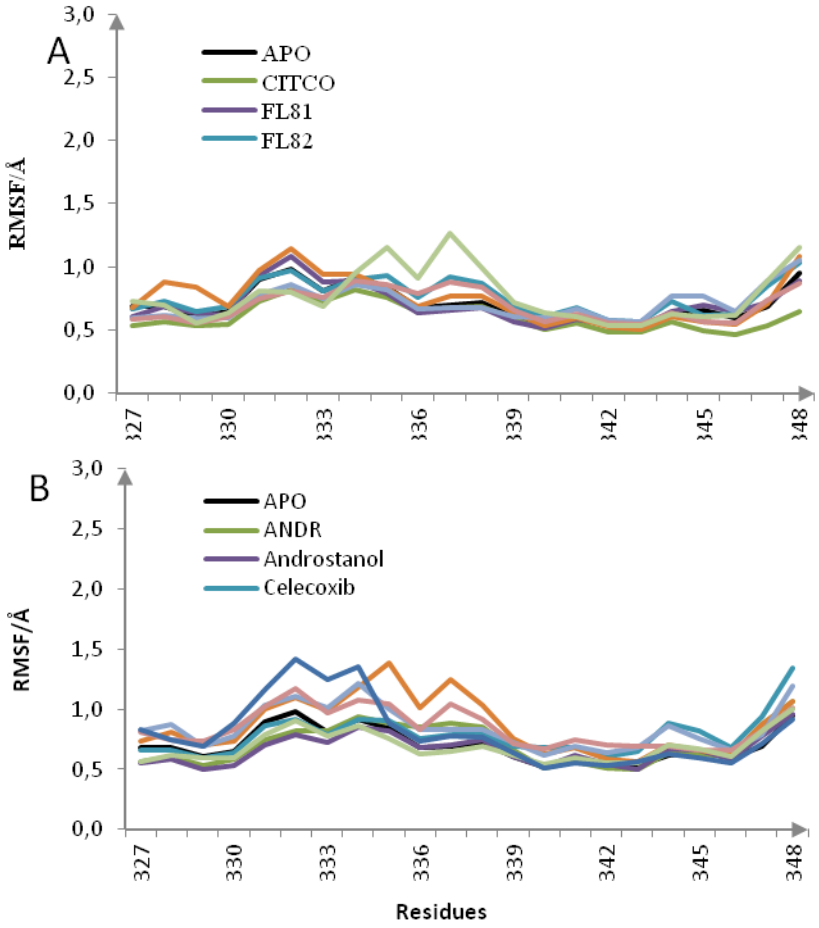

Figure 7. APF values of the C-terminal residues of hCAR-LBD in system VII. (A) agonists. B) inverse agonists.

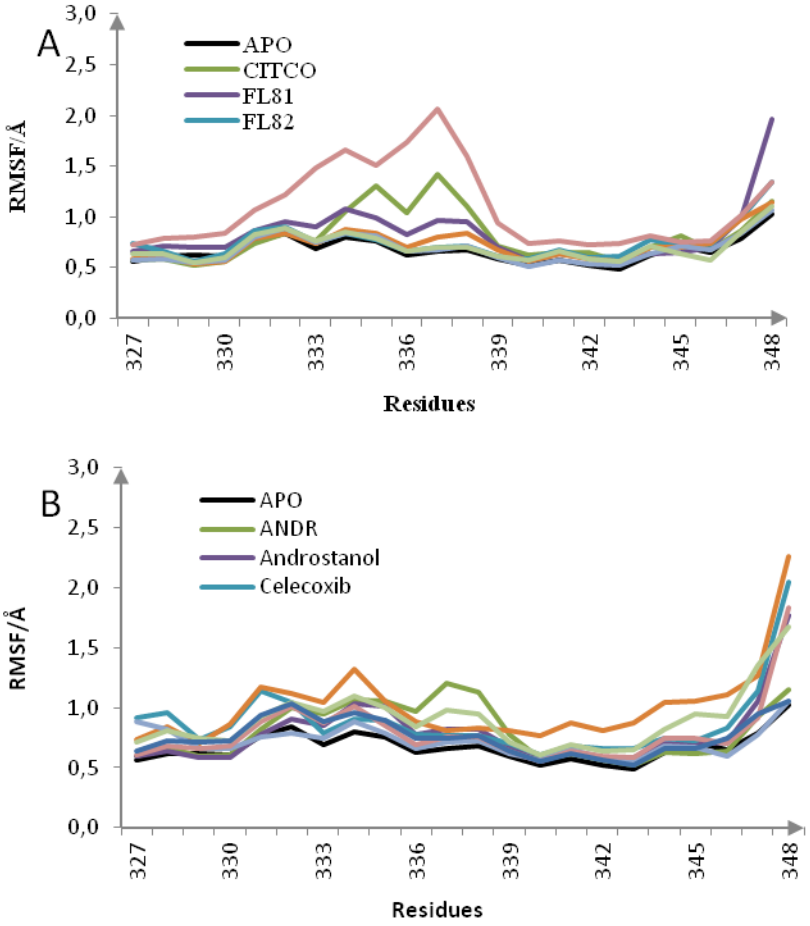

Figure 8. APF values of the C-terminal residues of hCAR-LBD in system VIII. (A) agonists. B) inverse agonists.

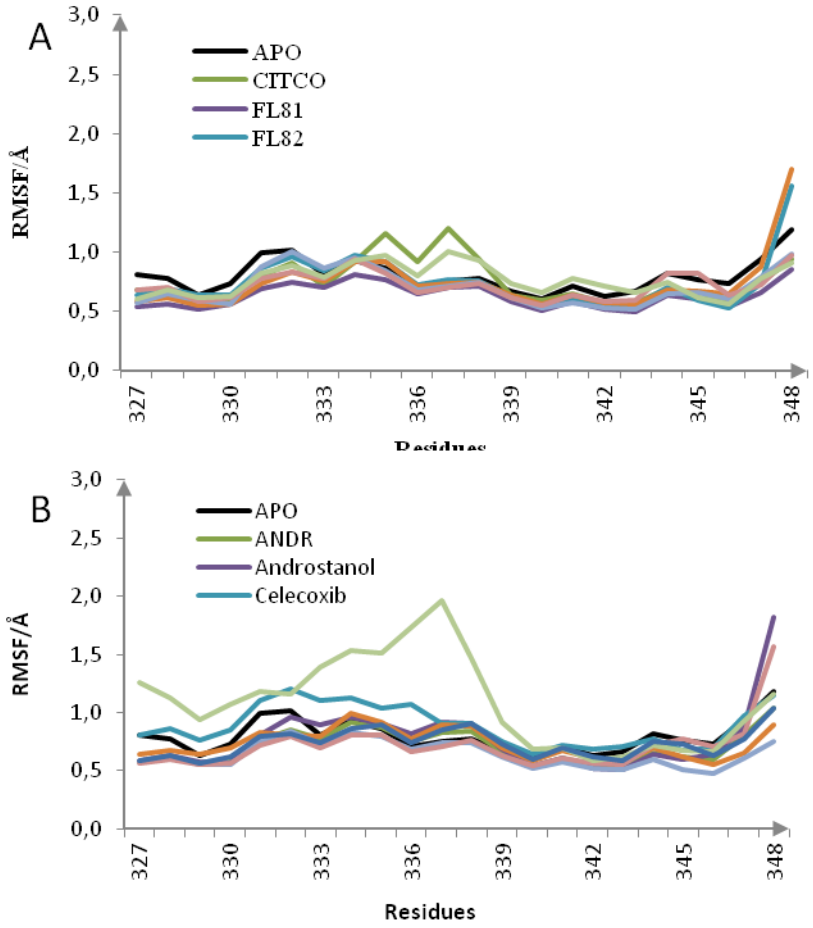

Figure 9. APF values of the C-terminal residues of hCAR-LBD in system IX. (A) agonists. B) inverse agonists.

Appendix V. Helical content (HC %) (% of the MD time when the residues stay in helical conformation) of the C-terminal residues of hCAR-LBD

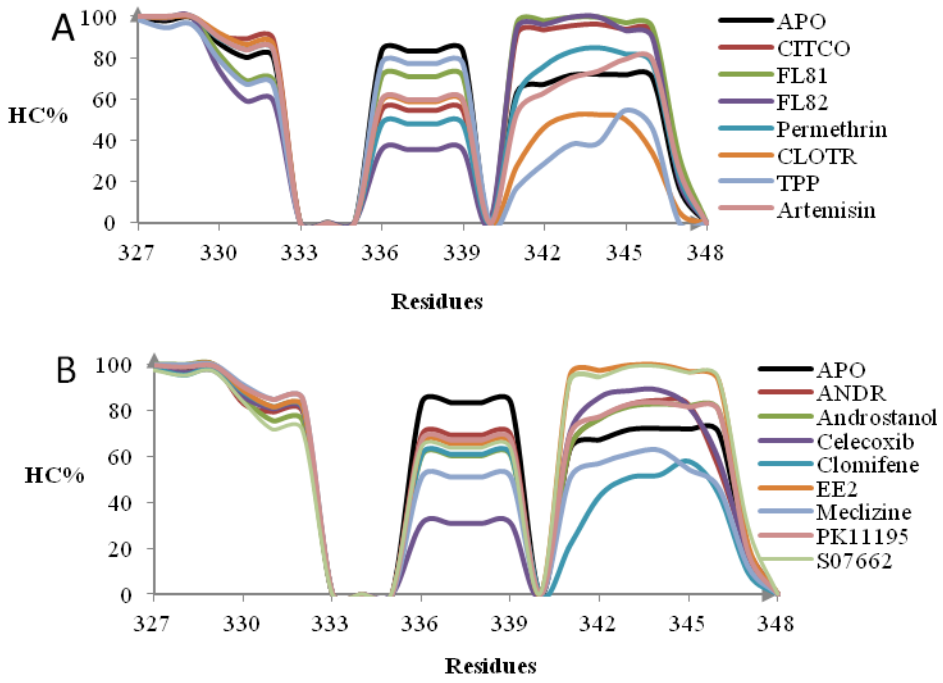

Figure 1. HC % values of system I that are in the presence (A) agonists and (B) inverse agonists. The C-terminal residues that are shown in x axis (amino acids: 327-348) include three helices, H10 (amino acids 327-332), HX (amino acids 336-339) and H12 (amino acids 341-347).

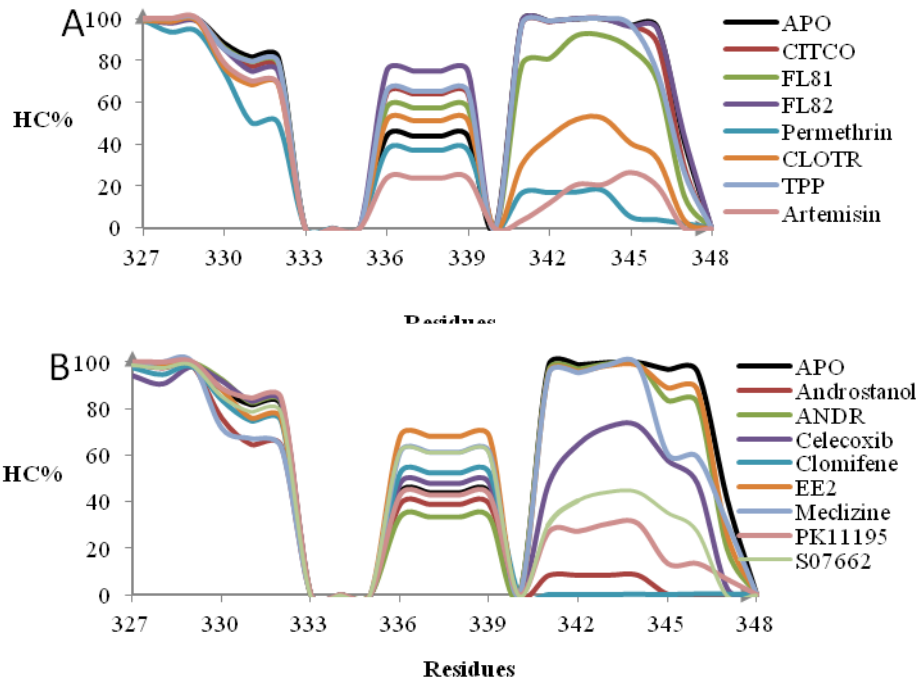

Figure 2. Helical content (HC %) of the C-terminal residues of hCAR-LBD during MD simulations. System II that are in the presence of (C) agonists and (D) inverse agonists.

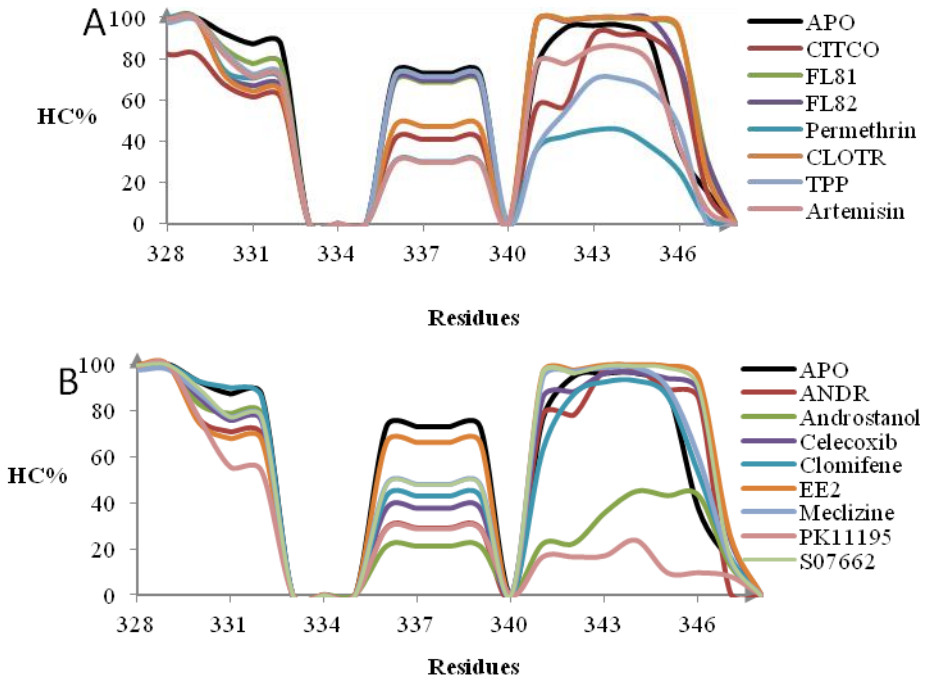

Figure 3. Helical content (HC %) of the C-terminal residues of hCAR-LBD during MD simulations. System III in the presence of (A) agonists and (B) inverse agonists.

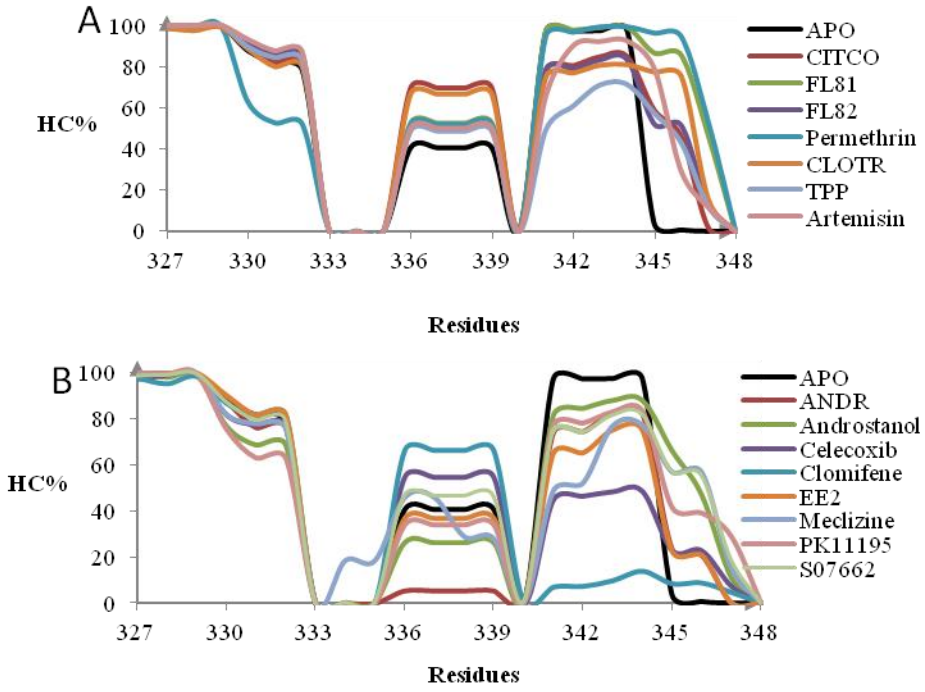

Figure 4. Helical content (HC %) of the C-terminal residues of hCAR-LBD during MD simulations. System IV in the presence of (A) agonists and (B) inverse agonists.

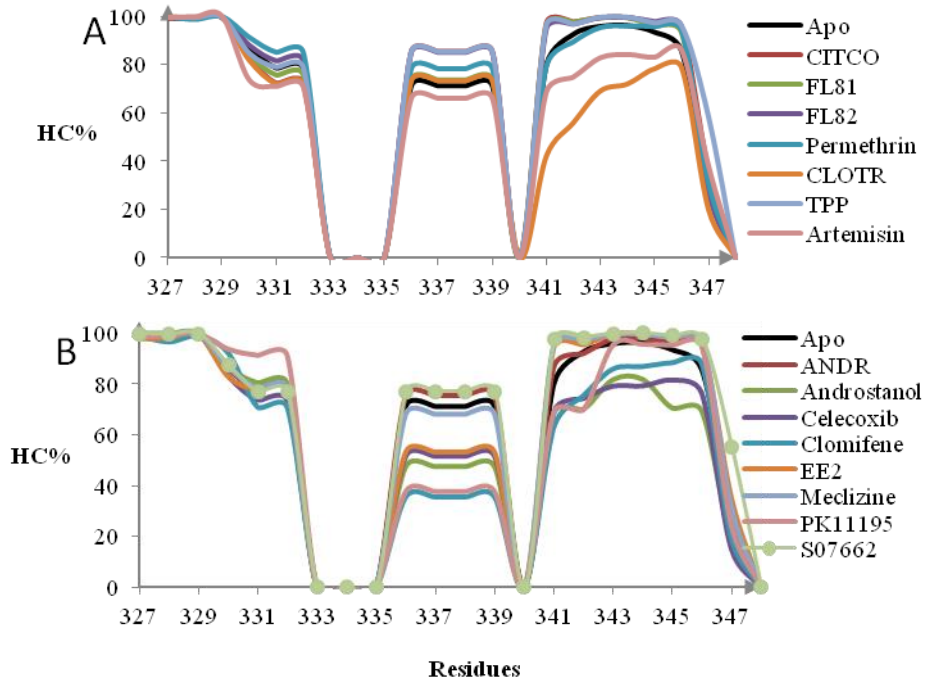

Figure 5. Helical content (HC %) of the C-terminal residues of hCAR-LBD during MD simulations. System V in the presence of (A) agonists and (B) inverse agonists.

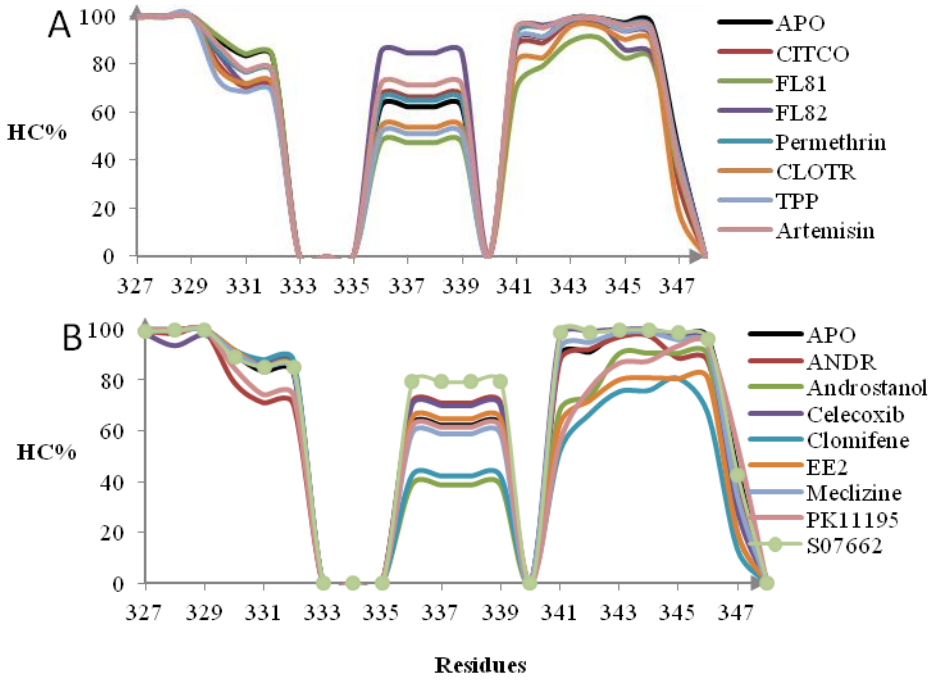

Figure 6. Helical content (HC %) of the C-terminal residues of hCAR-LBD during MD simulations. System VI in the presence of (A) agonists and (B) inverse agonists.

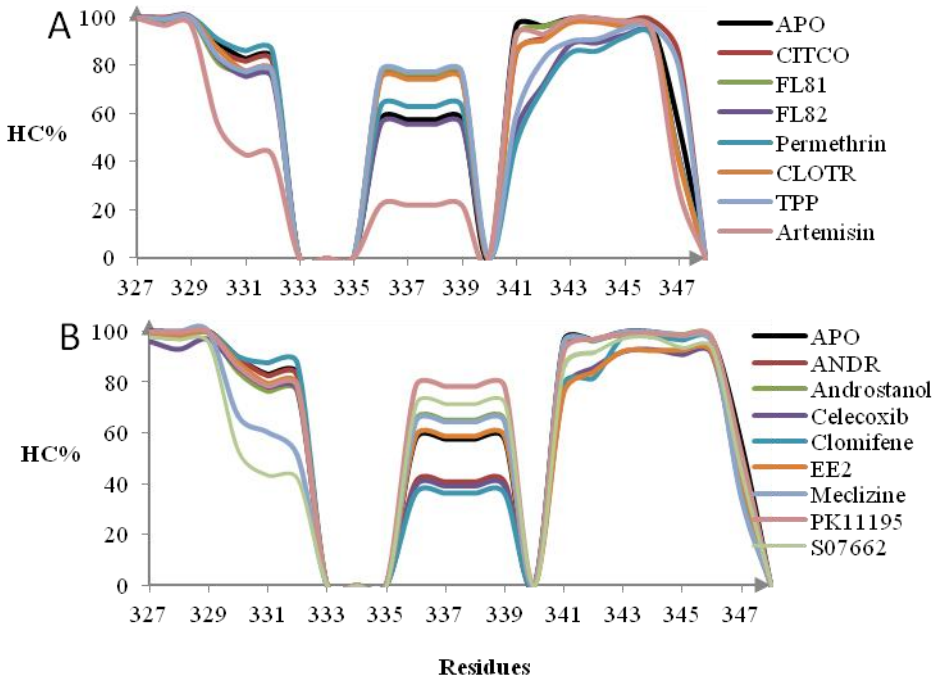

Figure 7. Helical content (HC %) of the C-terminal residues of hCAR-LBD during MD simulations. System VII in the presence of (A) agonists and (B) inverse agonists.

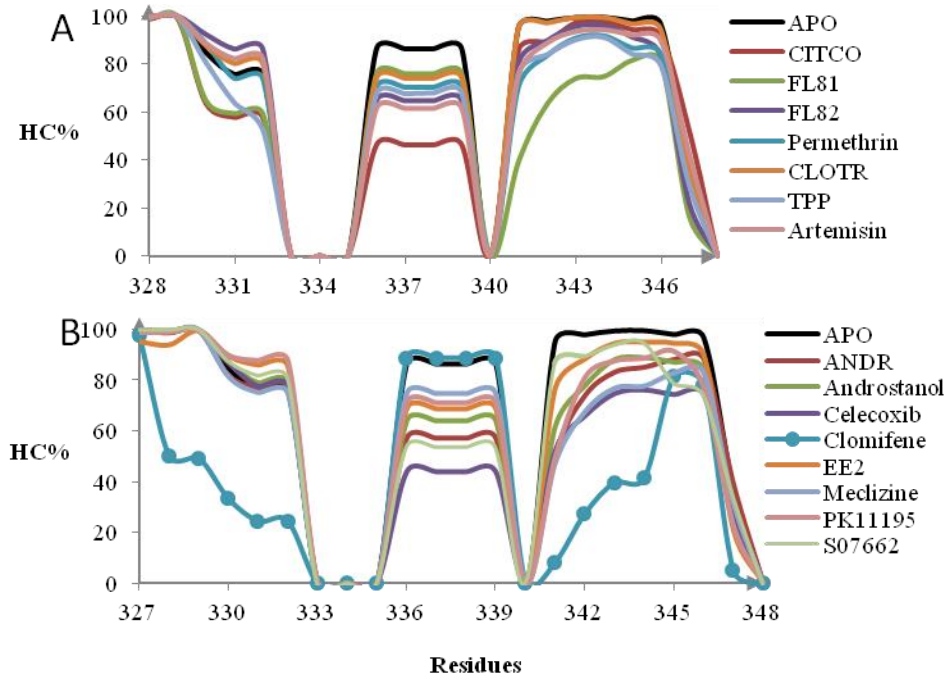

Figure 8: Helical content (HC %) of the C-terminal residues of hCAR-LBD during MD simulations. System VIII in the presence of (A) agonists and (B) inverse agonists.

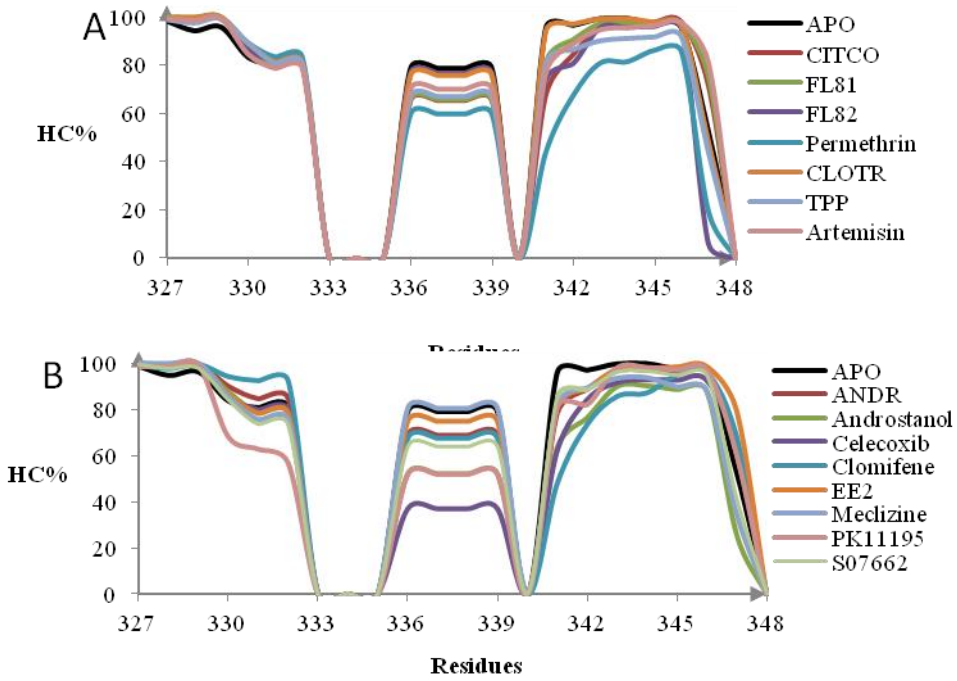

Figure 9: Helical content (HC %) of the C-terminal residues of hCAR-LBD during MD simulations. System IX in the presence of (A) agonists and (B) inverse agonists.

Appendix VI. The binding of apo-hCAR with co-regulator peptides

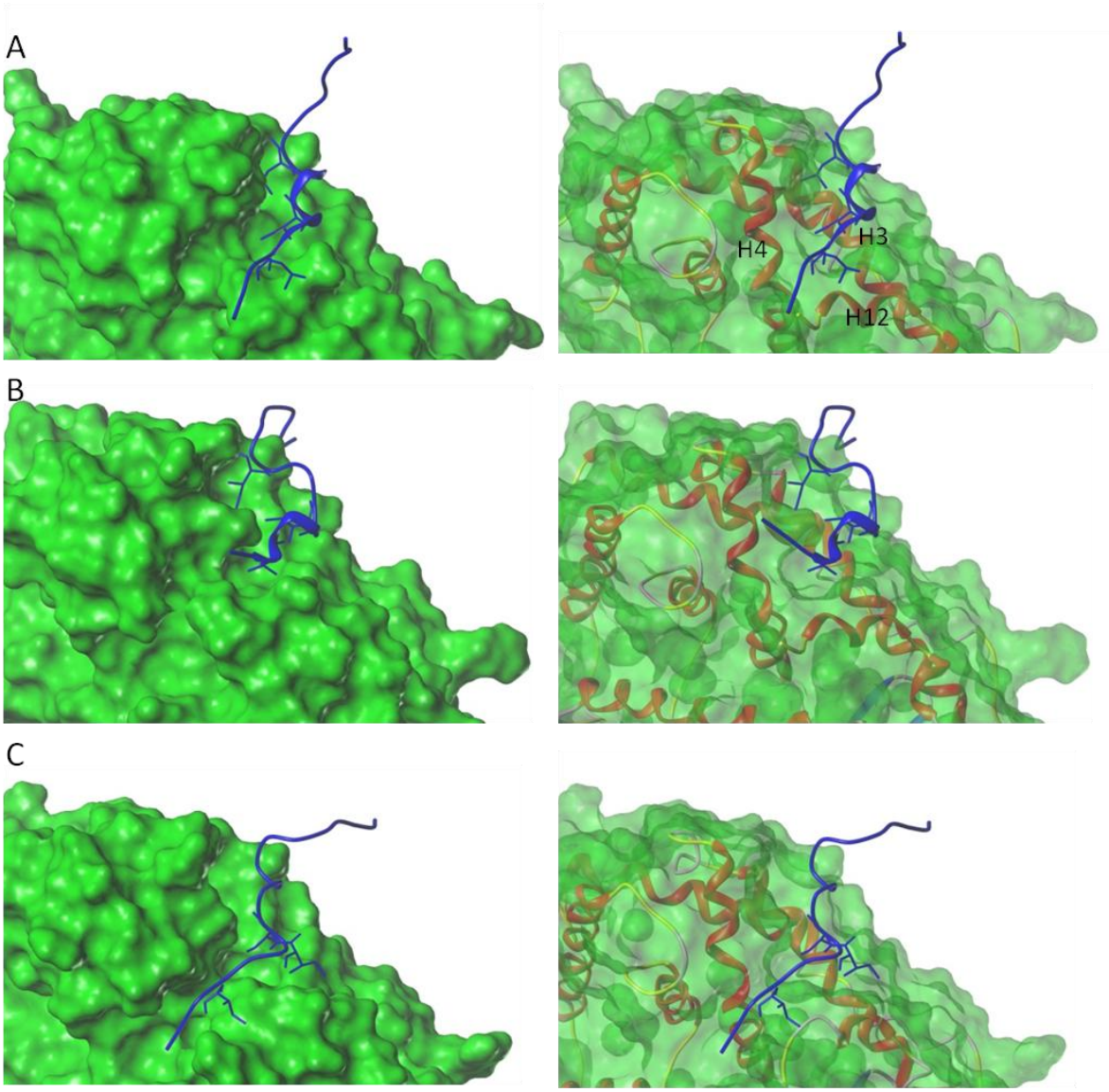

Figure 1. The binding of hCAR with co-repressor peptides. (A) NCoR ID2 binding, with showing the important residues of L1, I5 and L9 (boldface) of co-regulator peptides. (B) NCoR ID1a binding, with showing residues L1, I5 and I9 (boldface). (C) NCoR ID1b binding, with showing residues I1, I4 and I5 (boldface). Molecular surface (green) of hCAR-LBD are depicated in both transparent (right) and opaque (right) view. The ribbon that represent hCAR-LBD atoms is colored according to the secondary structure: α helix in red, β sheet in blue, others in pink or yellow. NCoR ID2, ID1a and ID1b peptides are shown in blue ribbon.

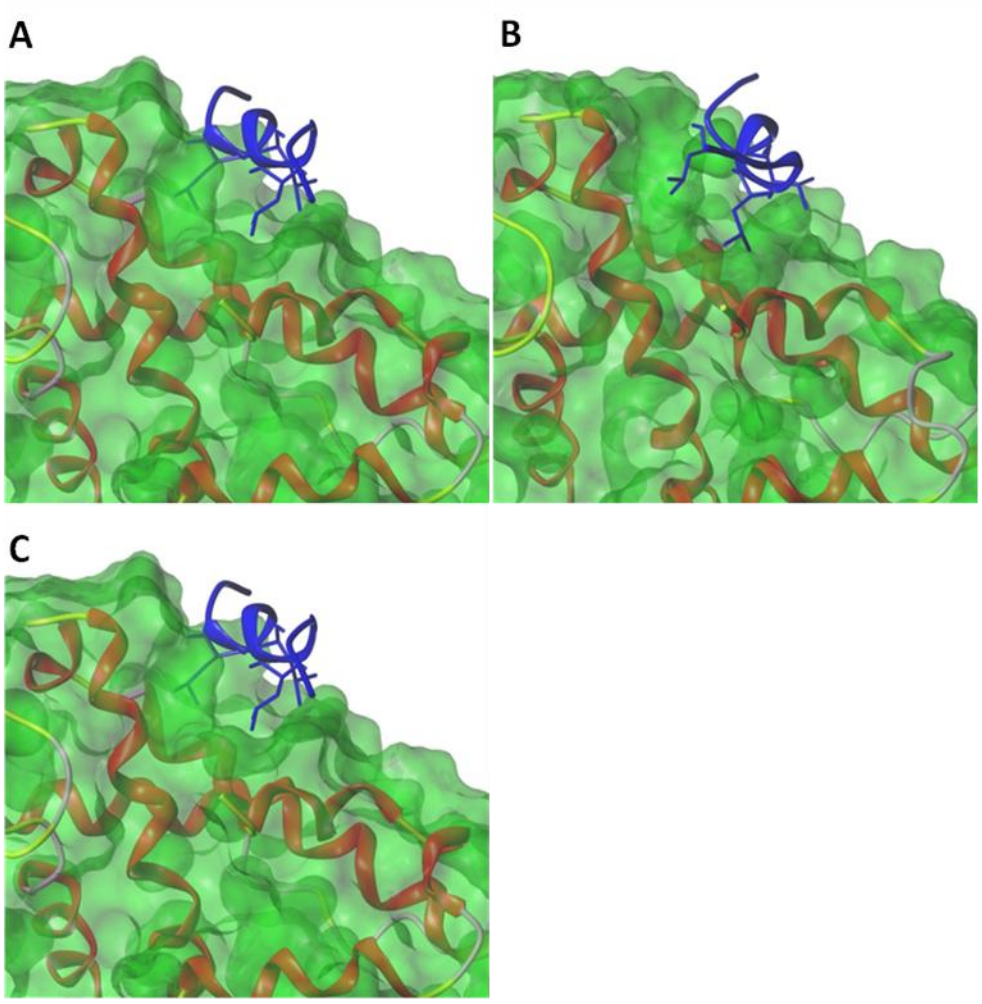

Figure 2. The co-regulator groove of hCAR with peptides from co-activator SRC-1. The important residues of L1, L4 and L5 (boldface) of peptides are shown. (A) NR1, (B) NR2 and (C)NR3 peptide binds onto apo-structure. The molecular surface of hCAR-LBD is shown in green, SRC-1 peptides is shown in blue.

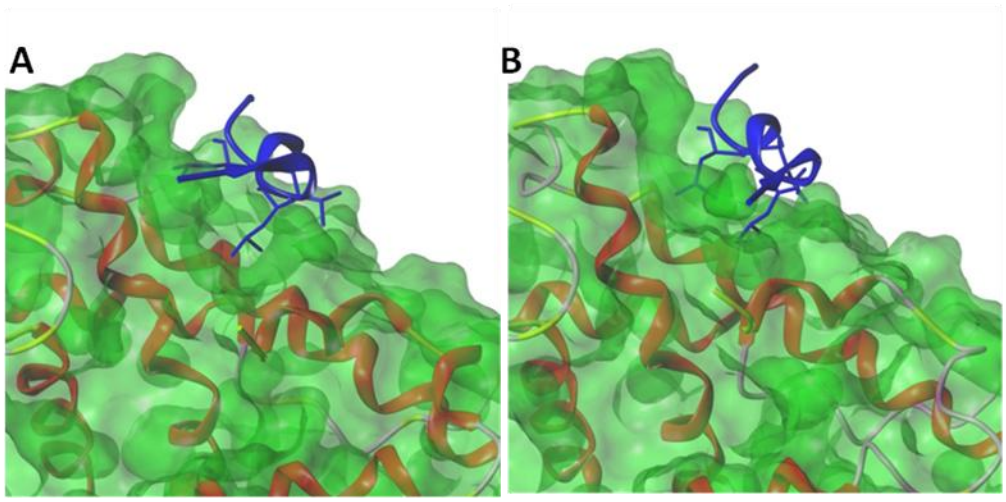

Figure 3. The co-regulator groove of hCAR with peptides from mediator TRAP. The important residues of L1, L4 and L5 (boldface) of peptides are shown. (A) NR1, (B) NR2 peptide binds onto apo-structure. The molecular surface of hCAR-LBD is shown in green, SRC-1 peptides is shown in blue.

Appendix VII. The core residues co-regulator peptides on the liganded structures

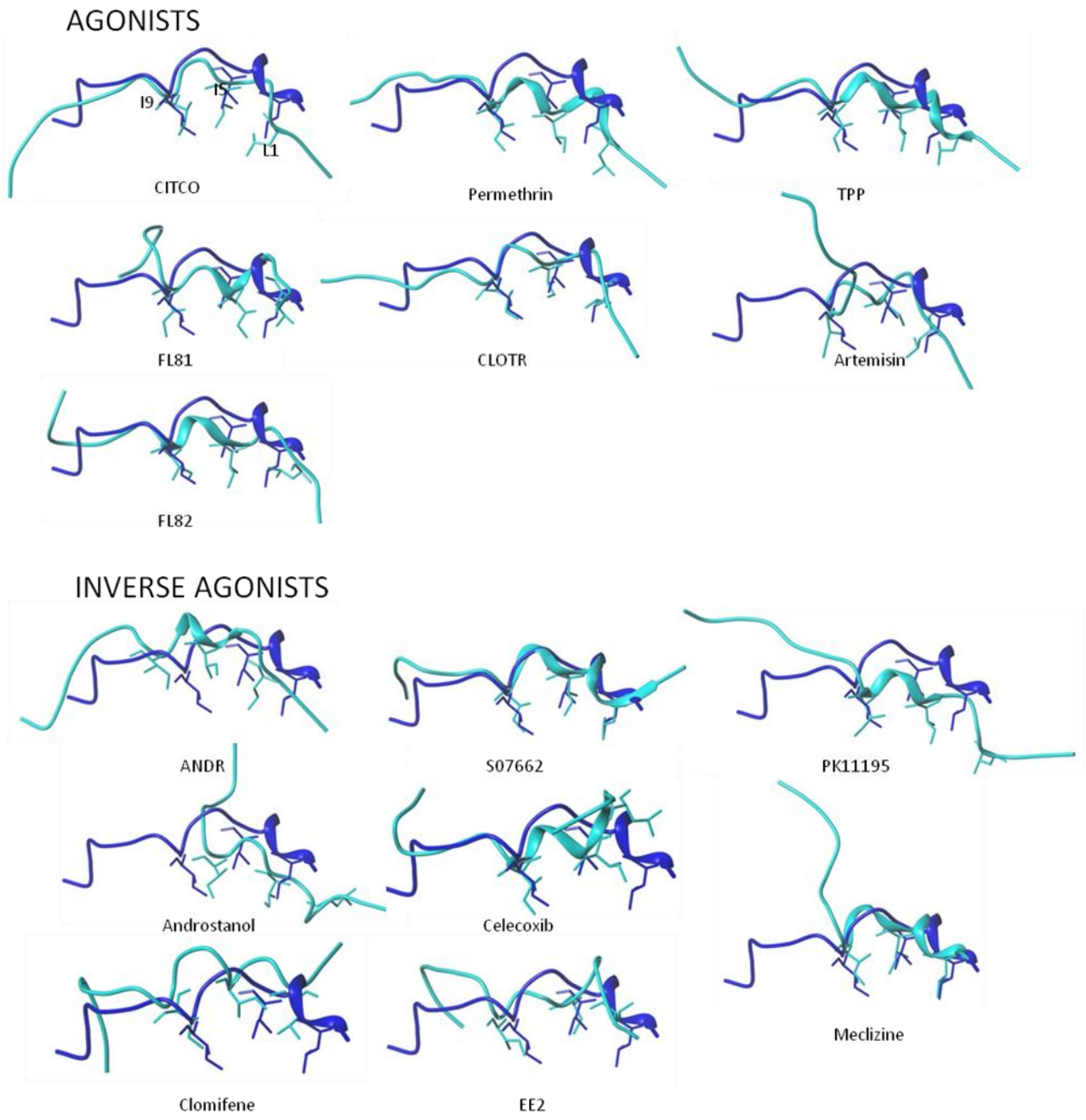

Figure 1. The core residues L1, I5 and I9 of NCoR ID1a on the liganded structures (cyan), compared to the apo-structure (blue).

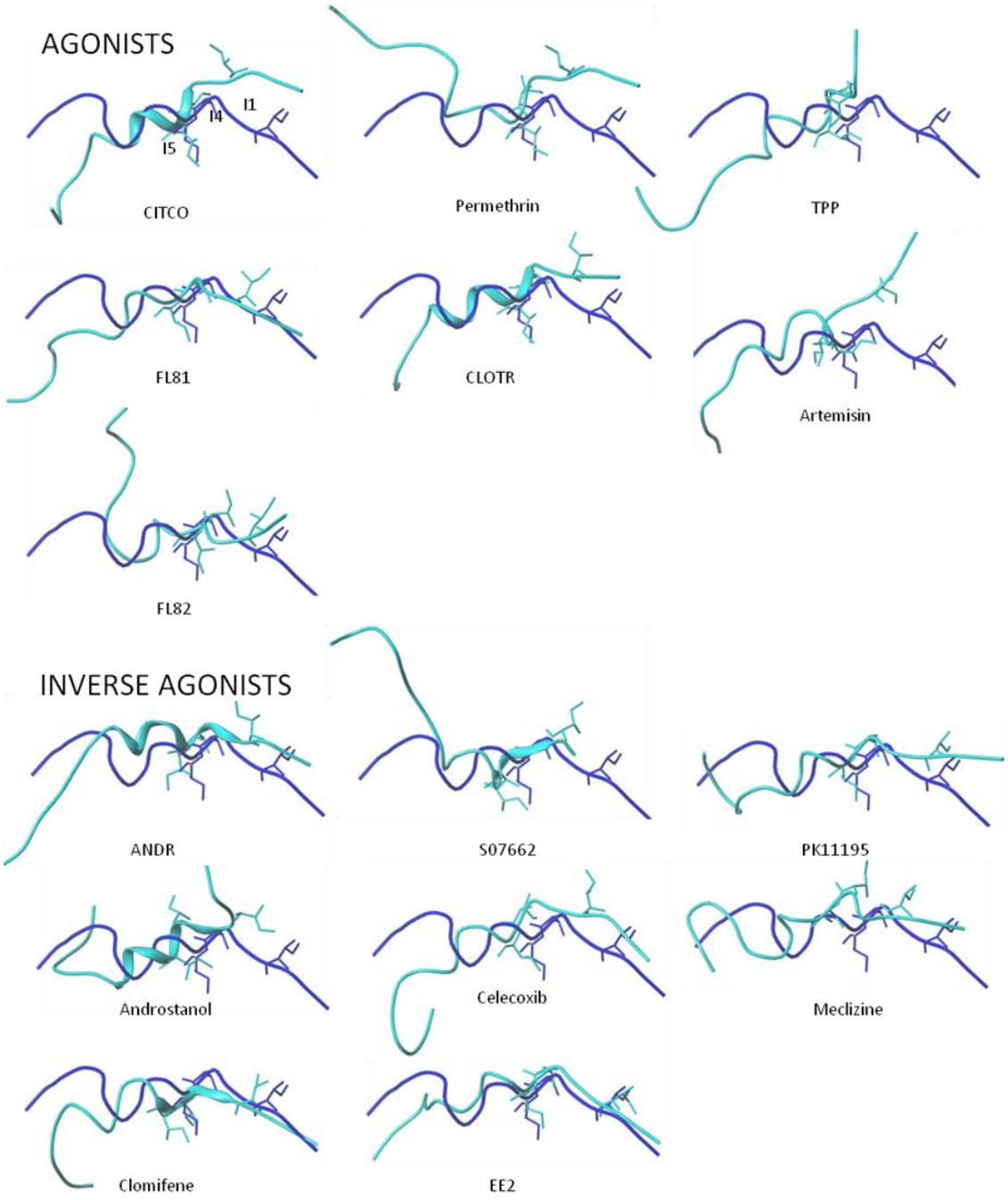

Figure 2. The core residues I1, I4 and I5 of NCoR ID1b on the liganded structures (cyan), compared to the apo-structure (blue).

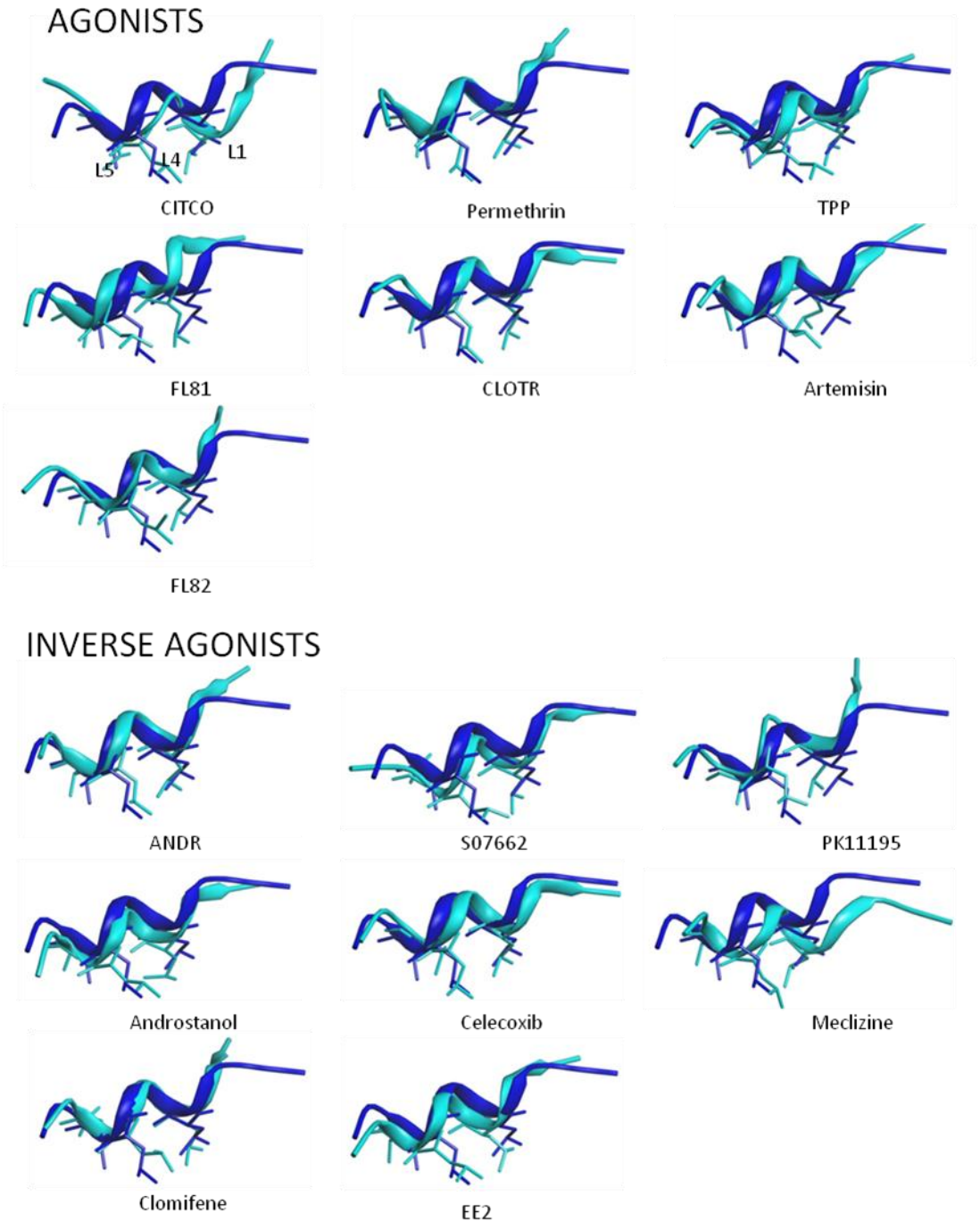

Figure 3. The core residues L1, L4 and L5 of SRC-1 NR1 on the liganded structures (cyan), compared to the apo-structure (blue).

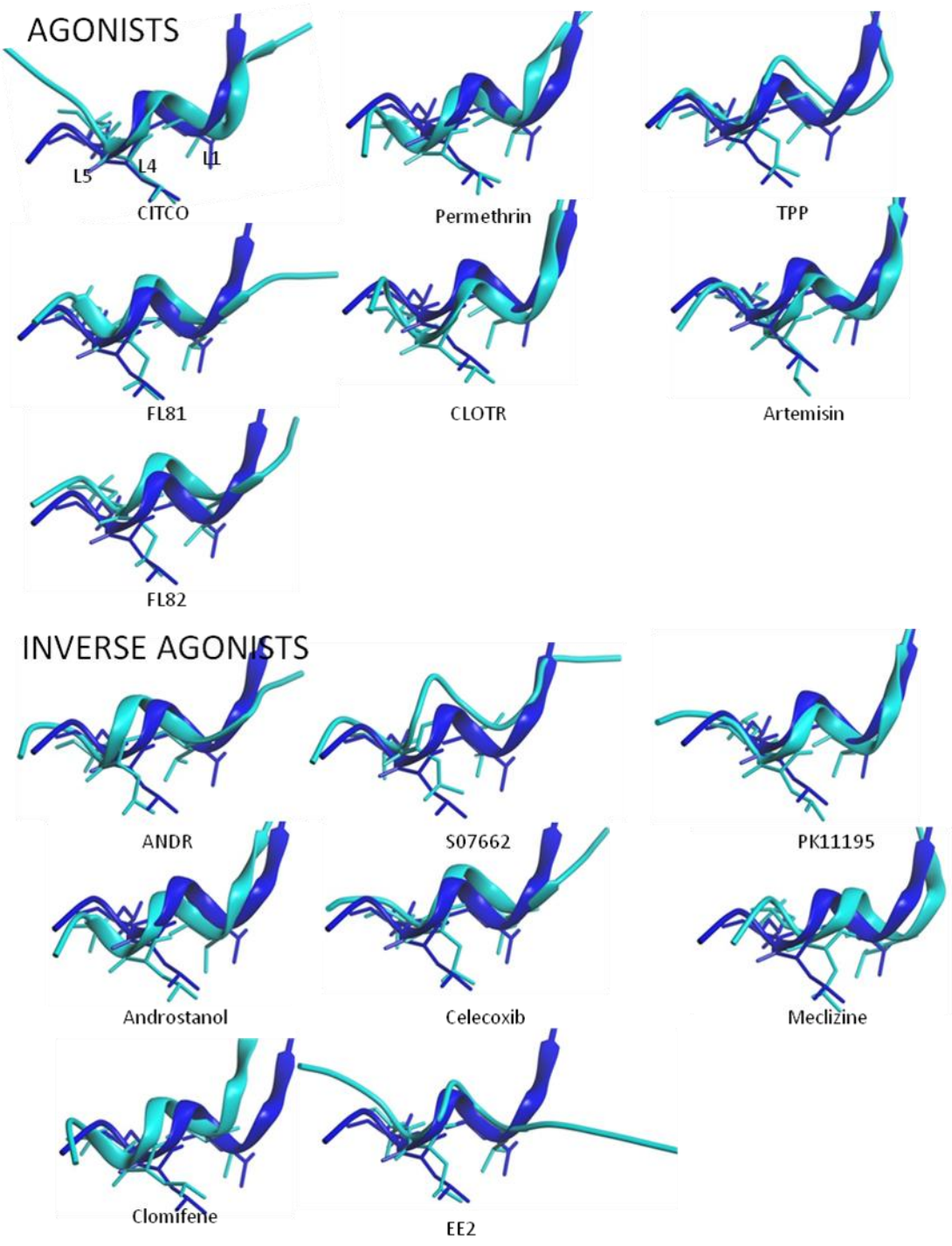

Figure 4. The core residues L1, L4 and L5 of SRC-1 NR2 on the liganded structures (cyan), compared to the apo-structure (blue).

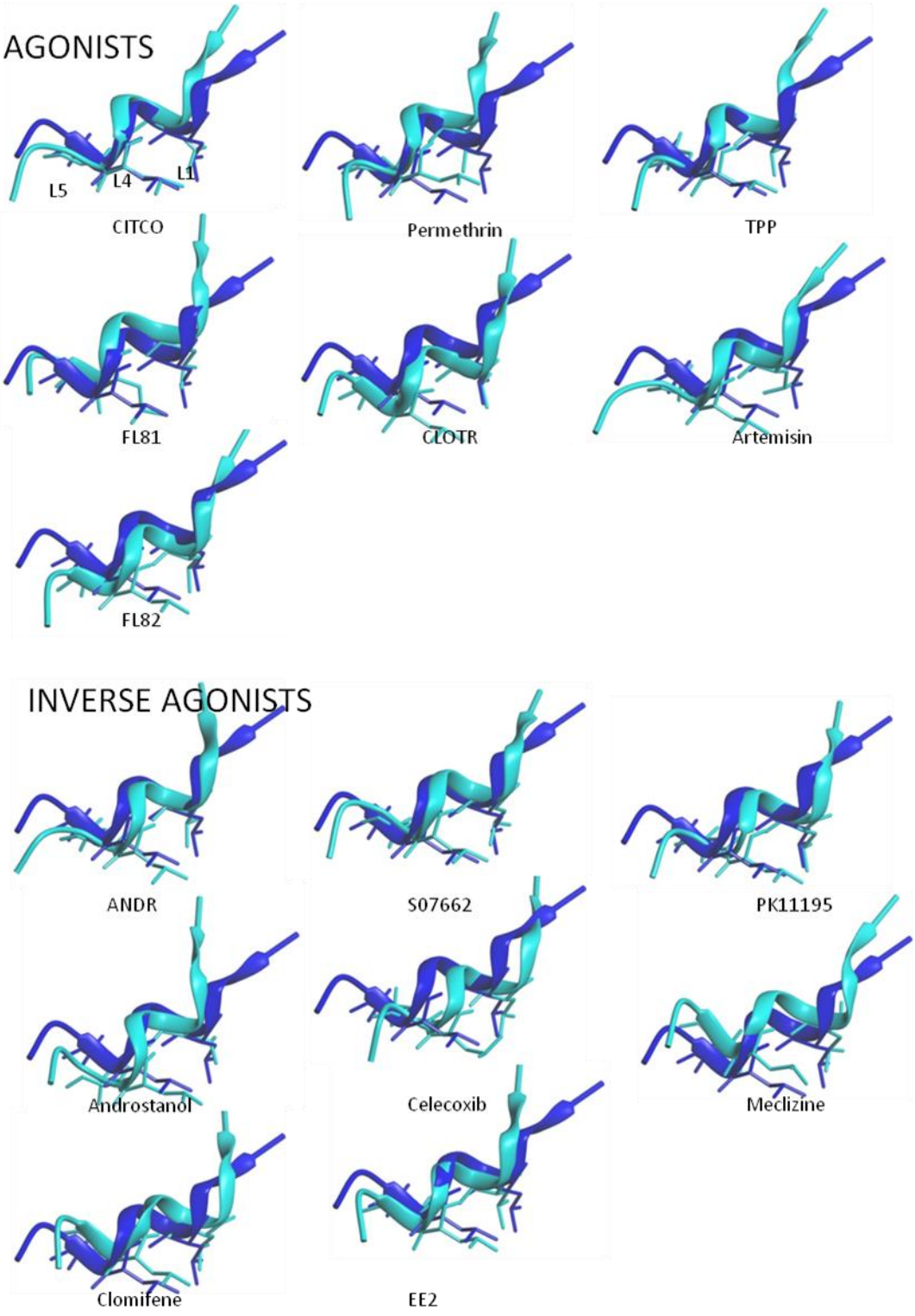

Figure 5. The core residues L1, L4 and L5 of SRC-1 NR3 on the liganded structures (cyan), compared to the apo-structure (blue).

Appendix VIII. Helical content (HC %) of the co-regulator peptides during MD simulations

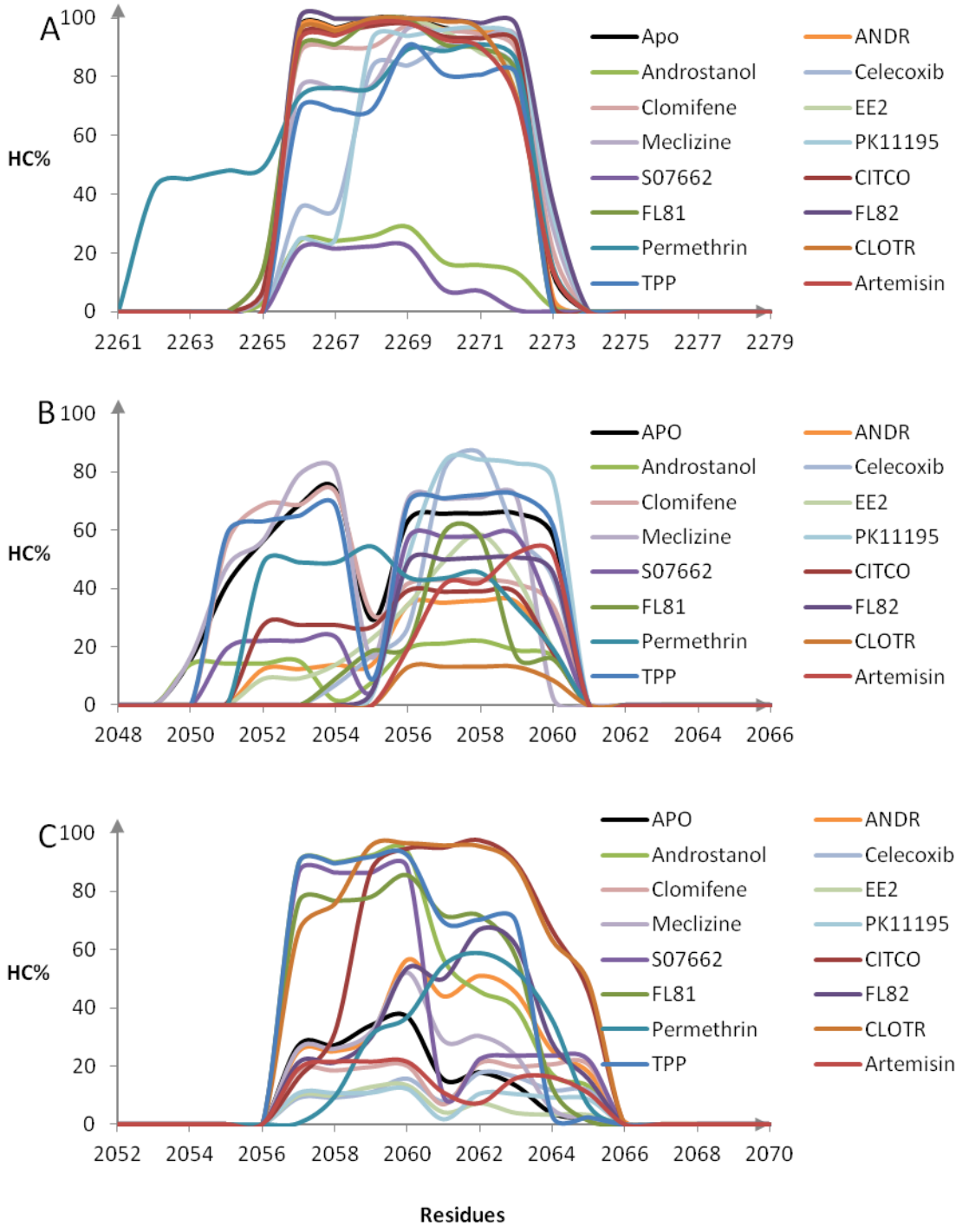

Figure 1. Helical content (HC %) of the peptide from co-repressor NCoR during MD simulations. (A) NCoR ID2 in system II and (B) NCoR ID1a in system III and (C) NCoR ID1b in system IV.

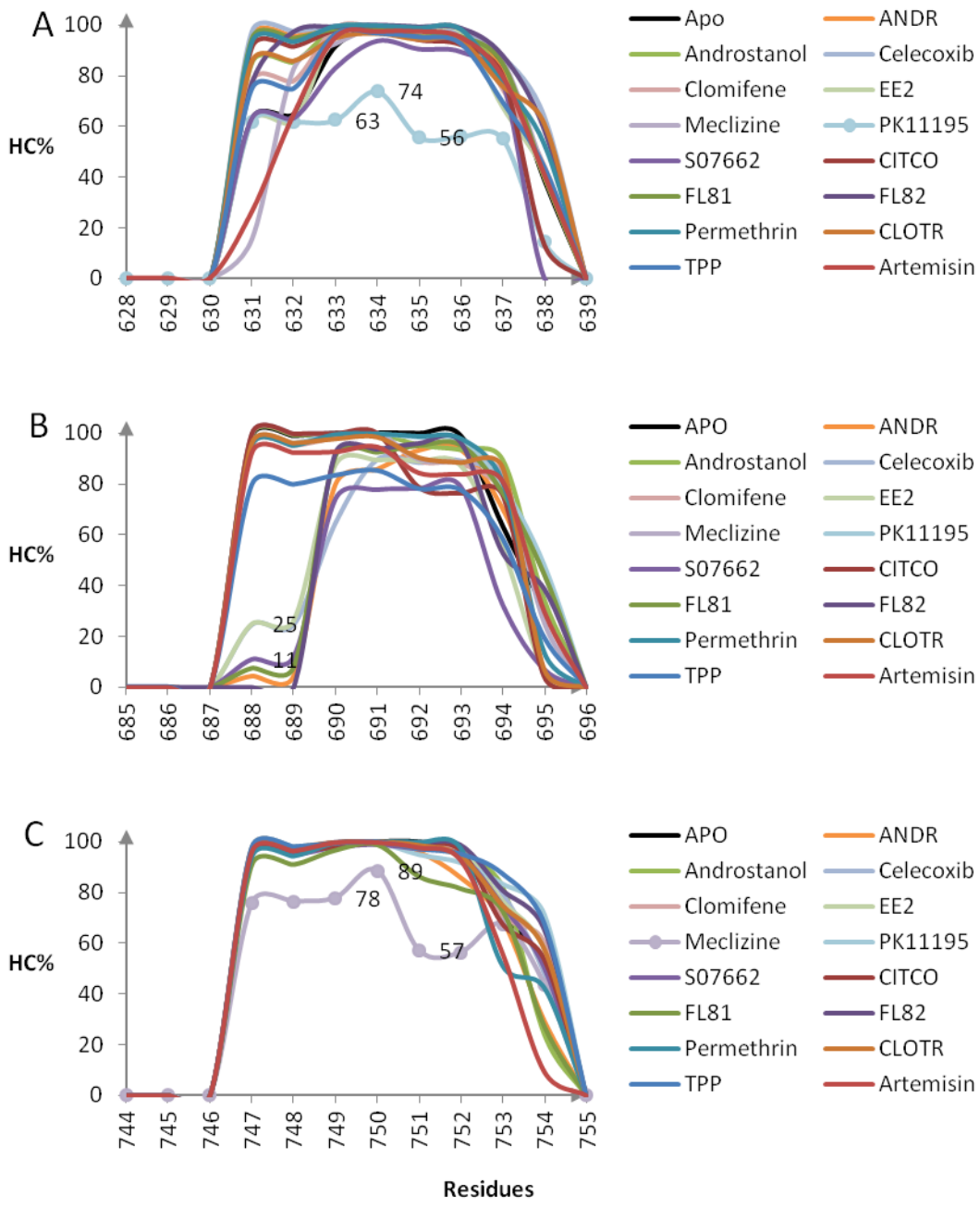

Figure 2. Helical content (HC %) of peptides from co-activator SRC-1 during MD simulations. (A) NR1 in system V and (B) NR2 in system VI and (C) NR3 in system VII.

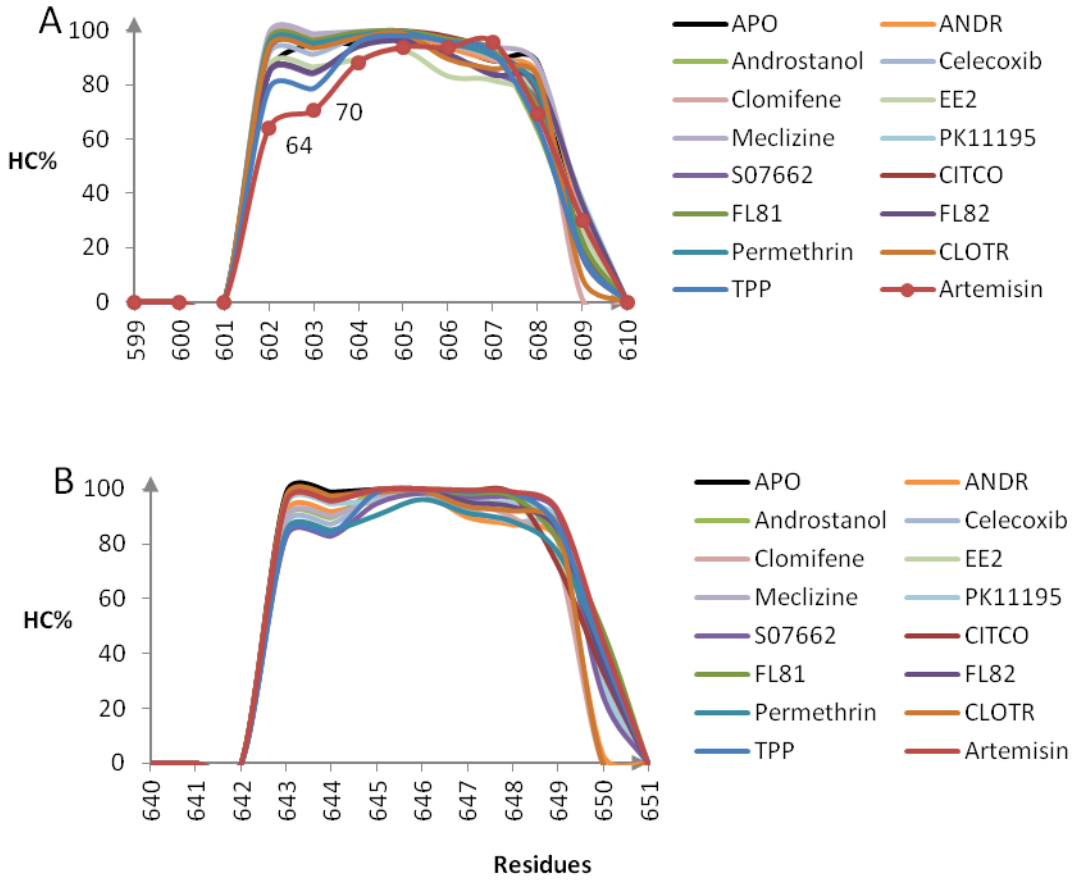

Figure 3. Helical content (HC %) of the peptide from TRAP during MD simulations. (A) TRAP NR1 in system VIII and (B) TRAP NR2 in system IX.

Appendix IX. Positions of H12 in the final structures from 10 ns MD simulations

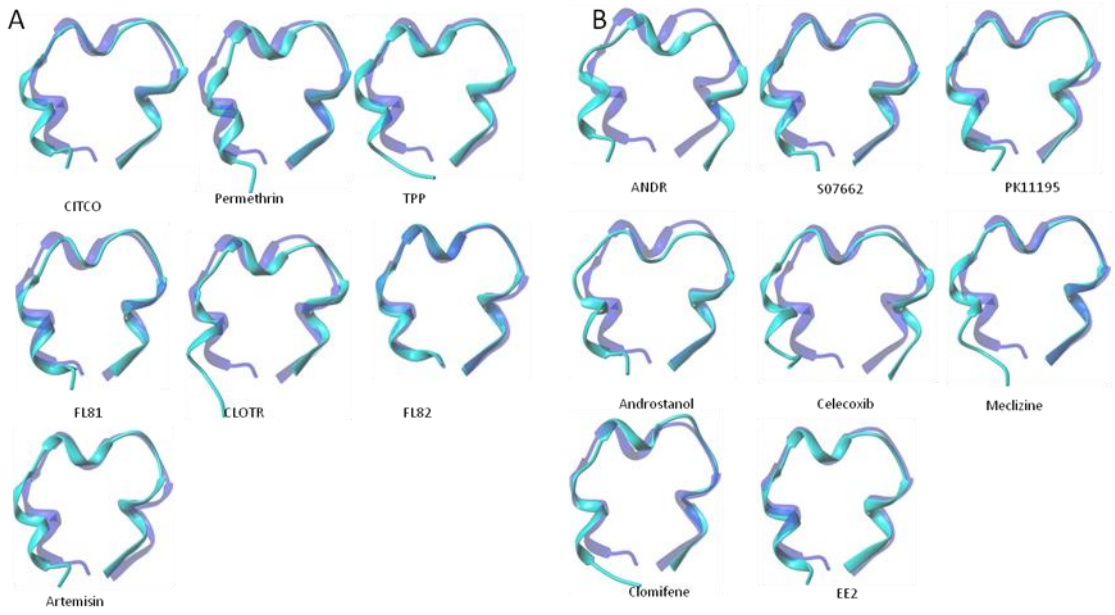

Figure 1. Positions of H12 in system I in the presence of (A) agonists and (B) inverse agonists. Apo (transparent, blue) is shown as a reference with each liganded structure (cyan).

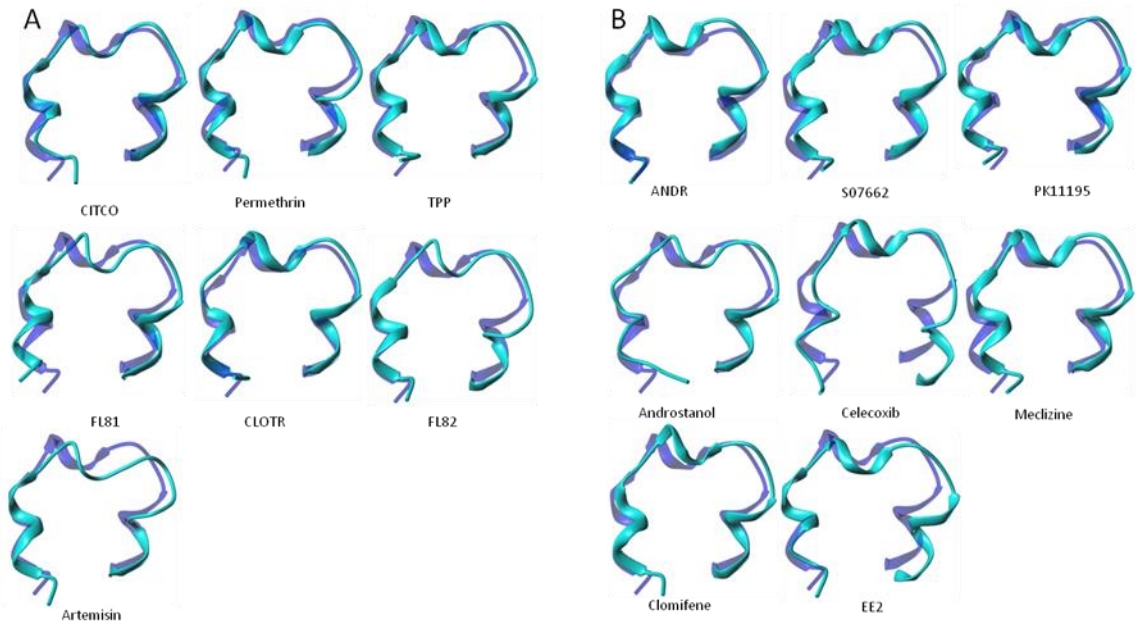

Figure 2. Positions of H12 in system V in the presence of (A) agonists and (B) inverse agonists. Apo (transparent, blue) is shown as a reference with each liganded structure (cyan).

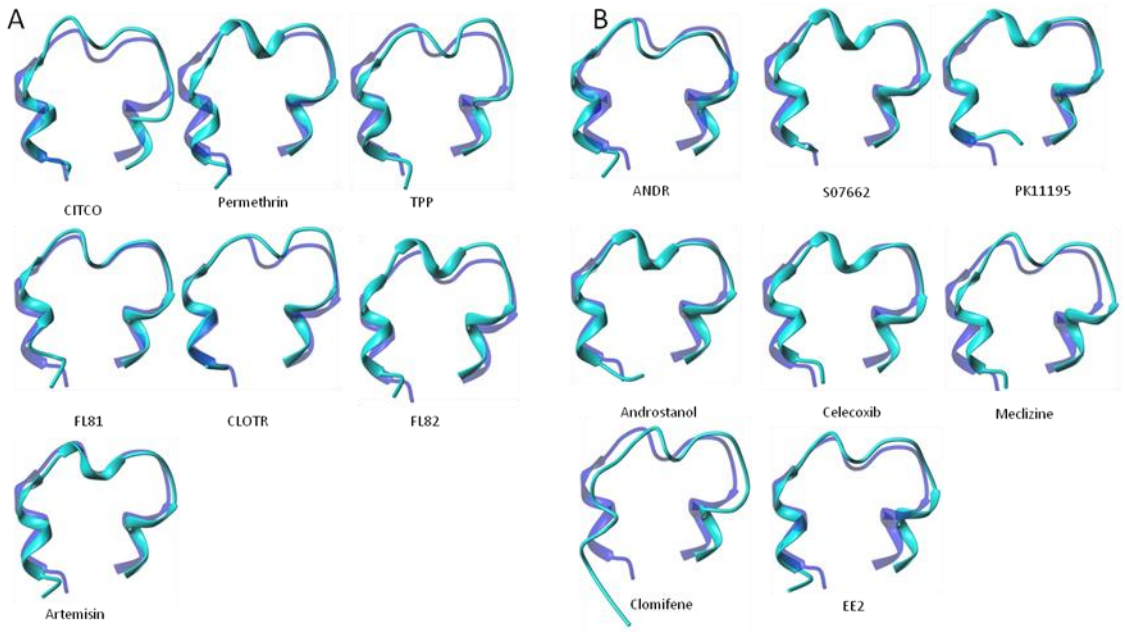

Figure 3. Positions of H12 in system VI in the presence of (A) agonists and (B) inverse agonists. Apo (transparent, blue) is shown as a reference with each liganded structure (cyan).

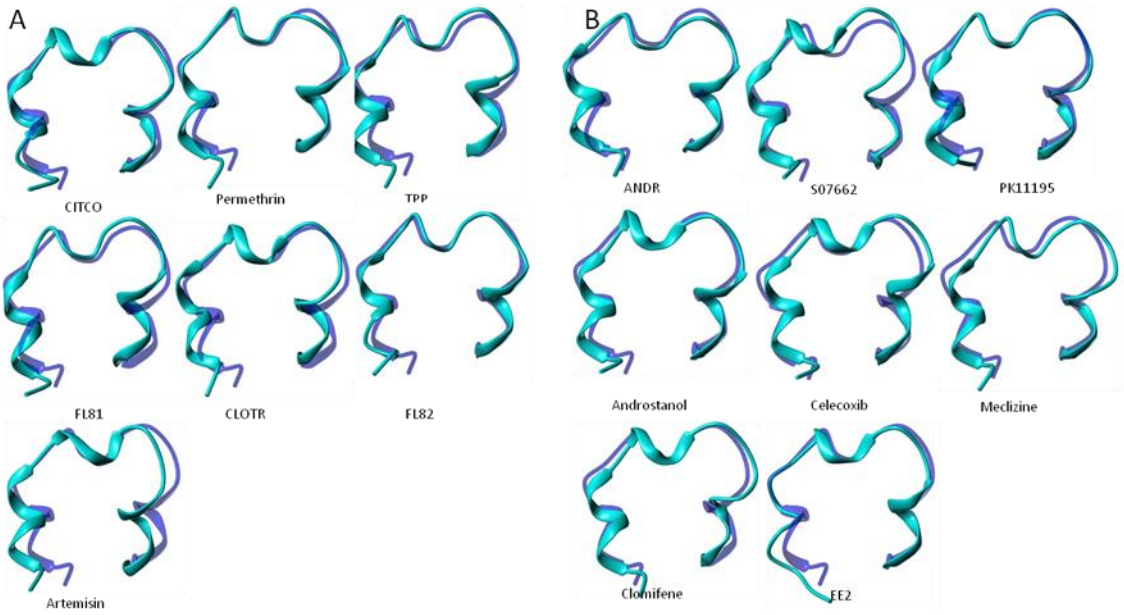

Figure 4. Positions of H12 in system VII in the presence of (A) agonists and (B) inverse agonists. Apo (transparent, blue) is shown as a reference with each liganded structure (cyan).

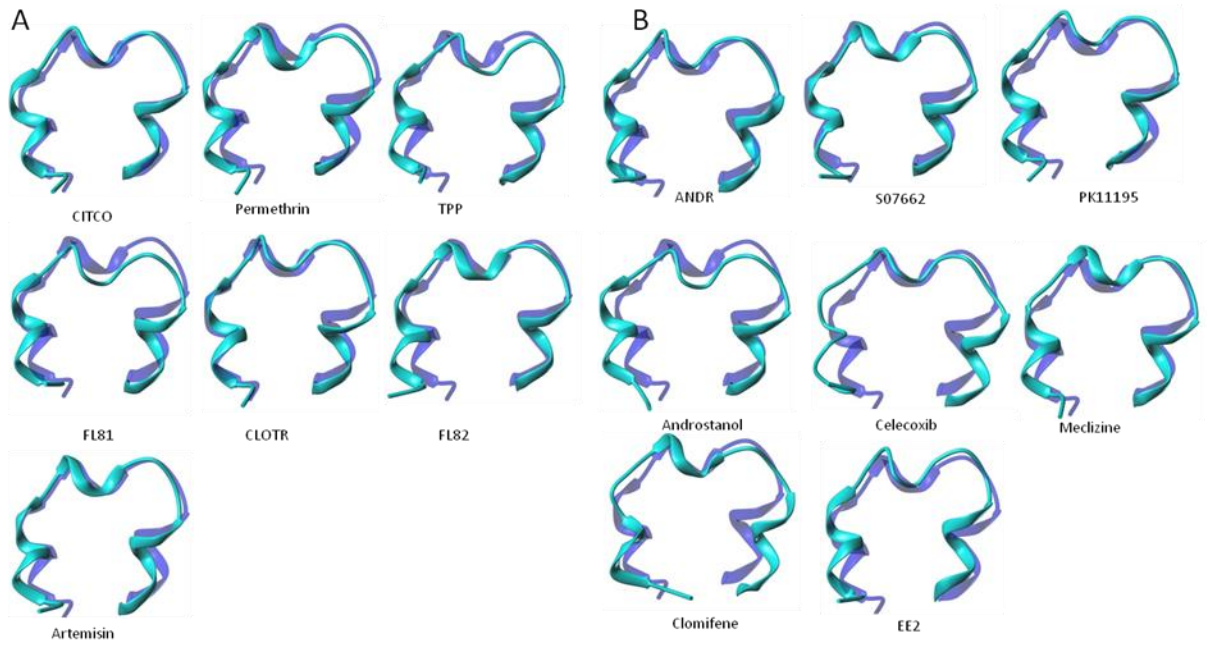

Figure 5. Positions of H12 in system VIII in the presence of (A) agonists and (B) inverse agonists. Apo (transparent, blue) is shown as a reference with each liganded structure (cyan).

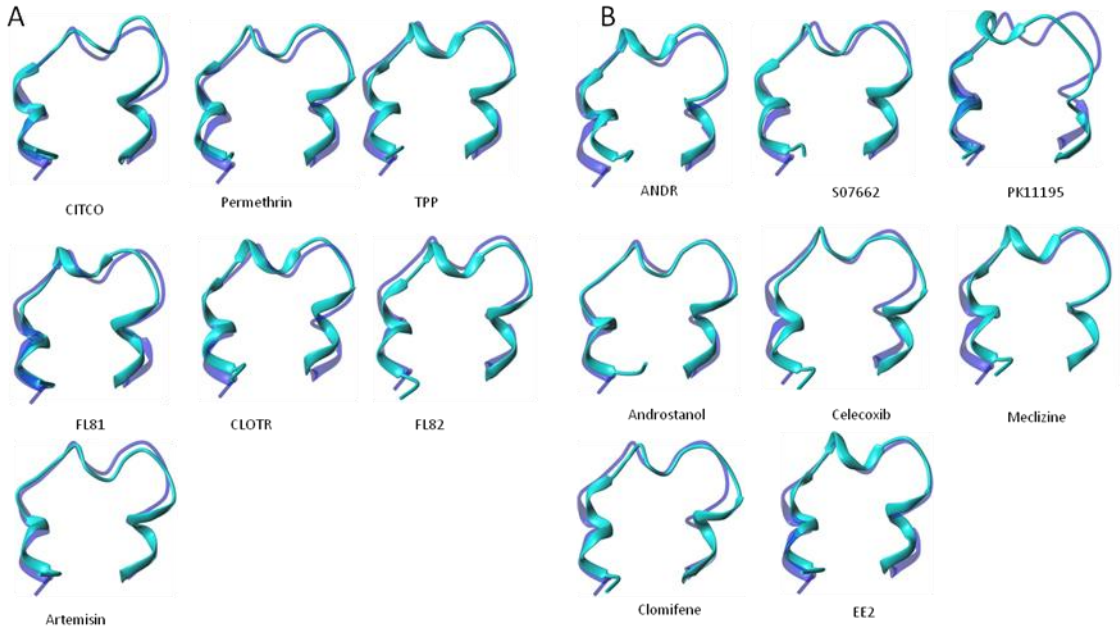

Figure 6. Positions of H12 in system IX in the presence of (A) agonists and (B) inverse agonists. Apo (transparent, blue) is shown as a reference with each liganded structure (cyan).

Appendix X. The helical content (% of MD simulation time when HX was stabilized in helical conformation) of HX

Ligand[a]	System								
	I	II	III	IV	V	VI	VII	VIII	IX
APO	83	44	73	41	71	62	58	86	79
CITCO*	55	64	41	70	86	66	75	46	65
FL82*	35	75	69	50	85	85	55	65	77
FL81*	71	57	69	53	74	47	76	76	66
Permethrin*	48	37	30	52	78	65	63	70	60
CLOTR*	59	51	47	66	73	54	74	74	76
TPP*	58	65	71	49	85	51	77	68	67
Artemisin*	59	24	30	50	66	71	22	62	70
EE2**	65	68	66	37	53	65	59	69	75
Androstanol**	60	39	21	26	47	39	65	64	52
ANDR**	69	33	29	5	75	71	41	57	69
PK11195**	67	43	29	34	38	61	78	71	52
S07662**	64	61	48	46	77	79	71	54	64
Clomifene**	61	52	43	66	35	42	36	89	68
Celecoxib**	31	48	37	55	51	70	39	44	37
Meclizine**	51	61	48	46	68	59	64	75	80

[a]agonist*; inverse agonist**

Appendix XI. APF values of the H2-H3 loop of hCAR-LBD

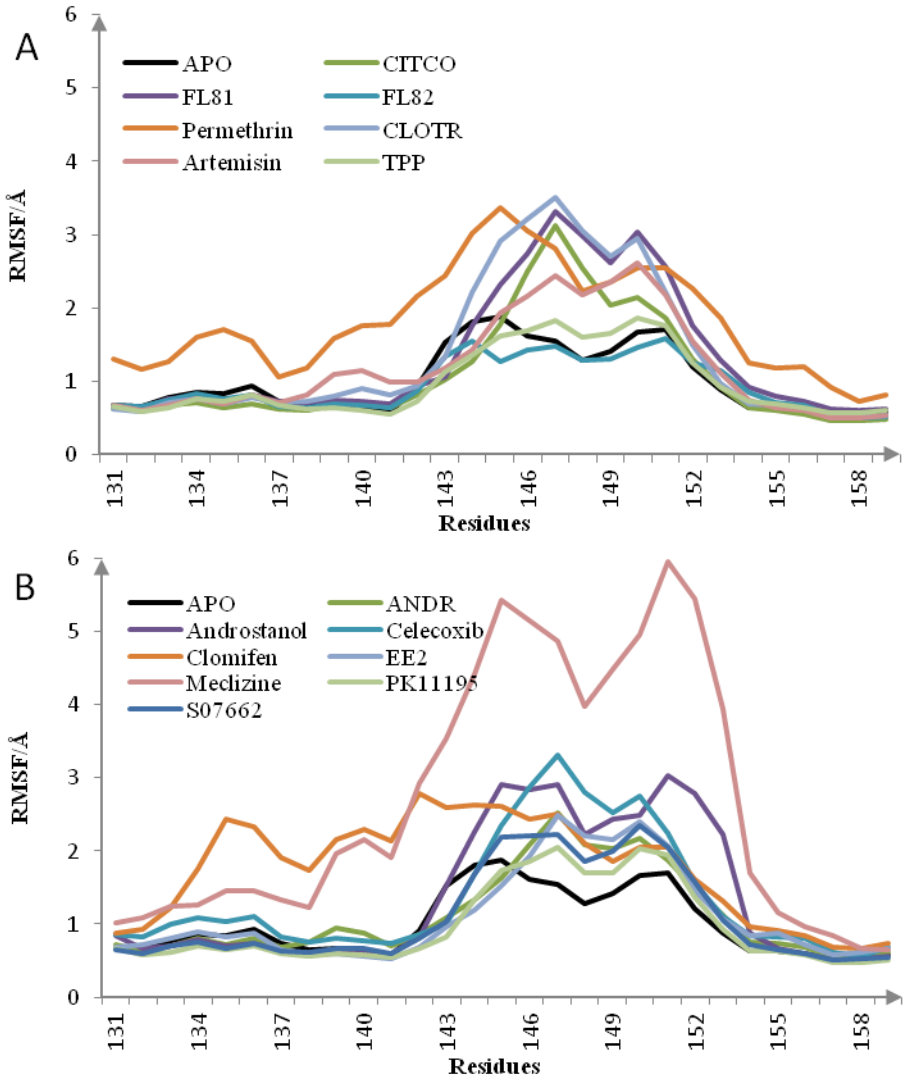

Figure 1. APF values of the H2-H3 loop of hCAR-LBD of system I in the presence of (A) agonists and (B) inverse agonists.

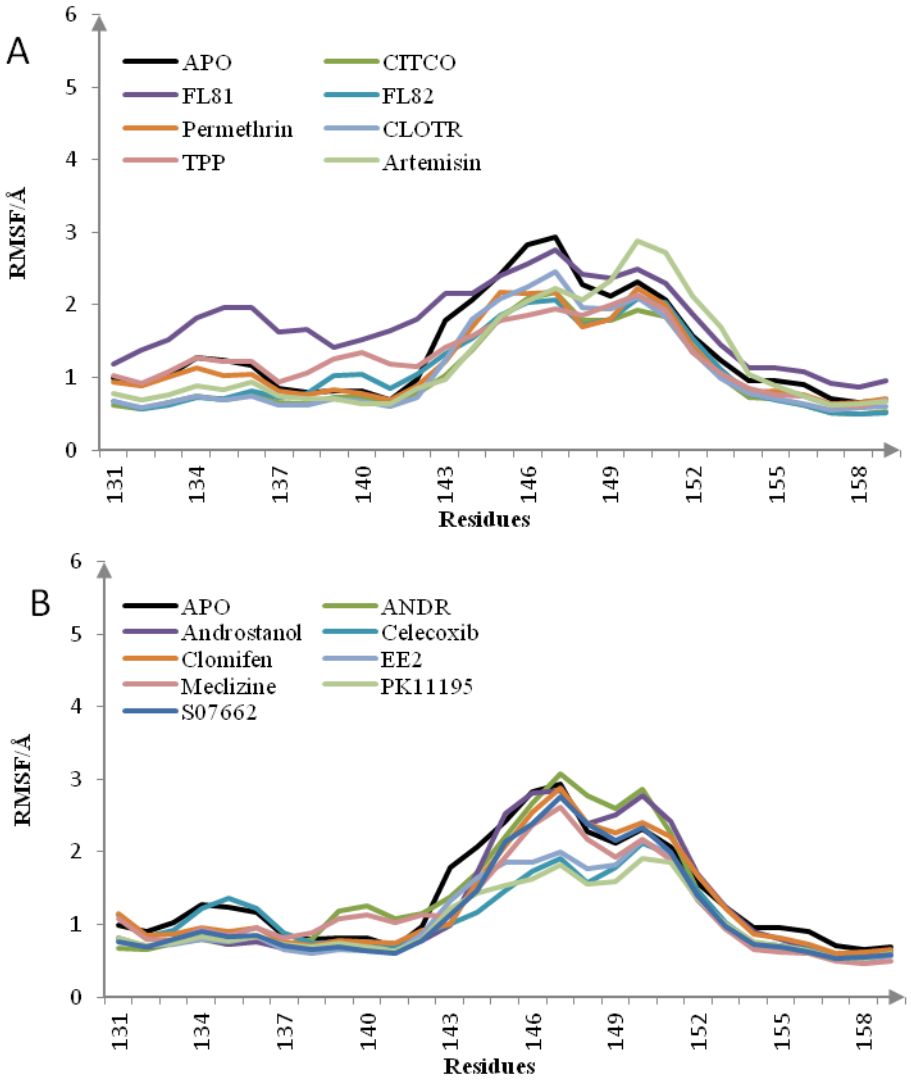

Figure 2. APF values of the H2-H3 loop of hCAR-LBD of system II in the presence of (A) agonists and (B) inverse agonists.

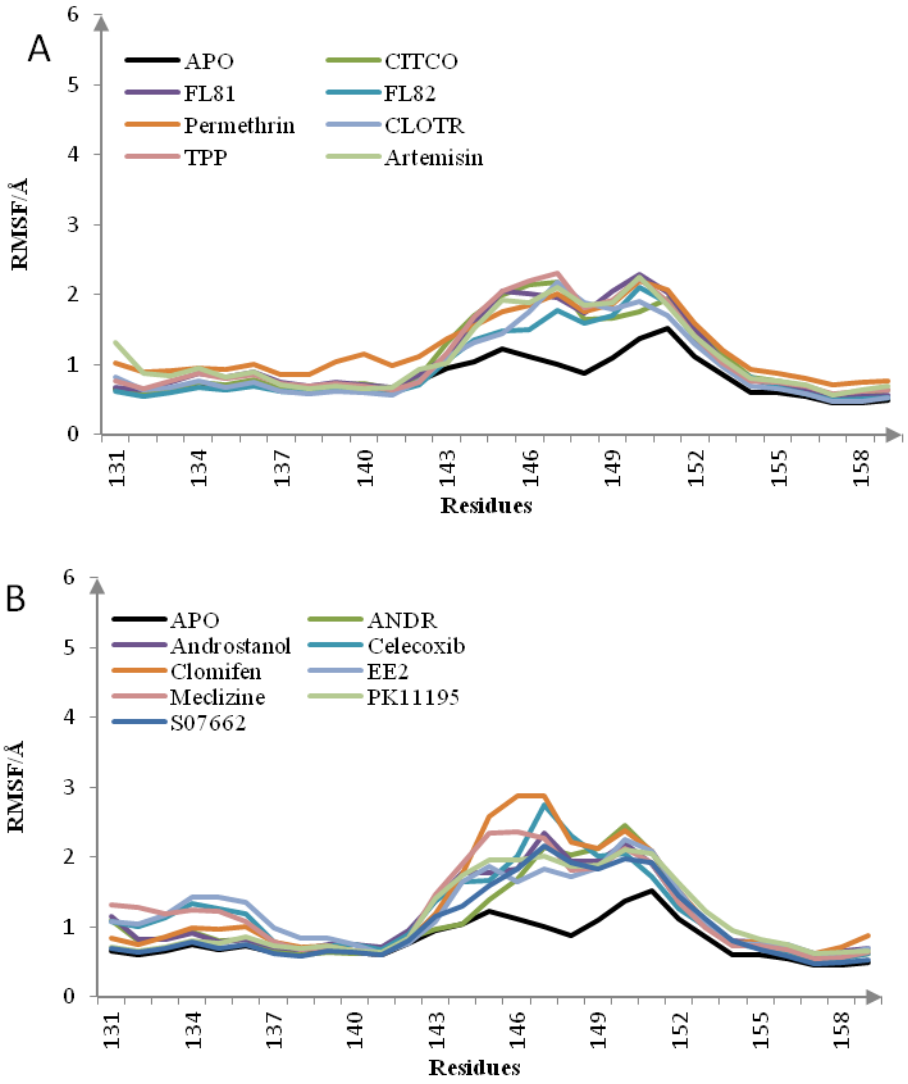

Figure 3. APF values of the H2-H3 loop of hCAR-LBD of system III in the presence of (A) agonists and (B) inverse agonists.

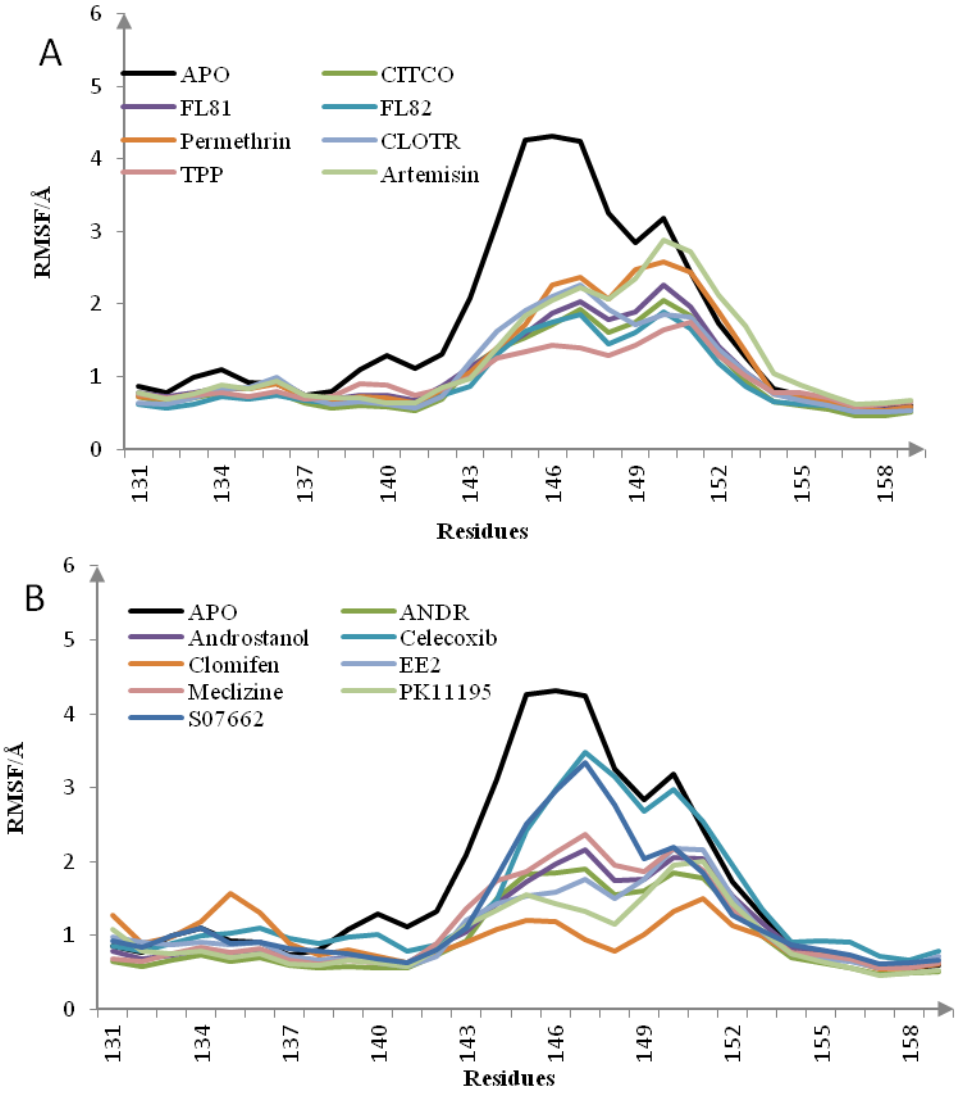

Figure 4. APF values of the H2-H3 loop of hCAR-LBD of system IV in the presence of (A) agonists and (B) inverse agonists.

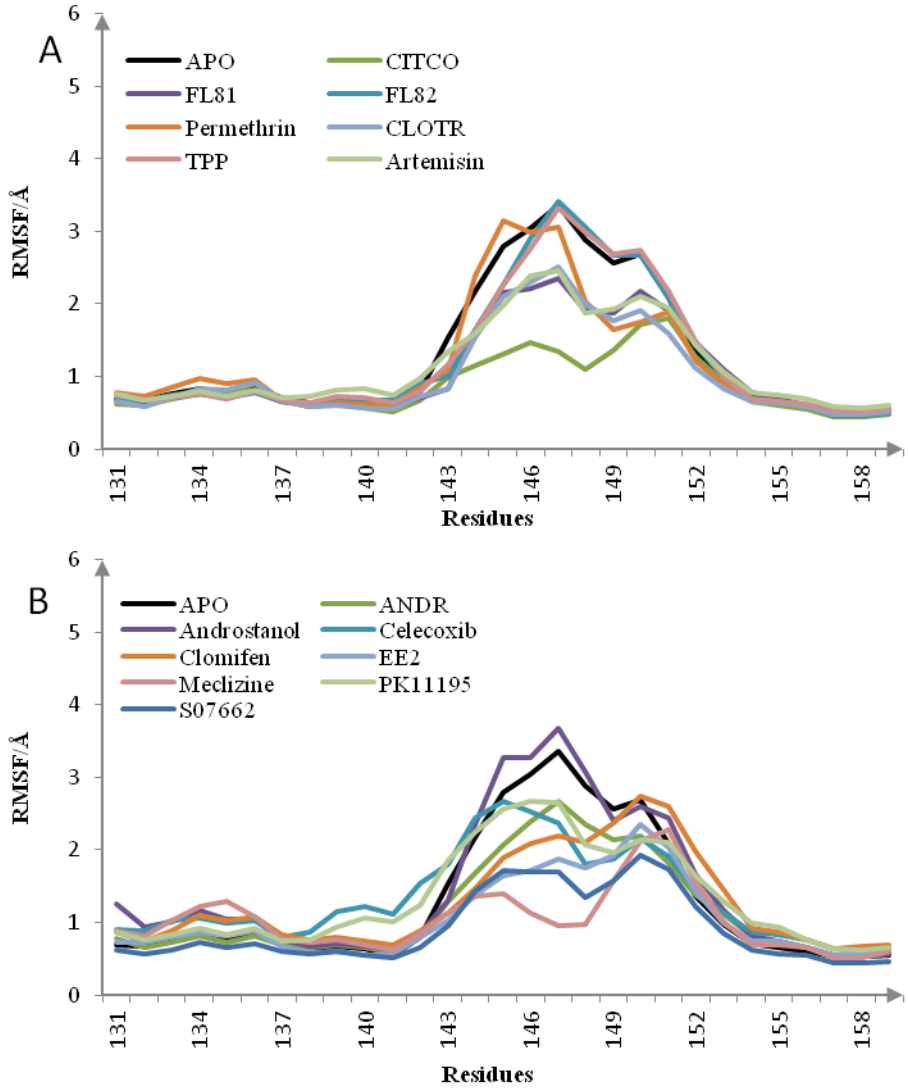

Figure 5. APF values of the H2-H3 loop of hCAR-LBD of system V in the presence of (A) agonists and (B) inverse agonists.

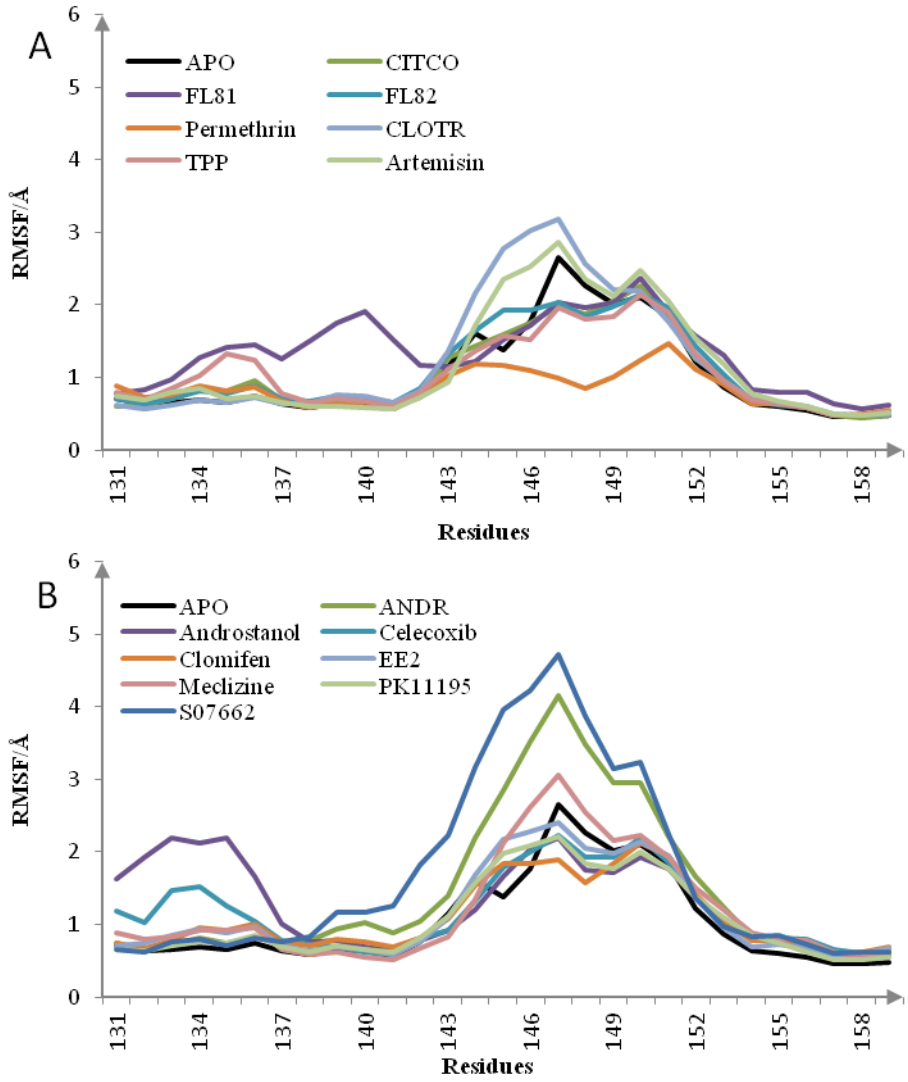

Figure 6. APF values of the H2-H3 loop of hCAR-LBD of system VI in the presence of (A) agonists and (B) inverse agonists.

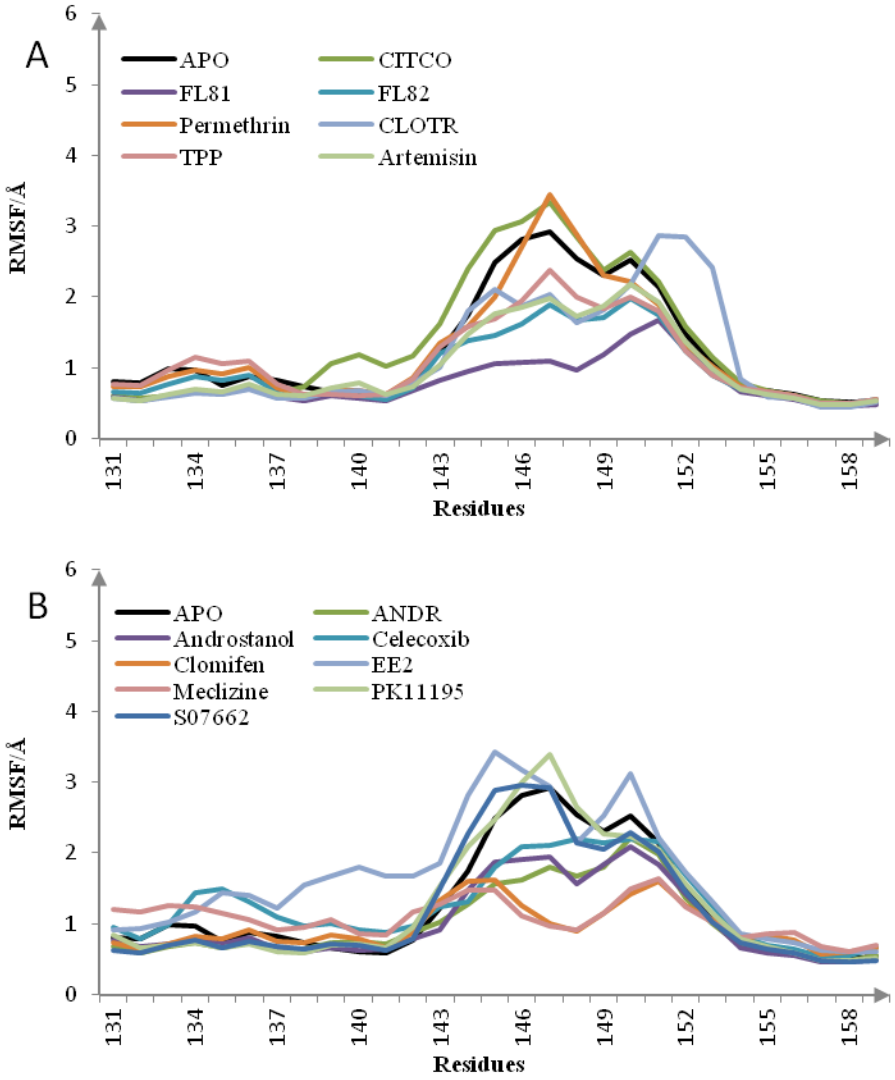

Figure 7. APF values of the H2-H3 loop of hCAR-LBD of system VII in the presence of (A) agonists and (B) inverse agonists.

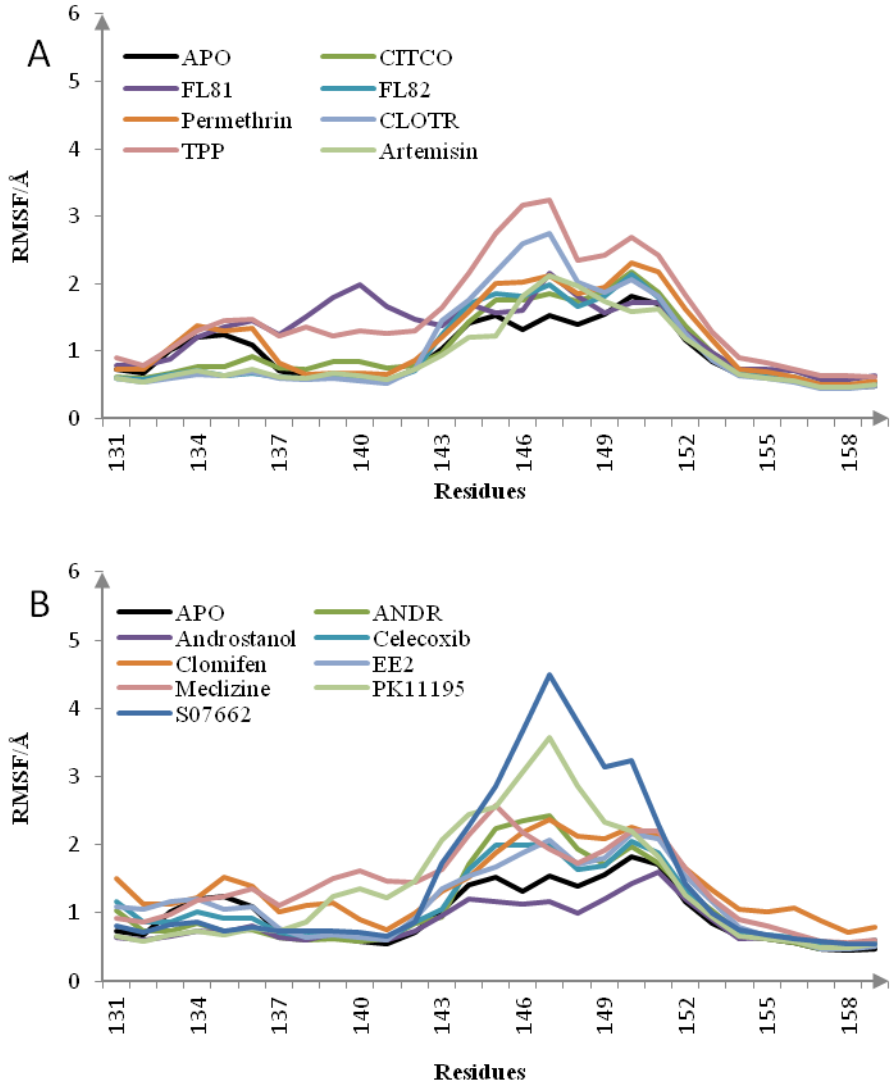

Figure 8. APF values of the H2-H3 loop of hCAR-LBD of system VIII in the presence of (A) agonists and (B) inverse agonists.

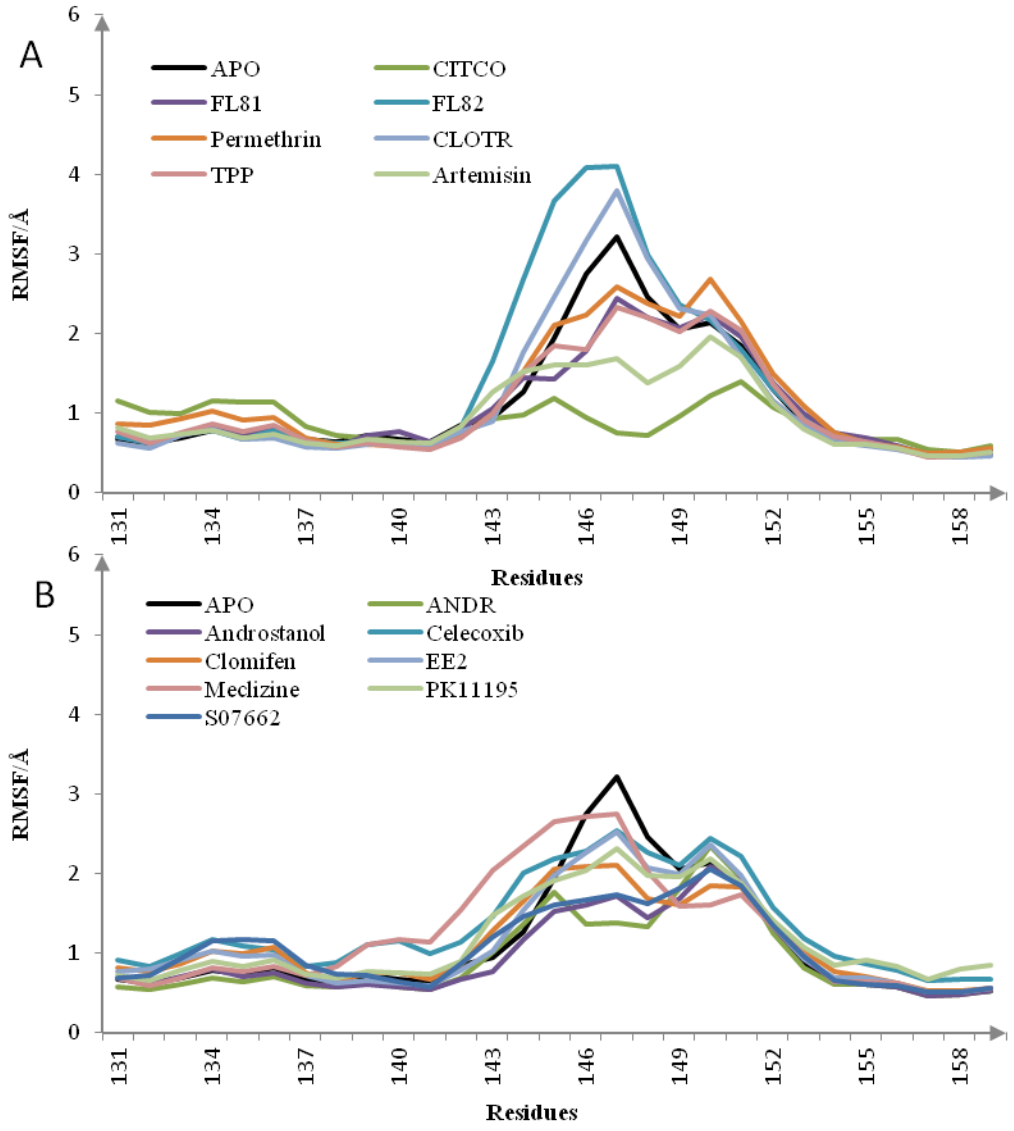

Figure 9. APF values of the H2-H3 loop of hCAR-LBD of system IX in the presence of (A) agonists and (B) inverse agonists.

Appendix XII. The ligand-protein interaction energy that were calculated with MM-PBSA method. CITCO, meclizine, clomifene and permethrin who have the highest molecular weight, gain the most favorable energy values.